University of Stavanger

Faculty of Science and Technology

MASTER'S THESIS

Study program/ Specialization: Well Engineering	Semester: Spring semester, 2014 Privacy status: Open
Writer: Edohamen Patrick Awannegbe	………………………………………. (Writer's signature)
Faculty supervisor: Bernt Sigve Aadnøy External supervisor(s): Ricardo Azevedo	
Thesis title: Characterization of flow regime of highly viscous oils using conventional ICD and BECH AICD	
Credits (ECTS): 30 points.	
Key words: ICD AICD Constant flow rate Inflow control Pressure drop Viscosity Density	Pages: 117 + enclosure: 14 Place and date: Stavanger, 16th June, 2014

ACKNOWLEDGEMENT

I would like to acknowledge the support of CNPq (Brazilian Federal Research Council), UiS, and the Statoil Akademia Program. Special appreciation goes to Prof. Bernt Aadnøy, a Drilling and Wells professor at UiS for providing enormous technical assistance with regards to the design/operational knowledge and technicalities of his BECH AICD patent used for this experimental work. More thanks to him for his expert technical input with the operation of our positive displacement pump and funds spent in procurement of fluids (in volumes of 20 liters) with varying rheological properties. Thanks to Dr. Ricardo Azevedo of the University of San Paulo who gave technical input and assisted me in taking accurate fluid throw measurements during his visits to UiS.

Furthermore, I wish to thank Per Eirik Widvey, a staff engineer and an industrial mechanic at UiS who helped me with the manual rig-up of the experimental apparatus. I also want to say thanks to Kim André Nesse Vorland a Head Engineer with UiS who helped with the operation of the university's state of the art rheometer for fluid viscosity measurement. Finally, I would like to say thanks to Dr. Oystein Djuve and Sivert Drangeid both of UiS for their input as regards personal safety and safety of equipment during flow experiments.

Stavanger 16/06/2014

Edohamen Patrick Awannegbe.

ABSTRACT

Horizontal wells are currently very common for oil production, because they can increase its efficiency. An offshore platform for instance, may have several wells all aiming to produce from a common reservoir. In addition, each well can produce more oil being in contact with a larger part of the reservoir rock. However, long horizontal wells are subject to water or gas coning. These fluids exist naturally in the reservoir, or are injected into it to increase pressure and oil production. Due to their greater mobility under high pressure differences which are common in wells of this caliber, they end up going through the oil layer and reaching the wellbore before the oil, thereby forming these cones. To prevent this, there are several types of passive Inflow Control Devices (ICD's) that can be placed along the horizontal part of the well which function by restricting its flow. Another important aspect here is that the production rates are normally higher at the heel of the well than at the toe. This is because the closer the fluid comes to the heel, the smaller the pressure it will face. One way to eliminate this issue is to simply make more perforations in the production tubing near the toe and decreasing the same near the heel.

Similarly, when using ICD's they usually provide different pressure drops, depending on their distances to the heel. In general they work very well and are very reliable, during the early stages of production. The problem is that, as the reservoir is depleted, the flow rate decreases and flow regimes change, which often comes to cause cones again, sometimes near other parts of the well. Besides that, the best possible production will no longer be reached. There are some devices in the market that can autonomously avoid water or gas inside the tubing, interrupting the flow when necessary. However, they cannot adjust the flow rates according to depletion, nor avoid the formation of cones. Currently, there is one type of Autonomous Inflow Control Device (AICD) called the BECH AICD patented by Prof. Aadnøy of the University of Stavanger who also happens to be the supervisor of this thesis work – that can do that. Experimentally, it would be demonstrated that constant flow throughout the life of an oil field, and along the well, can be achieved by incorporating the mentioned patent into the down hole completion equipment. This can eliminate the cones, thereby making the production more stable and increasing the final/cumulative oil recovery. Other possible uses for this device are also stated at a later stage of this report. The experimental results obtained points to the fact that it can be used also for injection wells or in any well operation where constant flow is needed. They are designed as stand-alone robust devices to withstand the adverse operating conditions of a well.

However, ICDs have mostly been used for light oils. For fluid compositions having low viscosities, the flow is not dependent on viscosity but only on the density of the flowing fluid. Therefore when fluid properties change from light oil to water, the flow rate reduces according to the square root of the density ratio between oil and water as would be demonstrated in Chapter 5 of this report. Highly viscous oils occasionally have a density approaching that of water, often with a negligible density contrast. The transition from turbulent to laminar flow occurs earlier, and viscous pressure drops may become more significant (i.e. the pressure drop seen in the ICD nozzle becomes governed by viscosity which is highly sensitive to changes in temperature and pressure).

In the forgoing thesis report, an experimental setup is proposed where fluids of various viscosities and densities are flow-tested. Correlations would be established to enable accurate definition of the behavior of passive inflow control systems in relation to highly viscous oils or highly viscous oil fields. Seating at the center of this experimental study is the introduction of a BECH company Autonomous Inflow Control Device patented by Prof. Aadnøy of the University of Stavanger. This would serve to illustrate the unique benefits of this patent in that it is able to maintain a constant flow rate through its nozzle irrespective of pressure variation. A detailed presentation of flow regime investigation using the Bernoulli model as a reference point also forms an important aspect of this thesis.

ABBREVIATIONS

AICD	Autonomous Inflow Control Device
BECH	Company which owns the legal rights to Prof. Aadnøy's AICD patent.
BS	Barents Sea
cP	Centi-poise (Unit for viscosity)
ERW	Extended Reach Well
ESP	Electrical Submersible Pump
GOC	Gas Oil Contact
HP	High Pressure (15+ bars). **Defined for the purpose of this thesis only, does not apply to practical calculations in industry.**
ICD	Inflow Control Device. **The word conventional/commercial is used to describe ICD technology currently available in the market.**
IPTC	International Petroleum Technology Conference
L	Denotes volume in cubic meters
LP	Low Pressure (0 bars – 15 bars). **Defined for the purpose of this thesis only, does not apply to practical calculations in industry.**
mL	Mililiters
NCS	Norwegian Continental Shelf
NPV	Net Present Value
OGC	Oil Gas Contact
OHGP	Open Hole Gravel Pack
OHHW	Open Hole Horizontal Well
OTC	Offshore Technology Conference
OWC	Oil Water Contact
PDP	Positive Displacement Pump
PPE	Personal Protective Equipment
R-Phrase	Risk Phrase
RA	Risk Analysis
Sec	Seconds

S-Phrase	Safety Phrase
SAGD	Steam Assisted Gravity Drainage
SAS	Stand Alone Screen
SPE	Society of Petroleum Engineers
t	Denotes time in seconds.
TAML	Technological Advancement for Multi-Laterals.
Three-D	3 Dimensional View.
UiS	University of Stavanger

LIST OF FIGURES

LIST OF TABLES

Content

1 INTRODUCTION

Sub-sea technology has evolved into horizontal wells, as in the Goliath field (OFFSHORE-TECHNOLOGY, 2014), in the Norwegian BS. These horizontal wells are popular for increasing production efficiency. In high costs areas like the BS, it is important to reduce the required number of wells to be drilled, but with the condition that they produce optimally. With larger exposure to the reservoir they also reach larger portions of complex reservoir geometries.

Source: Aadnøy B.S, Awannegbe Edohamen. P, De Azevedo Cabral. R. Autonomous Inflow Control Device for Horizontal Wells in the Barents Sea. SPE work shop in Harstad Norway, 2014.

However along with the oil, large quantities of water and gas can also reach the wellbore. These fluids exist naturally in the reservoir or are injected into it to increase pressure and oil production. The problem is that when they reach the well, they are also produced thereby reducing the hydrocarbon production index. Long horizontal wells are also subject to the formation of the so-called cones of water or gas. This is because these fluids, due to their greater mobility under the high flow and pressure differences common in this kind of well, end up crossing the oil layer and reaching the wellbore before the oil.

1.1 Brief account of the birthing of the ICD era in well completions

The ICDs are basically flow restriction devices (chokes) that avoid water coning in wells irrespective of trajectory type, following the Bernoulli law for low-viscous fluids (AADNØY, 2012, 2012a). They are installed in regular intervals along the horizontal path of a well as an integrated part of the down hole completion equipment. As the pressure is not constant along the well, different setups are used for each inflow point. The flow is complex, ranging from laminar flow in the reservoir, through screens and conduit, to turbulent flow through ICDs. In long horizontal tubing, the well bottom will have a laminar flow, whereas at the production packer it is fully turbulent.

The early development of ICDs was driven by the need to ameliorate early water break-through from the heel of an ERW. This design was originally based upon equalizing flux (i.e. hydrocarbon flow rate per unit length of horizontal well section). During a typical production operation, this was achieved through a mechanism which chokes flux in the heel region where the higher pressure drop is expected due to higher frictional effects. The choking system principally functions based on the proportionality relation that exists between choking level and flow rate. This therefore enables it to automatically produce a more uniform flow profile.

It had always been common practice for an oil well to be drilled with a vertical trajectory profile from seabed to target depth. However, the natural occurrence of the following challenges associated with oil wells/reservoirs has necessitated the use of directional drilling technologies.

a) Need for a sidetrack due to an irrecoverable fish and a subsequent plug and temporary abandonment situation.
b) Need for control of vertical holes (i.e. compensation for bit walk by making adequate tool face re-orientation)
c) Drilling to avoid geological problems.
d) Drilling beneath obscure/inaccessible locations.
e) Off-shore development drilling.

Over the years, the aforementioned technology has come to be widely accepted as a more economically efficient drilling practice. Several well control problems are likely to occur during the drilling, completion and production of the complex well trajectory of an extended reach well. One of such problems as already mentioned is the early breakthrough of gas or water. It should be noted that a problem of this nature can also occur in conventional vertical wells. However, the major difference is that with the ERW, an ICD is needed down hole to control the well whereas the vertical well due to the presence of very small variation in pressure drop, is typically controlled from surface to prevent breakthroughs. The following undeniable benefits, which are mainly linked to project economics, make an ERW desirable in spite of the mentioned disadvantages.

a) Increased penetration of the producing formation.
b) Increased efficiency of Enhanced Oil Recovery (EOR) techniques.
c) Improved productivity in fractured reservoirs by intersecting a number of vertical fractures.
d) Increased drainage area of platform.

However, the problem is that as the reservoir is depleted the flow rate decreases and the flow regimes change. These often cause cones again maybe near other parts of the well at a later stage of production, following the redistribution of fluids in the reservoir. Another problem is that the conventional ICD chokes too much in depleted stages of the reservoir thereby reducing production to an unacceptable degree. Therefore one of the core purposes of this experimental thesis work is to develop ways to prevent the formation of these cones over time while achieving the goal of optimal production which eliminates intervention/work over downtime.

1.2 Objectives of thesis

a) To experimentally prove that the BECH AICD (Prof. Aadnøys patent) guarantees constant flow rate regardless of reservoir pressure.
b) To investigate the extent to which the constant flow feature of the BECH AICD remains independent on the Darcy model and fluid viscosity.
c) To experimentally prove that the BECH AICD can potentially drain a reservoir nearly 2 times as fast as today's commercial/conventional ICD. This then implies quicker financial turn-around and overall better project economics in terms of NPV of the reserves which would directly impact project capital expenditure (CAPEX) and operational expenditure (OPEX).
d) To reveal the limitations of today's conventional ICD by making a comparison to BECH AICD.
e) To reveal the limitations of the BECH AICD.
f) To investigate the flow regime in the nozzles of ICDs and AICDs using fluids with varying properties.
g) To depict what is obtainable in the arctic reservoir environment of the Norwegian Continental Shelf by careful selection of fluids for experimental work.
h) To investigate the viscosity range within which flow is governed by density both in BECH AICD and conventional ICD.
i) To investigate the viscosity range where viscous effects creates laminar flow both in BECH AICD and conventional ICD.

1.3 Overview of Inflow control problems

Problems associated with the flow of hydrocarbon/reservoir fluids into the well are often exacerbated in down-hole conditions where there is a natural, design-induced or operation-induced occurrence of one or a combination of the following:

Please note that the list below does not in any way represent an exhaustive range of possible inflow problems.

a) Highly viscous fluids.
b) Reservoir lithology which is prone to erosion.
c) Partially open horizontal wells i.e. selective completion design.

d) Soft sand formation which necessitates the use of SAS, OHGP technology or perforated / slotted liner in horizontal wells.
e) Scaling reservoir environment.
f) Complex deep gas reservoir environment.
g) Reservoir featuring thin pay zone with bottom water drive.

Passive Inflow Control Devices (ICDs) as already stated were developed to counteract the horizontal well's hell-toe effect whereas Active Interval Control Valves (ICVs) were used originally for controlled and commingled production from multiple reservoirs.

Figure 1.1 and Table 1.1 which represent the outcome of comprehensive reservoir engineering uncertainty quantification, serve to illustrate an acceptable decision making modality on a "ICDs vs ICVs" compromise based design concept selection. This is largely dependent upon prevailing down-hole conditions and project needs/economics.

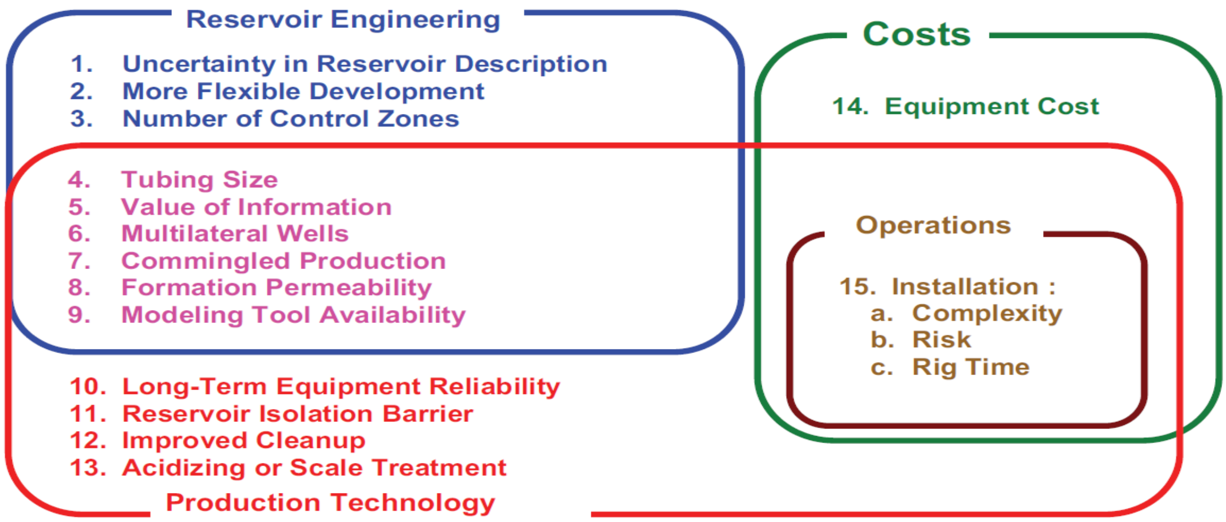

Figure 1.1: A comprehensive approach to the selection between Passive and Active inflow control in completion design. F.T. AL-KHELAIWI, V.M. BIRCHENKO, M.R. KONOPCZYNSKI, and D.R. DAVIES 2010. SPE.org.

TABLE 1—CONVENTIONAL CASED-HOLE, ICD, AND ICV COMPLETIONS COMPARED*			
Aspect		ICD vs. Cased Hole	ICD vs. ICV
Uncertainty in reservoir description		D	V
More flexible development		D	V
Number of controllable zones		D	D
Inner flow conduit diameter		=	D
Value of information		=	V
Multilateral wells	Control of lateral	=	V
	Control within lateral	D	D
Multiple reservoir management		D	V
Formation permeability	High	D	D
	Medium-to-low	D	V
Modeling tool availability		C	V
Long-term equipment reliability		C	D
Reservoir isolation barrier		=	V
Improved well cleanup		D	V
Acidizing/scale treatment		D	V
Equipment cost		D	D
Installation (risk, cost and complexity)		D	D
Gas production	Gas inflow equalization	D	D
	Water control	C	V

* C: cased hole, D: ICD, V: ICV, =: equal performance

Table 1.1: A comprehensive approach to the selection between Passive and Active inflow control in completion design. F.T. AL-KHELAIWI, V.M. BIRCHENKO, M.R. KONOPCZYNSKI, and D.R. DAVIES 2010. SPE.org.

To reduce/eliminate inflow control problems, several suppliers of ICDs/ICVs technologies some of which are delineated in Chapter 3 have developed unique designs for creation of the required pressure drop to delay/prevent water coning. These designs currently include nozzles, orifices, tubes and helical and labyrinthine channels. However, the size of the restrictions is set before or at the time of well completion. This makes it impossible to make a later adjustment of the flow restriction diameter without an intervention/work over operation.

The BECH AICD which will be experimented and discussed in the forgoing thesis work totally eliminates the need for a time consuming and cost-ineffective intervention work at a later stage of reservoir production. This is achieved by Prof. Aadnøy's design which features a valve stem that is hydraulically controlled by prevailing reservoir pressure. This design allows for an increased opening of the valve stem at low reservoir pressures and likewise, a corresponding reduction in opening at high reservoir pressure. Hence the flow rate is maintained from start of production to point of complete reservoir drainage.

1.4 Quick quiz which shows advantages and limitations of conventional ICDs

Q: If I use 10 small nozzles instead of one large nozzle what is the difference in behavior?

A: If the sum of the nozzle areas of the small nozzles equals the one large nozzle, they will behave exactly similar.

Q: Will the commercial ICD work well also in a depleted phase of a reservoir?

A: No. The flow inside the long horizontal tubing is complex, and when the flow decreases, the ICDs may no longer be optimal. Water coning may therefore occur at a later stage of depletion.

Q: Will the flow rate change after water breakthrough in the heel of the well?

A: Yes. Again from Bernoulli relation, if the incoming water has 15% higher density than the produced oil, flow rate will decrease by 8%. This may not be a strong effect.

Q: Although the density is often constant in a field, the viscosity may vary significantly during the life of the field. How important is the viscosity?

A: The variations in viscosity are not important. The nozzle alone controls the pressure drop, and because this has a high turbulent flow, variations in viscosity have no effect. This is beneficial because we would not have appreciated the opposite.

Q: Some ICD suppliers argue that they are viscosity sensitive because they are also passing the oil through some tubes in addition to the nozzle. This is not correct then?

A: Actually no for the common ICD scenario. Computer simulations have shown that for viscosity to dominate the pressure drop, the tubes must be much longer than a 10-meter SAS section, which is difficult to implement in practice.

Q: If suppliers advertise a combined solution, an ICD consisting of a tube and a nozzle in series, is this not an improvement?

A: Technically speaking it is correct, but usually the nozzle dominates such that variations in viscosity are negligible.

Q: You mean that all usual brands of ICDs actually behave exactly similar?

A*:* Yes, most ICDs are passive choke devices aimed at reducing the flow.

Q: Limiting ourselves to simple mechanical devices, how can we improve the ICD function?

A*:* An ICD can be considered a first generation flow control, with the limitation that it is statically fixed. A second generation would be an autonomous control valve that by sensing the reservoir pressure using hydraulic feedback could maintain constant flow even during reservoir depletion.

Aadnøy and Hareland, 2009; Gimre, 2012.

2 BACKGROUND

2.1 Objectives of Inflow Control Devices

a) To prevent or at least delay gas/water coning.

b) To create a uniform inflow profile across the sand screen.

c) To equilibrate pressure throughout the length of the horizontal well bore (i.e. heel to toe).

d) To obtain higher total hydrocarbon recovery.

2.2 Synoptic view of ICDs

1) Darcy Flow – Inflow from the reservoir is governed by the radial flow equation derived from Darcy's law and it is:

$$Q = \frac{2\pi kh}{\mu} \times \frac{P_{res} - P_{well}}{\ln \frac{r_e}{r_w}} - - - - - - 2.1$$

From equation 2.1 it is clear that the flow rate Q is directly proportional to the drawdown $P_{res} - P_{well}$ and permeability k but inversely proportional to the fluid viscosity µ. r_e and r_w represent the radius of the reservoir and wellbore respectively.

When entering the well the fluid changes direction and regime, passing from laminar to turbulent. This implies that flow is not anymore fully governed by equation 2.1; instead it is being more dependent on its density than viscosity. The insertion of ICD's makes this study even more complex because it also results in changes of flow regime.

Assume a long horizontal well, the figure below shows the coning problem. The consequence of the wellbore pressure drop is a higher flow at the heel of the well, controlled by the following:

a) Viscosity (All Darcy Parameters).
b) Permeability variations.
c) Along hole turbulence
d) Pressure

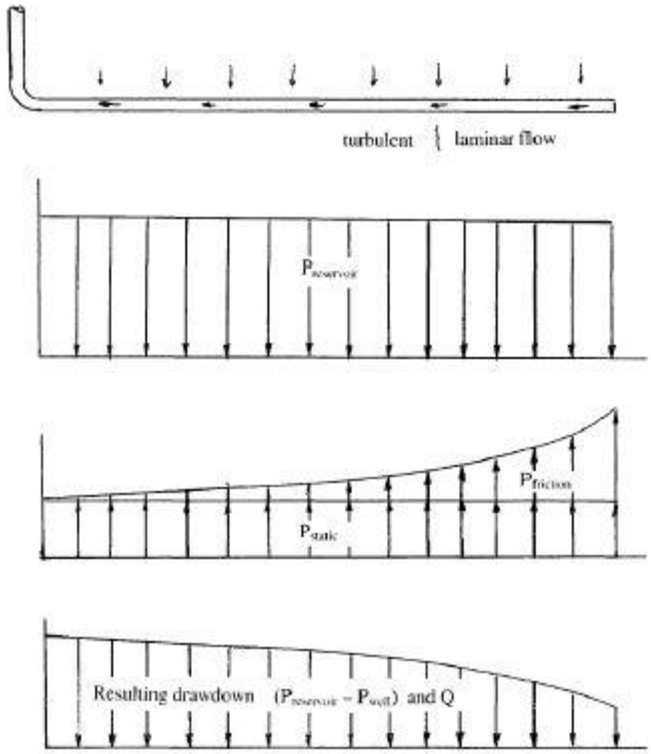

Figure 2.1: Illustration of drawdown profile for Darcy controlled OHHW. Aadnøy and Hareland, 2009; Gimre, 2012. SPE.org.

2) Current Commercial Inflow Control Devices – Flow here is changed by installing chokes at regular intervals. Since the drawdown is not constant along the well, different chokes should be applied. The flow is therefore not totally Darcy but a combination of Darcy and choke.

   During depletion, the pressure changes in particular inside the well that again leads to uneven flow controlled by:

   a) Along hole turbulence
   b) Permeability variations
   c) Density
   d) Pressure.

   The diagram below illustrates this concept.

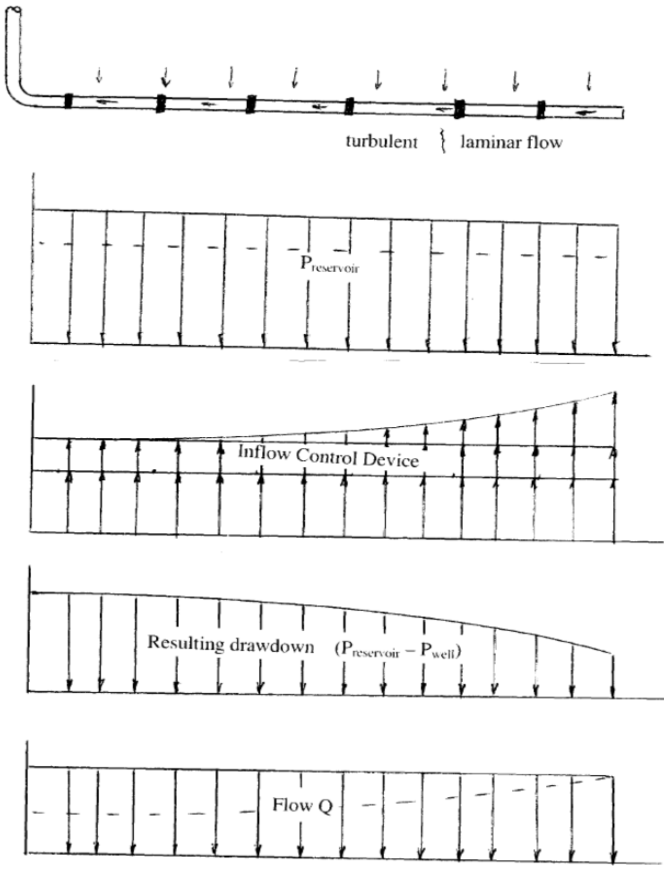

Figure 2.2: 2012 Illustration of drawdown profile in partial Darcy controlled/partially choked OHHW. Aadnøy and Hareland, 2009; Gimre 2012. SPE.org.

3) The BECH constant flow valve.

For illustrative purposes, the reservoir pressure, permeability and the well pressure are varied. The resulting flow rate is still constant. The flow is therefore not dependent on reservoir or wellbore condition. This is weakly controlled by density.

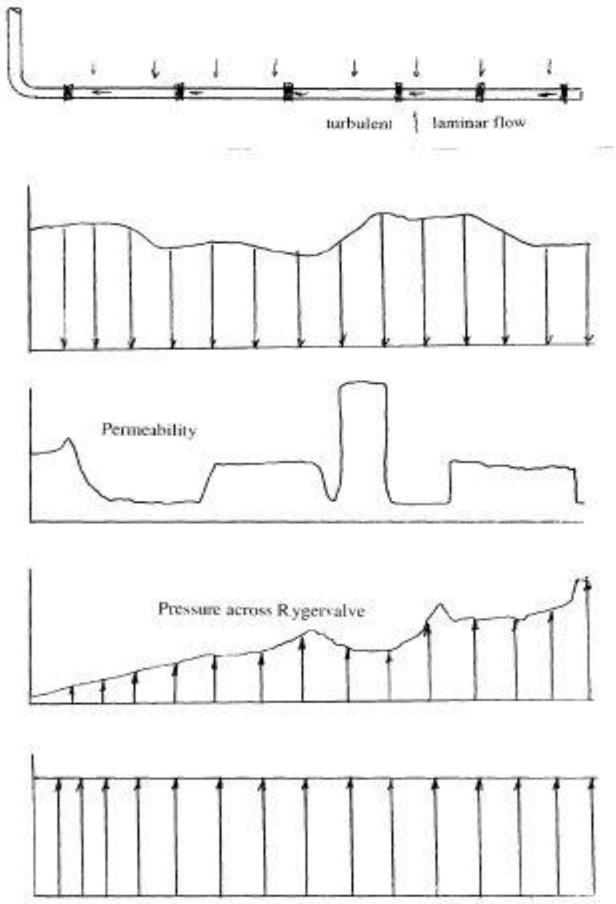

Figure 2.3: Drawdown profile for flow controlled OHHW. Aadnøy and Hareland, 2009; Gimre, 2012. SPE.org.

2.3 Conventional ICD design available in industry

Figure 2.4 below is a Three-D view of an ICD and it shows the areas where pressure drop occurs as the hydrocarbon flows from the reservoir into the production tubing.

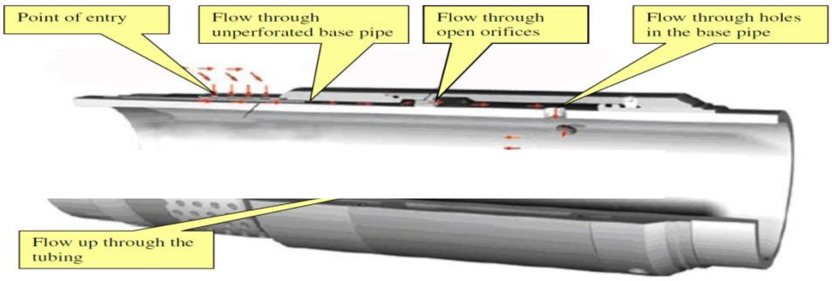

Figure 2.4: Illustration of the flow path that the hydrocarbon follows before flowing through the ICD nozzle. Weatherford FloReg™; Torbergsen, 2010. SPE.org.

In extended reach wells, the use of very long production tubing introduces very large pressure drops with the highest production rates at the heel and the lowest at the toe of the production tubing. The potential for this to cause the occurrence of water/gas coning necessitates the implementation of Inflow Control Devices to realize the objectives listed in Section 2.1.

The breakthrough of water/gas at the heel would significantly reduce the hydrocarbon Production Index of the well. This is true because the hydrocarbon at the toe of the wellbore exhibits significantly lower mobility than the breakthrough water/gas at the heel.

The Inflow Control Device therefore achieves its objectives by reducing flow in the regions of high productivity as illustrated in Figure 2.5b. Figure 2.5a is an illustration of the vast disparity in heel to toe pressure drop which is prevalent in an extended reach well completed without an ICD.

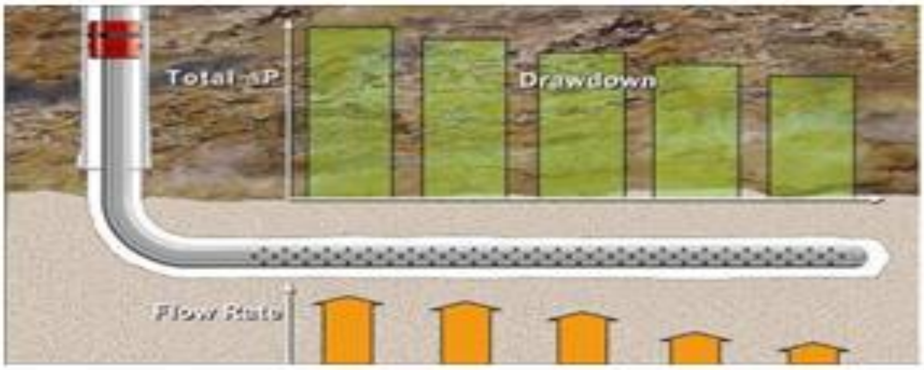

Figure 2.5a: Heel to toe pressure drop profile of well completed **without** ICD. Gimre, 2012. Halliburton.com.

Figure 2.5b: Heel to toe pressure drop profile of well completed **with** ICD. Gimre, 2012. Halliburton.com.

The above picture illustrates the results that can be obtained from utilizing current commercial ICDs. However, the fact that there exists an uneven/non-linear profile throughout the productive life of a typical reservoir is a very important factor/consideration that must be taken into account when designing an ICD. The details of such non-linear profile can be obtained from reservoir characterization studies based on estimated reservoir depletion rates which continually alter pressure profile.

At this junction it is clear that the primary function of current commercial Inflow Control Device put simply, is to optimize production by equalizing reservoir inflow along the length of a horizontal well bore.

2.3.1 Economic justification for ICD inclusion in completion design.

Typical intelligent well business drivers are shown in Figure 2.6. The figure shows that increased total recovery has the highest relative business value.

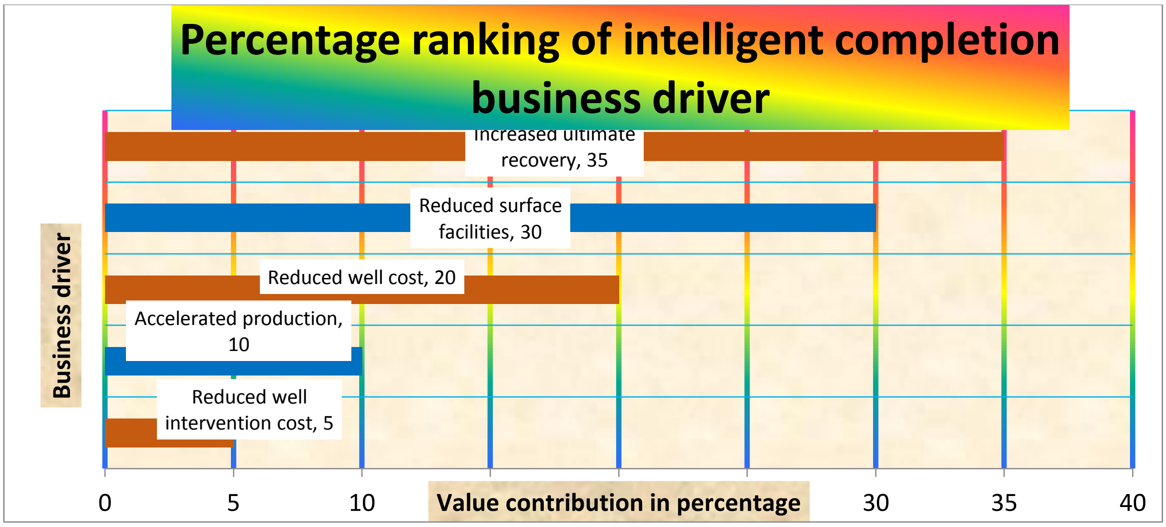

Figure 2.6: Relative business value contribution of a typical intelligent well completion technology as evaluated in the Norwegian oil industry.

Increased ultimate recovery is shown to be the most important factor. If this goal is to be achieved, it would demand a very long term horizon. More often than not, the industry looks at accelerated production as the most important driver for ICD inclusion in completion design. This owes to the fact that the industry is more interested in creating best possible value now (i.e. NPV), and draining the reservoir in the most cost effective way. Evaluations need to be done constantly by the key players in the industry on how best to optimize production.

In performing an economical evaluation for project, ICD inclusion in completion design would normally be less expensive than including an ICV. However, the issue of cost comes in as one of the several criterions when faced with the decision of which completion technology should be implemented. This therefore implies that an overall sensitivity and characterization study of the reservoir must be performed, well communicated and deeply understood before making a completion choice.

Source: Jeanette Gimre, Master Thesis 2012. Efficiency of ICV/ICD systems.

2.4 Description and Illustration of water/gas coning phenomena

Generally, in the reservoir rocks, the effect of gravity causes the water to remain below the oil, and the oil below the gas, based on their differences in density. However, the water and the gas usually have greater mobility. Therefore, when subjected to large pressure differences, caused by a producing well, these fluids can move more quickly than the oil, reaching the well first.

Water and gas coning is formed exactly when this situation occurs. These “cones” are preferential paths of the fluids into the wellbore. This causes increased water/oil ratio (WOR) or gas/oil ratio (GOR) inside the well, with consequent loss of oil production. Both oil and gas-producing wells, vertical or horizontal, can potentially present the formation of cones. Although the properties of fluids may accentuate it, the differential pressure between the reservoir and the well is what causes this phenomenon. In lower permeability reservoirs, such as those observed in the Brazilian pre-salt layer, it is necessary to establish a large pressure differential to achieve the desired production level, thereby increasing the risk of cones formation. Another factor that may increase this risk is the existence of a large number of fractures in the reservoir, which is also often the case in a pre-salt lithology. The water and the gas flow more easily through these fractures, due to their high conductivity.

In vertical production wells, the pressure gradient is much higher in the immediate vicinity of the well than in the rest of the reservoir. In the case of horizontal wells, this gradient is practically uniform in the reservoir, increasing only slightly near the well. Due to their higher productivity, the horizontal wells can be produced with lower pressure gradients, which generally minimize or retard the formation of cones.

The vertical wells may be re-completed at higher portions of the reservoir, when hit by water, or lower portions, when affected by gas from the top of the reservoir. Horizontal wells, on the other hand, generally will be hopelessly lost when invaded by these cones, for not having portions above or below to be re-completed. Thus, these wells are designed to operate with flow rates low enough to prevent the coning formation. However, many times this flow reduction is not a practical alternative, as it reduces their productivity and, in particular, the oil recovery. Many authors have presented several correlations for the estimation of critical flow of oil in the presence of water and gas in horizontal wells. The critical flow is defined as the maximum possible flow in the well without producing unwanted fluids by the formation of cones.

Figure 2.7a below presents a Two-D view of a water coning mechanism. This picture is based on the assumption that the OWC is perfectly parallel to the production tubing as shown. The effect of this assumption would be seen in calculations later-on in this chapter.

Due to the much greater mobility of gas than that of the oil, at high flow rates and high pressure differences, the recovery of oil from a field is significantly reduced. This effect is called water or gas coning. To avoid it, Inflow Control Devices are installed as an integrated part of the completion equipment as already stated in the introduction of this report.

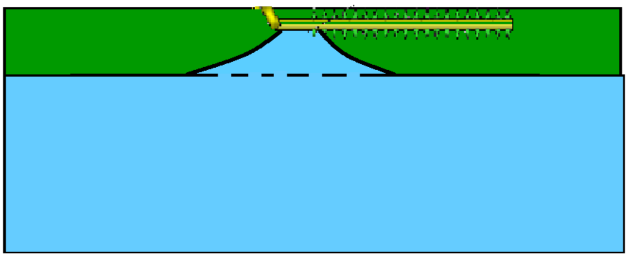

Figure 2.7a: Water coning effect observed in an extended reach well. Inikori 2002. Schlumberger glossary.

Figure 2.7b is a Three-D view showing the OWC and OGC. The change in the OWC and OGC profile is largely as a result of varying draw-down pressures during production. For the purpose of this thesis work, the term draw-down is used to infer the difference between the reservoir pressure and the bottom hole pressure of the well.

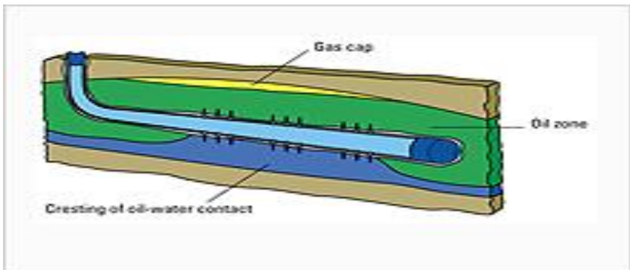

Figure 2.7b: Water and gas coning effect observed in an extended reach well. Inikori 2002. Schlumberger glossary.

2.5 Flow regime investigation through constrictions of ICDs/AICDs

Inflow control devices as already mentioned are developed to prevent water/gas coning in long horizontal wells and they have been used with great success in the last 15 years. Pressure drop is a major issue and this occurs in the following regions of the completion tool, before hydrocarbons actually flow up the production tubing.

a) In the reservoir
b) Through the screen
c) Through the flow conduit
d) Through the ICD nozzle
e) Finally in the production tubing
f) Pressure drop in the lower completion which consists of:
    i) Wash pipe
    ii) Screen packer
    iii) Cross-over valve

Real-field-data-based evaluation of existing models associated with current commercial ICDs shows clearly that the pressure drop through the ICDs is dominated by turbulence and it is established from fluid mechanics that turbulent flow is principally controlled by the density of the fluid or fluid mixture. This can be evaluated as an advantageous feature since density does not vary nearly as much as viscosity during the productive life of a typical NCS reservoir.

Once again, it becomes necessary to develop an ICD that is independent of reservoir depletion and variation in reservoir pressure profile. In other words, an ICD that allows constant flow rate regardless of reservoir pressure at a given time. This ICD should be sufficiently robust in design such that it also allows very minimal changes in flow rate even with vastly changing viscosity of produced hydrocarbon. This can be achieved through a feedback system that is controlled hydraulically, mechanically, electrically or otherwise. For the purpose of this thesis, the hydraulics of an Autonomous Inflow Control Device is investigated. This serves to optimize the coning prevention feature of an ICD no matter what phase of production the reservoir is placed (i.e. ability to prevent water/gas coning both during linear and non-linear production phase of reservoir).

2.5.1 Inflow control problems associated with extended reach wells.

There exists very high pressure drop in production tubing used in an extended reach well. Basically, the toe of the well accounts for the lowest pressure drop and the heel accounts for the highest. Upon this premise, the reservoir section close to the heel will produce more liquid hydrocarbons since the flow rate is proportional to pressure drop as would be established mathematically later. This will then result in the coning of either the water-oil contact from below the tubing or the gas-oil contact from above the production tubing. It is seen once again that this coning will definitely occur first at the heel at a distant time period before it gets the chance to occur at the toe of the well. The inevitable consequences of the above explained scenario includes but are not limited to the following.

a) Coning of water/gas which would subsequently accelerate leading to a drastic reduction in oil production from the heel.
b) Greater challenge for the oil in the toe section of the well to overcome pressure drop in the heel due to its significantly less mobility in comparison to the breakthrough fluid.
c) More problems associated with the disposal of water in terms of time and cost.
d) Borehole cleaning in this case is generally more challenging and time consuming.

As a consequence of the second pit fall stated above in line item b), most of the oil near the toe of the production tubing can only be produced by drilling new wells for its drainage thereby ramping up project capital and operational expenditure.

Figure 2.8a is a Two-D representation of a coning mechanism in an extended reach well completed without an ICD. Figure 2.8b shows a Two-D view of the near-parallelism between the OGC above the production tubing and the OWC below. This near-parallelism in practice is only achievable in a well completed with a SAS having an integrated ICD technology, and it forms the basis for flow regime investigation as seen later-on in this chapter.

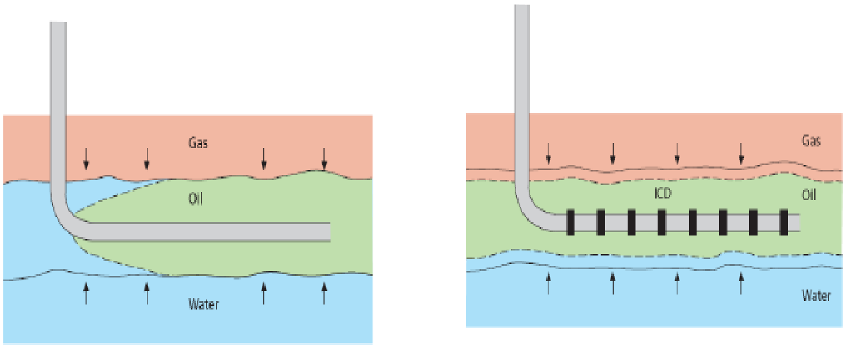

Figure 2.8a and b: OWC and OGC phenomena in extended reach wells in wells with and without ICD in completion design respectively. Aadnøy and Hareland, 2009; Gimre, 2012. SPE.org.

In order to equilibrate drawdown pressure throughout the length of the horizontal tubing, ICDs are installed at every connection in the production tubing. These ICDs apply restrictions by a calculated percentage, thereby reducing or controlling coning. However, they are limited in that they fail to perform during the depletion phase of the reservoir implying that coning could still occur at a later phase.

In the following analysis, we seek to establish turbulence through the ICD nozzle under the assumption that the water-oil and gas-oil contact is perfectly parallel to the production tubing.

2.5.2 Hydraulic model for ICDs

Figure 2.9 shown below is a Three-D representation of the integration of the BECH AICD nozzles into the body of the completion equipment.

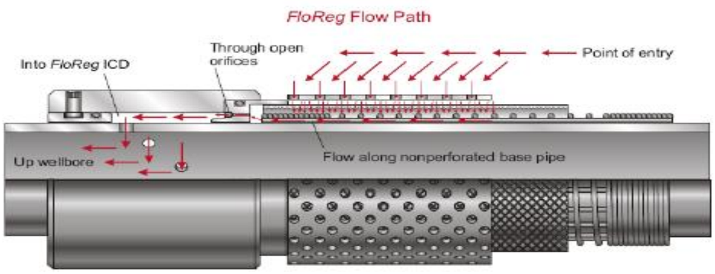

Figure 2.9: A typical ICD geometry showing orifices and integration of ICD into the sand screen. Aadnøy and Hareland, 2009; Gimre, 2012. SPE.org.

Figure 2.9 shows how an ICD nozzle is integrated into the body of a typical pre-packed sand screen. Oil from the reservoir through an entry point, enters the outside of the screen assembly. It flows through the screens into a pathway on the base pipe from where it enters a chamber before going through several orifices. It then flows through a number of large holes inside the casing. It is important to note that the orifices are actually the ICD which control the flow.

The hydraulic model here represents the pressure drop from the reservoir through the ICD and into the base pipe of the screen. The pressure losses before the hydrocarbon flows up the production tubing can be seen in sections as follows.

a) The outer screen
b) Conduit below outer screen
c) The chamber
d) The orifices
e) Holes through the casing.

Analysis of the geometry of the screen does reveal that 11% of the outside surface is the actual flow area. The area is therefore calculated to be 12320 mm^2 for one meter length of screen.

Inflow velocity when calculated in terms of flow rate is given as:

a) THE OUSIDE SCREEN.

$$v\left(\frac{m}{s}\right) = \frac{q}{A} = \frac{Q\left(\frac{m^3}{\sec}\right)}{12320 * 10^{-6}m^2} = 81.17Q - - - - - 2.2$$

If we model pressure drop as laminar flow between 2 plates as defined by Bourgoyne et.al (1986) the following is true.

$$Q = \frac{wh^3}{12\mu} \times \frac{\Delta P}{L} - - - - - 2.3$$

$$\Delta P(bar) = \frac{12\mu QL}{Ah^2} = 15.58 \times 10^4 \mu Q - - - - - 2.4$$

Where $h = 0.25 \times 10^{-3} m$

Assuming a typical North Sea oil viscosity of 0.5 Poise, the above equation becomes:

$$\Delta P(bar) = 799Q(m^3/\text{sec}) - - - - - 2.5$$

b) CONDUIT BELOW THE SCREEN

Hydraulic radius is given by:

$$R_H(mm) = \frac{Area}{Wetted\ Perimeter} = \frac{9.7 \times 5.1}{2(9.7 + 5.1)} = 1.67mm - - - - 2.6$$

The hydraulic diameter is four times the hydraulic radius of 6.69mm. Laminar pressure drop for a circular pipe is given by:

$$\Delta P(bar) = \frac{32\mu v}{d^2} \times L = 203000\mu Q - - - - -\ 2.7$$

Assuming that $\mu = 0.5\ cp$

$$\Delta P(bar) = 11.5Q\left(\frac{m^3}{sec}\right) - - - - - 2.8$$

c) THE CHAMBER

Because the chamber is relatively large, the velocity is small and thus the pressure drop is negligible.

d) THE NOZZLES

We start by assuming fully turbulent flow through the nozzles and using the pressure drop across a nozzle from Bourgoyne et.al.

$$\Delta P(Pa) = \frac{1}{2}\rho v^2 = \frac{\rho Q^2}{2A^2} - - - - - 2.9$$

Nozzle radius for each nozzle is 1.59 mm. The density of the oil is assumed to be 0.75 specific gravity. The pressure drop is then given by:

$$\Delta P(bar) = 5.98 \times 10^7 Q^2 - - - - - 2.10$$

e) THE PRODUCTION TUBING

The pressure drop upstream from the nozzle is considered negligible.

Total pressure drop

$$\text{Total pressure drop} = 779\frac{Q}{L} + 11.5Q + 5.98 \times 10^7 \frac{Q^2}{n} - - - - - 2.11$$

Typical values for the parameters in the North Sea are as follows:

Flow rate, $Q = 3.2 \times 10^{-4} m^3/sec$

Length of screen, $L = 10\ m$

This would yield:

$$\Delta P(bar) = 0.0098 + 3.69 \times 10^{-3} + \frac{6.12}{n} - - - - - 2.12$$

This illustration is based on a worst case scenario where all 10 nozzles are open which yields a total pressure drop of 6.12bar at the nozzles.

Pressure drop distribution

5m Screen → 0.16 % having a flow area of 61600 mm^2

Conduit → 0.06 % having a flow area of 2177 mm^2

10 nozzles → 99.76 % having a flow area of 20 mm^2

Source: Aadnøy and Hareland, 2009; Gimre, 2012. SPE.org.

Analysis shows that the nozzles are the main controlling point for pressure drops. Since its flow area is only 0.03% of the screen area and only 0.9% of the conduit area.

From the above results, turbulent flow is confirmed on commercial ICDs which is not sensitive to variations in viscosity but controlled by density.

Flow regime evaluation

The regime of flow is investigated further by using a laminar to turbulent transitional Reynolds number of 2320, where in a laminar flow the pressure drop depends on the viscosity of the fluid.

For Reynolds number higher than 2320, the flow regime is considered turbulent and pressure drop is therefore dependent on the fluid density.

$$Re = \frac{vd}{V} \leq 2320 - - - - - 2.13$$

Where $V = Average\ flow\ velocity$

$$d = Pipe\ diameter$$

$$v = Kinematic\ viscosity$$

$$v = \frac{\mu}{\rho} - - - - - 2.14$$

Where $\mu = Fluid\ viscosity$

$$\rho = Fluid\ density$$

Therefore, the transitional velocity between laminar and turbulent flow regime is expressed as:

$$v\left(\frac{m}{sec}\right) = \frac{2320 \times v(m^2/sec)}{d(m)} = \frac{2320 \times \mu(Pa.s)}{\rho\left(\frac{kg}{m^3}\right) \times d(m)} - - - - - - 2.15$$

Assuming an average reservoir temperature between 50 and 100 degrees, water dynamic viscosity is $5 \times 10^{-4} Pas$ and for light oil $0.5 \times 10^{-4} Pas$.

Inserting these values into the above equation yields the following critical velocities.

For water:

$$V\left(\frac{m}{sec}\right) = \frac{1.16 \times 10^{-3}}{d(m)} - - - - - - 2.16$$

For oil:

$$V\left(\frac{m}{sec}\right) = \frac{1.16 \times 10^{-4}}{d(m)} - - - - - - 2.17$$

The critical flow rates results obtained from the velocity expression given in equation 2.17 is summarized in Table 2.1.

Path	Fluid	Diameter (m)	Critical velocity (m/sec)	Critical Flow rate (l/hr.)
Screen	-	-	-	-
Conduit	Water	0.00669	0.17	26.4
Conduit	Light Oil	0.00669	1.74	2.64
Nozzles	Water	0.0032	0.36	0.3
Nozzles	Light Oil	0.0032	3.63	0.03

Table 2.1: Summary of the critical flow rates for the different sections of the integrated sand screen and ICD design. Aadnøy and Hareland, 2009; Gimre, 2012. SPE.org.

The flow regimes in the various parts of the ICD is calculated by determining the transitional velocity for oil and water and then multiplying by the total flow area to obtain the critical flow rates. For a typical North Sea flow rate of 18.9 l/min, only the nozzles yield turbulent flow, the other parts of the ICD are evaluated to be at laminar flow. **Hence the initial assumption of turbulence (i.e. density governed flow) is authentic.**

2.5.3 Evaluation of possibility of designing an ICD tool with viscosity controlled flow at nozzle

This in concept is achievable with the use of a very long pipe which obviously has very large frictional pressure drop that ultimately brings the flow velocity within the laminar domain.

In this case, pressure drop in a circular pipe is modelled as

$$\Delta P = \frac{32\mu v \times L}{d^2} ----- 2.18$$

Once again, the transitional Reynolds number is give as:

$$Re = \frac{Vd}{v} = \frac{\rho v d}{\mu} \leq 2320 ----- 2.19$$

From equation 1

$$L(m) = \frac{Pd^2}{32\mu V} ----- 2.20$$

Critical transitional speed between laminar and turbulent flow is

$$V = \frac{2320 \times \mu}{\rho d} ----- 2.21$$

Table 2.2 shows the pipe length required to achieve certain critical velocities in order to stay within laminar flow regime. Equation 2.20 above is used for the pipe length calculation.

Field	Oil density (kg/m^3)	Oil viscosity (cP)	Dynamic viscosity (Pas)	Critical velocity (m/sec)	Pipe length (m)
Balder	914	3.0	300×10^{-5}	2.38	28
Draugen	824	0.68	68×10^{-5}	0.60	480
Gulfaks	838	0.40	40×10^{-5}	0.35	1400
Gyda	822	0.28	28×10^{-5}	0.25	2800
Heidrun	922	2.29	229×10^{-5}	1.80	48
Heidrun	882	0.75	75×10^{-5}	0.62	422
Oseberg	850	0.43	43×10^{-5}	0.37	1232
Smorbukk	832	0.14	14×10^{-5}	0.12	11667
Snorre	690	0.42	42×10^{-5}	0.44	1061
Frigg	835	4.83	483×10^{-5}	4.19	10
Troll	900	1.60	160×10^{-5}	1.29	95
Ekofisk	838	0.13	13×10^{-5}	0.11	13706
Eldfisk	842	0.10	10×10^{-5}	0.09	21778

Table 2.2: Summary of the critical flow rates in application to development fields in the NCS. Aadnøy and Hareland, 2009; Gimre, 2012. SPE.org.

Results shown in Table 2.2 show that if 1/8" tubes are wrapped around the base pipe, they must be very long. More so, if 10 orifices should be replaced by long tubes, the tubes must be wrapped in parallel around the base pipe. This is deemed impracticable in the oil fields obtainable in the Norwegian Continental Shelf.

Hence above analysis points to the fact that today's commercial ICDs are controlled by turbulent flow regime and are not sensitive to viscosity. In other words, todays commercial ICDs are not sensitive to variations in fluid viscosity, an oil property that is experientially proven to vary a lot as the reservoir depletes. This is evaluated to be a desirable feature since there is comparatively insignificant variation in reservoir fluid density.

2.6 Limitations of today's commercial ICDs and features of BECH valve

a) They cannot maintain constant flow through the depletion of the field for the following reasons.
   i. Flow through ICD depends on pressure drop (i.e. the higher the pressure drop, the higher the flow through the nozzle of the ICD)
   ii. Pressure drop is proportional to density and the squared flow rate, both of which changes as depletion of reservoir progresses.

Figure 2.10 below shows the non-linear relationship between flow rate and pressure drop.

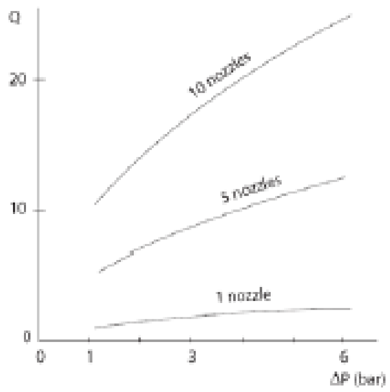

Figure 2.10: Presentation of flow rate vs pressure drop relationship with the closure of 1, 5 and 10 nozzles. Weatherford FloReg^{TM}; Torbergsen, 2010. SPE.org.

Figure 2.11 below shows the operation of a BECH AICD which utilizes a hydraulic feedback principle to achieve constant flow rate at all pressures. This technology presents the benefit of moving the oil-gas and oil-water contacts parallel to the well. Accurate knowledge of the initial distance between the fluid contacts and the well trajectory will guarantee maximum recovery.

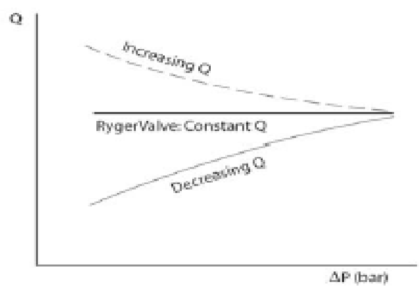

Figure 2.11: Performance characteristics of the BECH autonomous flow control valve. The horizontal axis is the pressure drop from the reservoir to the production tubing. Aadnøy and Hareland, 2009; Gimre, 2012. SPE.org.

The new valve can be calibrated both for constant flow, increasing flow and decreasing flow as shown in the figure above. This therefore implies that for complex reservoirs an optimal design can always be found. The new ICD can actually be used as a designer ICD for advanced reservoir depletion design.

In summary, the following can be said with a great degree of certainty about ICDs

a) The outer screen is always in laminar flow.
b) Nozzles are always in turbulent flow
c) More than 99% of the total pressure drop occurs at the nozzle.
d) Pressure drop through the ICD tool is therefore controlled by density of the produced fluid.
e) Fluid viscosity has negligible effect on pressure drop.
f) Hypothetical analysis reveals that in order to design a tool where pressure drop is controlled by viscosity, the tubes replacing the nozzles must be significantly longer than the screen on which the ICD is installed.
g) Based on data and dimensions used in the North Sea today, it is unrealistic to build a viscosity controlled tool.
h) With the Ryger valve tool, the reservoir engineer can control the flow through the depletion resulting in optimal recovery.

2.7 Inflow control devices from a near wellbore perspective

One of the challenges in long horizontal completion is the accrued formation damage and well clean up. Another challenge is the heel-toe effect caused by flow friction in the pipe, which leads to gas or water coning in the heel and limited drainage from the toe. This ultimately leads to an overall reduction in production index of hydrocarbon.

Implementation of Inflow Control Devices provides a controlled pressure drop which is a function of flow rate. It restricts high producing zones and stimulates low producing zones which in effect yield the following benefits.

a) Improved well clean-up, minimizing the effects of formation damage caused by drilling.
b) Equalizing the flux along the well path, thereby giving reduced possibility for water/gas coning.
c) Reduced annular flow which reduces the risk of sand production behind the screen and subsequent plugging or erosion.

Traditionally, completion is done by running a liner which is cemented and perforated in a cased hole completion strategy. In the case of long horizontal wellbores, this operation becomes complicated and expensive. Hence the development of pre-packed sand screen which gives the advantage of preventing sand production from unconsolidated sandstone reservoir. However, there still exist challenges with the usage of this technology. In order to limit inflow variation due to frictional pressure drop along the liner, a technology named variable perforation density was developed. There however exists some unpredictability both in the penetration and in the local reservoir conditions around the penetration. Inflow control devices integrated in the base pipe of the pre-packed screen helps overcome these uncertainties as experiments and experience shows. The implementation of the ICD does not only optimize performance but also helps in the efficient removal/transportation of drill fluids, solids and mud-cake from a long horizontal well. Hence in the foregoing literature, we seek to establish a relationship between completion design, hole clean-up and resulting inflow performance.

2.7.1 Typical commercial ICD design

The working principle with current Inflow Control Devices is based upon choke restriction. On the upstream side, the choke unit connected to a sand screen made by wrapping wire is wrapped around and tack welded to a set of axial rods which circumferences the base pipe as shown below in Figure 2.12.

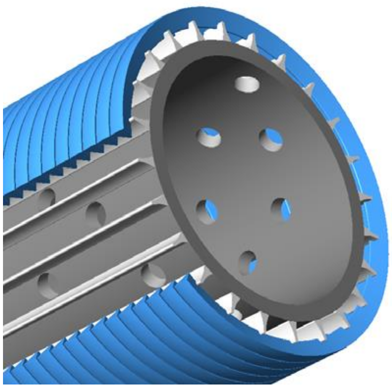

Figure 2.12: Sample of a wire wrapped screen. A triangular shaped wire makes precise slot opening. By using tall axial ribs, the flow cross section area is large, thus reducing the pressure drop to a minimum. T. Moen, H. Asheim 2008. SPE.org.

The screen design is based on the fluid flow through a filtering media and into a drainage layer. The drainage layer allows the fluid to flow from the filter media into the perforations in the base pipe or into the ICD housing which is normally located at the end of the screen jacket as shown below in Figure 2.13.

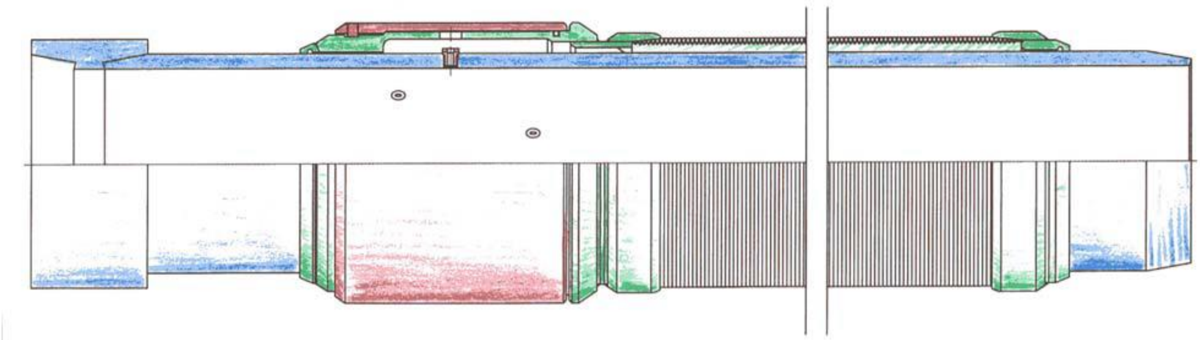

Figure 2.13: A nozzle based ICD screen. The fluid flows in through the wrapping of the screen section, along the axial ribs of the drainage layer, into the housing and through the nozzles. T. Moen, H. Asheim 2008. SPE.org.

A nozzle based ICD screen is show in Figure 2.9. The fluid flows in through the wrapping of the screen section, along the axial ribs of the drainage layer, into the housing and through the nozzles.
In this design, the nozzles are the only flow constrictions in the system. Analyzing the non-Newtonian properties of the drilling fluid, the required differential pressure to ensure backflow of the drill fluid through the screen is given as:

$$\Delta P = \frac{\tau_b \times c \times L}{A} ------ 2.22$$

Where:

$$\tau_b = Shear\ strength\ of\ the\ bingham\ fluid$$

$$c = Circumference\ of\ the\ flow\ channel$$

$$L = Length\ of\ the\ flow\ channel$$

$$A = Cross\ sectional\ area\ of\ flow\ channel$$

From Equation 2.22, it is clear that geometry plays a key role in the determination of pressure drop. To buttress this fact, a nozzle based ICD design is compared with a tube design used as a flow constriction design. To obtain same pressure drop through both constriction designs, analysis show that the tube diameter should be approximately 50% bigger than that of the nozzle while its length should be 100 times longer.

From the given equation, the required pressure to initiate flow becomes at least 67 times higher for the tube according to the following calculation.

$$\left\{\frac{\tau_b \times 100L \times \pi \times (D + 0.5D)}{\pi/4 \times (D + 0.5D)^2}\right\} : \left\{\frac{\tau_b \times L \times \pi \times D}{\pi/4 \times D^2}\right\} - - - - - 2.23$$

$$= \left\{\frac{266 \times L \times \tau_b}{D}\right\} : \left\{\frac{4 \times \tau_b \times L}{D}\right\} - - - - - 2.24$$

= 67:1

2.7.2 Heel-to-toe effect and ICD efficiency in well bore cleaning

The heel to toe effect is a result of the frictional pressure drop causing a variable draw-down along the well. In the heel of the well, the fluid encounters less resistance when compared to the toe because this fraction is also exposed to friction pressure drop along the length of the completion interval.

To calculate this, a well is separated into 10 zones where each zone is assumed to be at radial Darcy flow. Effects of relative permeability or variations between vertical and horizontal permeability are considered. A filter cake pressure drop is included, where flow rate from this zone is assumed to be zero. This then results in higher flow rates through the other zones.

ICDs based on nozzles are also included in the model. This gives pressure drop proportional to the fluid density and the square velocity. The fluid flows into the base pipe and the pressure drop is based on the accumulated flow rate from each zone. This is done to capture the heel-toe effect. When the drawdown pressure is applied, it is assumed that the filter cake is lifted off in the heel end of the well. This leads to a flow and pressure drop across formation nozzles and through the tubing. This process continues gradually toward the toe until the drawdown pressure becomes too small to lift off the filter cake.

When a nozzle based ICD completion is used, the tubing pressure becomes lower due to pressure drop through the ICD. Since the pressure drop is a function of flow rate squared, it therefore follows that zones with no flow will have zero pressure drop through the nozzles. Because of this, the applied differential pressure across the filter cake increases.

A set of simulation was performed based on data and performance of a North Sea well completed with ICD screens. The well was reported to perform much better than similar wells completed with screen only. It was also observed that there is an uneven flux in the wells with screen completions, more so the toe parts of these wells do not contribute at all to production.

In the figure below, the violet line indicates filter cake pressure below the formation pressure. As long as the tubing pressure is below this line, the clean-up process continues to the next zone. Hence the smallest flow rate that still allows for the removal of the filter cake is calculated as $1575\,\frac{m^3}{d}$ before the last zone kicks in and increases the flow rate to $1685\,\frac{m^3}{d}$.

Shown in Figures 2.14 and 2.15 are detailed component pressures obtained during the process of hole cleaning. Figure 2.14 illustrates the more efficient hole clean-up achievable when an ICD is included in the completion tool as compared to Figure 2.15 where a standard sand screen completion is used without the inclusion of an ICD.

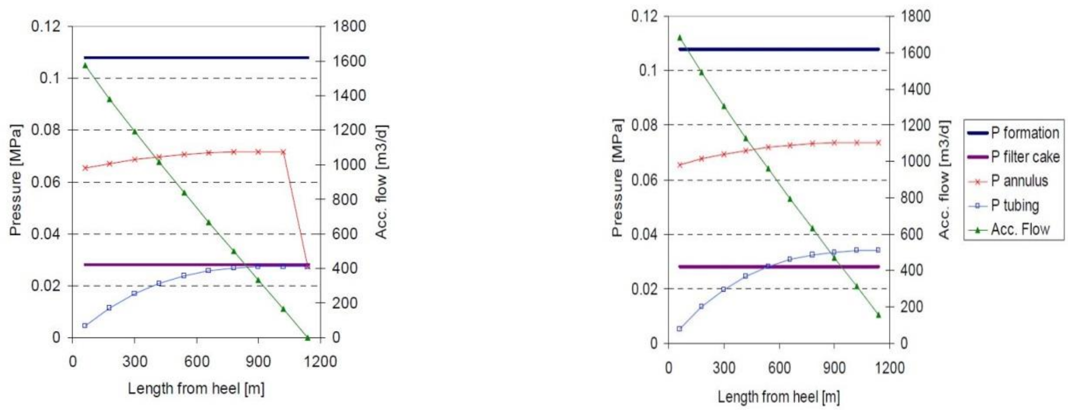

Figure 2.14a and b: Pressure profile and accumulated flow rate required for clean-up of an ICD completion. The tubing pressure is still below critical pressure before the last section has been cleaned up (left). Finally the tubing pressure exceeds the critical filter cake threshold pressure indicating that the clean-up process stops. T. Moen, H. Asheim 2008. SPE.org.

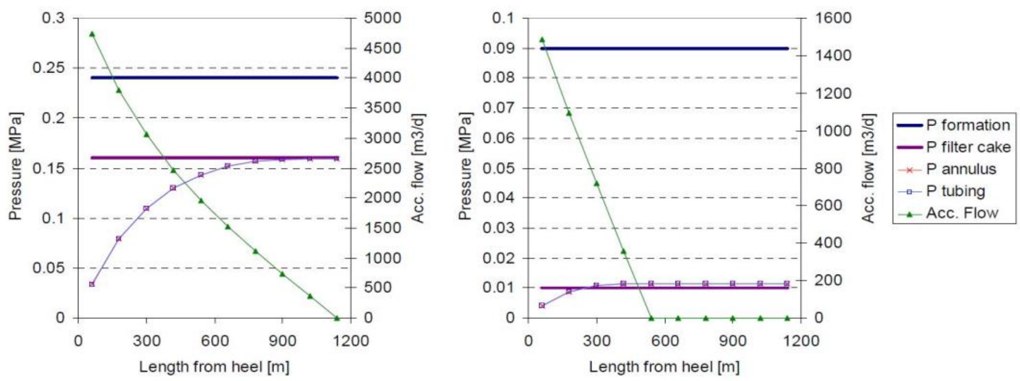

Figure 2.15a and b: Standard screen completion with pressure profile and flow rate required to clean up the whole interval (left). Here well is completed **without** ICD. T. Moen, H. Asheim 2008. SPE.org.

As seen in Figures 2.15 a) and b) above, the same calculation is done with a standard screen completion. It should be noted that the tubing and annular pressures are equal as the screen itself does not provide any significant pressure drop. The critical flow rate to clean up the whole well before the last zone starts is $4740\,\frac{\mathrm{m}^3}{\mathrm{d}}$. With the last zone included, the required flow rate is $4800\,\frac{\mathrm{m}^3}{\mathrm{d}}$. The drawdown in this case is smaller because the screen has capacity to produce all that comes from the first zones. In this case, no production is expected from the toe part, implying that significant reserves are left unproduced.

The facts presented above are indicative of how the added pressure drop across the flowing nozzles reduces the tubing pressure and consequently stimulates well clean-up. In the screen only well, a much higher flow rate must be used to achieve the same clean-up. In the non-stimulated case the flow is nearly 3 times higher than for the stimulated case. It could be a challenge to achieve this required high flow rate due to limitations in inflow capacity and drawdown pressure. This therefore implies that the risk of improper well clean-up is high when running a screen-only completion in a long horizontal well. It is therefore true that the integrated ICD and screen design has a significant impact on hole cleaning performance of the drilling fluid design. The risk associated with the backflow of the drill fluid is highly dependent on design details of the ICD screen.

A simplified calculation as shown already indicates that 67 times higher differential pressure is required to get a Bingham fluid to start flowing through a tube type ICD than a nozzle type ICD. The use of ICD technology is significantly changing the clean-up performance of wells by using a proper nozzle setting. This allows for the stimulation of the sections which are difficult to clean up. This stimulation serves as an added pressure drop to these sections until they contribute to production with a proper flow rate.

3 MODELS IN CONTEMPORARY OIL INDUSTRY

3.1 Norsk Hydro – Now Statoil

This ICD patent which functions by restriction to reduce flow rate was obtained in the year 1993. It features a variable flow area which enables a more uniform inflow and enhanced phase filtering. The phase filtering is designed such that the unwanted phase is choked and the flow of oil is facilitated. This concept is shown in Figure 3.1a.

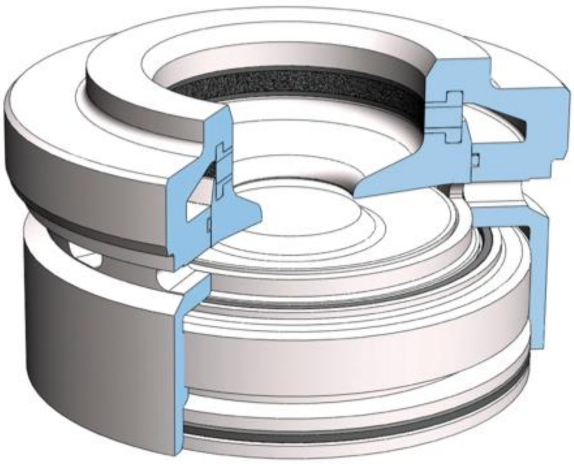

Figure 3.1a: Three-D model of Inflow control device with variable flow area (Inflow Control Company, Tonsberg, Norway 2013).

The ICD shown in Figure 3.1a is able to adjust to different reservoir conditions as follows.

a) Highly viscous oil reservoir with water drive – The water is stopped.
b) Oil reservoirs with water drive – The water gets stopped at a given draw down in order to avoid highway zones of water coning as seen in Figure 3.1 b).
c) Extra highly viscous oil reservoirs such as the bitumen obtainable in oil sands shallow reservoirs – The steam is stopped.
d) Oil reservoirs with gas cap – The gas is stopped.

Figure 3.1b below is an illustration of how coning is prevented using the ICD technology shown in Figure 3.1a.

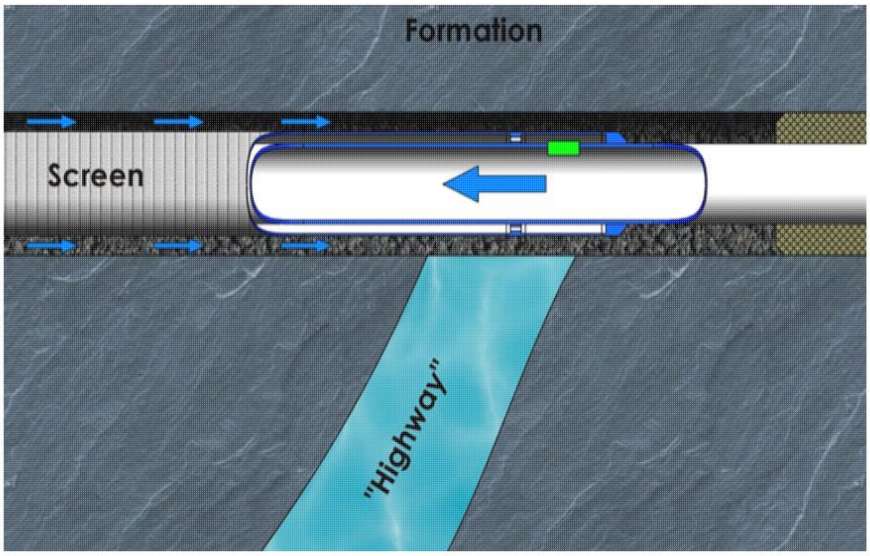

Figure 3.1b: Illustration of water coning in high way zones (Inflow Control Company, Tonesberg, Norway 2013).

3.2 Halliburton

Figure 3.2 below shows the mechanism by which hydrocarbon makes an entrance into the nozzle of an ICD patented by Halliburton.

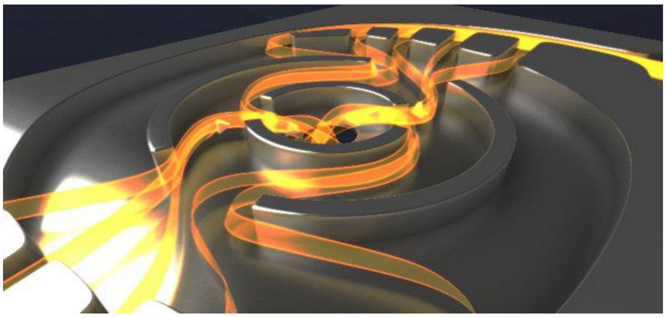

Figure 3.2: Picture of Halliburton EquiFlow Autonomous ICD. Halliburton.com.

The EquiFlow AICD shown in Figure 3.2 works by directing fluids through different flow paths within the tool. Higher viscosity oil takes a short, direct path through the tool with lower pressure differential as shown in the figure. Water and gas spin at high velocities before flowing through the tungsten carbide assembly, creating a large pressure differential.

3.3 Schlumberger – Reslink ResFlow

The ICD patent represented graphically in Figure 3.3 below, is called ResFlow which is originally a Reslink company patent. The acquisition of Reslink by Schlumberger took place in 2006. The ICD nozzles are designed to be around a collar. Flow rate is controlled by plugging a given number of nozzles. Like the other commercial ICDs the flow rate in this case also changes as the pressure drop varies.

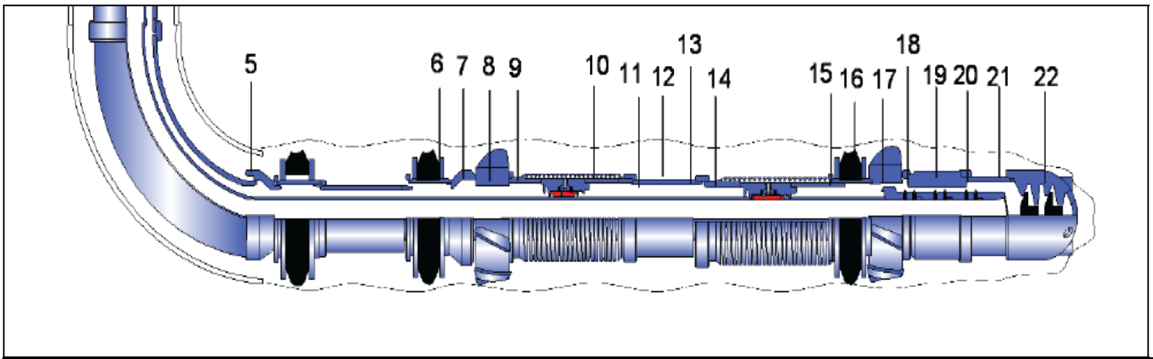

5 to 6: Blank pipe and an oil swellable packer (heel) 6: Oil swellable packer 9 to 11: ICD joints 12: Blank pipe	13: BTC box 14 to 15: ICD joints 16: Oil swellable packer	17: X-over 18: BTC box 19 to 22: Seal Receptacle, X-over, Spacer, Double Poppet wash down shoe End of string

Figure 3.3: Drawing of Schlumberger/Reslink ResFlow ICD integrated into a swell-able packer. Schlumberger.com.

3.4 Weatherford patent

Figure 2.4, as shown in Chapter 2 is a Three-D cut view of the Weatherford ICD patent. Variations in this patent are discussed further below.

3.4.1 FlowReg Tool

This functions very similarly to Reslinks ResFlow tool with a little difference in design.

3.4.2 US 6,371,210 B1

This features a variable flow valve consisting of a spring loaded sliding sleeve which presents the following operational challenges.

3.4.2.1 Control Action.

The control action which is based on a dynamic pressure across the sleeve is inherently unstable. The BECH AICD is based on a static pressure drop, which provides a much more stable solution.

3.4.2.2 Challenges with sliding sleeve.

Since the sliding sleeve is subject to friction and also exposed to debris, the sleeve can be locked easily. Frictional pressure drop can easily exceed the pressure drop of only 2-3 bars seen in the ICD nozzle hence the need for proper design of the sliding sleeve.

3.5 Baker oil tools

The patent shown in Figure 3.4a and b below is called the equalizer ICD. The biggest difference in this tool is seen in its flow restriction which utilizes a helical path around the pipe as opposed to a nozzle. This helical path provides a long narrow conduit causing pressure drop. However, like the other commercial ICDs, it still functions as a mere restriction where flow rate is not constant as pressure drop changes.

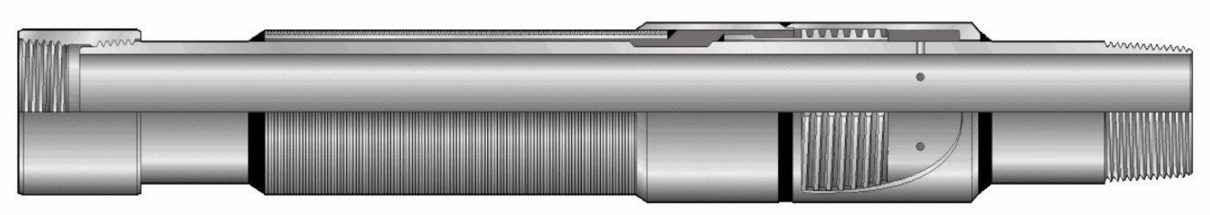

Figure 3.4a: Baker Hughes equalizer ICD designed with an integrated debris filter for application in carbonate formations. Bakerhughes.com.

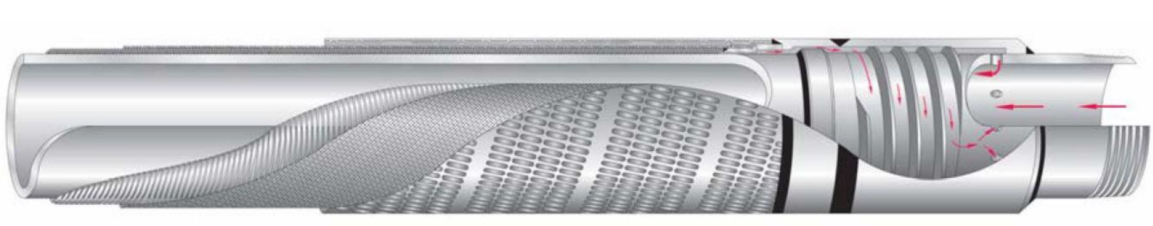

Figure 3.4b: Cut-away view of the equalizer ICD with premium sand screen and path for hydrocarbon production. Bakerhughes.com.

3.6 Autonomous flow control valve or intelligent ICD

ICDs are always installed in long horizontal wells since experience show that these types of wells are prone to water or gas coning which leads to production losses. It becomes necessary to utilize ICDs with autonomous control over flow rate as depletion sets in the reservoir yet for the prevention of coning at late production times.

The autonomous ICD is able to maintain constant flow rate throughout the productive life of the field, thereby eliminating water or gas coning. This presents the obvious advantage of increased recovery. More so, the implementation of this Autonomous ICD creates a high chance for the water fronts to enter the tubing over the entire length which then guarantees ultimate recovery.

Current commercial ICDs are only based upon a restriction principle and can simply be modelled as a nozzle. However these commercial ICDs are unable to maintain constant flow. As reservoir pressure declines, the flow through the nozzle also declines and due to reliability concerns, the use of pressure feedback systems through electronics application is avoided. This then creates a high probability for coning to occur at a later production stage.

3.6.1 3 levels of pressure drop in an ERW as postulated by the BECH company model.

a) Reservoir drawdown pressure controls the flow capacity of the well. Weighing into the flow capacity of the well includes parameters such as permeability, exposed rock area and fluid viscosity as seen in the Darcy flow equation.

$$\Delta P = \frac{Q\mu}{2\pi kh} \ln \frac{r_e}{r_w}$$

b) The pressure drop along the horizontal production tubing leads to coning at the heel of the well where the smallest pressure drops is encountered in a typical North Sea well. There exists a laminar flow (i.e. viscosity controlled) at the toe due to the low pressure drop. However, toward the heel, the flow is turbulent (i.e. controlled by density).

   It is therefore seen that the plot of flow rate vs pressure drop is non-linear and varies with the degree of depletion.

c) The pressure drop characteristic of the area across the Inflow Control Device – Modelling and field data has demonstrated that the nozzle of current ICDs are at turbulent flow which is desirable since density varies very slightly throughout the productive life of the reservoir.

LAMINAR FLOW: $\Delta P \sim \mu Q$

TURBULENT FLOW: $\Delta P \sim \rho Q^2$

Where ΔP= Pressure drop

Q = Flow rate

$\mu = Fluid\ viscosity$

$\rho = Fluid\ density$

In the case of a vertical well, the vertical production tubing is exposed to the following pressure drop.

a) Reservoir laminar flow (viscosity controlled)
b) Turbulent flow in the ICD nozzle (density controlled)
c) Laminar/Turbulent flow in the production tubing (both viscosity and density controlled)
d) Turbulent flow from heel of the well due to minimal pressure drop.

From Darcy's equation it is seen that high changes in fluid viscosity and changes in toe to heel pressure drop can alter the relative flow through the various ICDs.

3.6.2 BECH Company Autonomous Inflow Control Valve

This patent though pending was developed by Prof. Aadnøy of the University of Stavanger to overcome the non-linearity of flow regulated/traditional ICDs, which obviously leads to a relative flow change between the heel and the toe of the horizontal well. This invention would provide a constant flow rate from both toe and hell of the well regardless of pressure variations. The valves in this case are set such that the entire reservoir is depleted before water or gas gets the chance to breakthrough. The new valve maintains constant flow through a mechanism consisting of a spring/loaded membrane with a needle, keeping the simplicity whilst at the same time eliminating reliability issue that could arise in the use of complex electronic feedback system.

The reservoir pressure is choked through a nozzle which forms the principle element for setting flow rate before fluid flows in the production tubing. Hence when reservoir pressure is low, the spring/needle will open, maintaining constant flow and likewise when reservoir pressure increases (which is unrealistic in nature except in a gas injection operation), the pin closes to maintain a constant flow rate as shown in Figures 3.5a, b and c below.

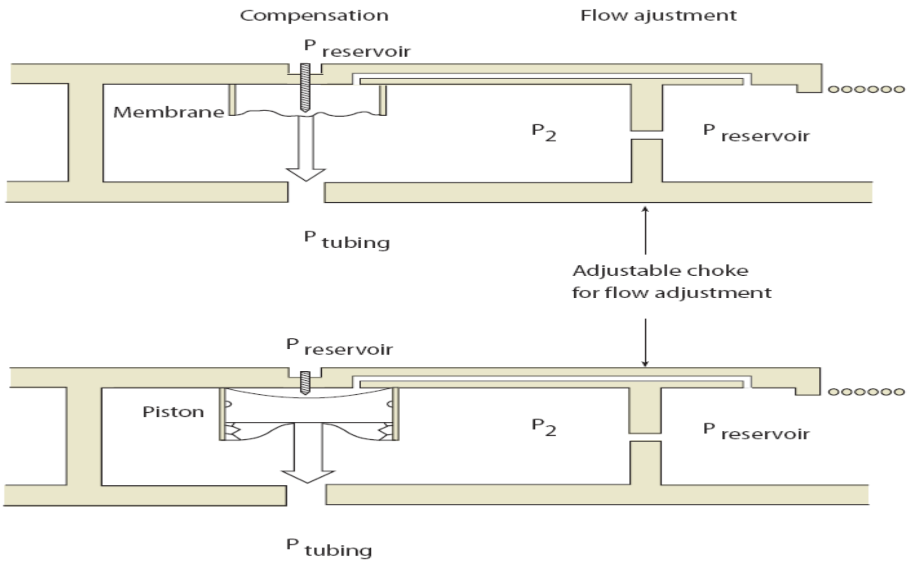

Figure 3.5a: Illustration of piston and membrane flow control. Aadnøy and Hareland, 2009; Gimre, 2012. SPE.org.

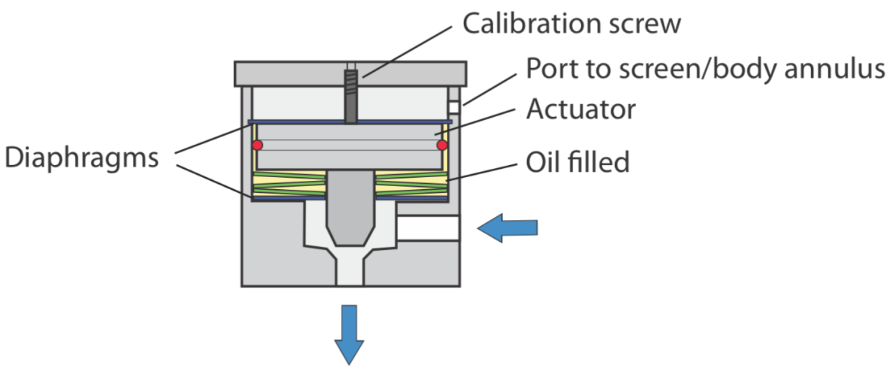

Figure 3.5b: A clearer illustration of the AICD piston/membrane. Aadnøy and Hareland, 2009; Gimre, 2012. SPE.org.

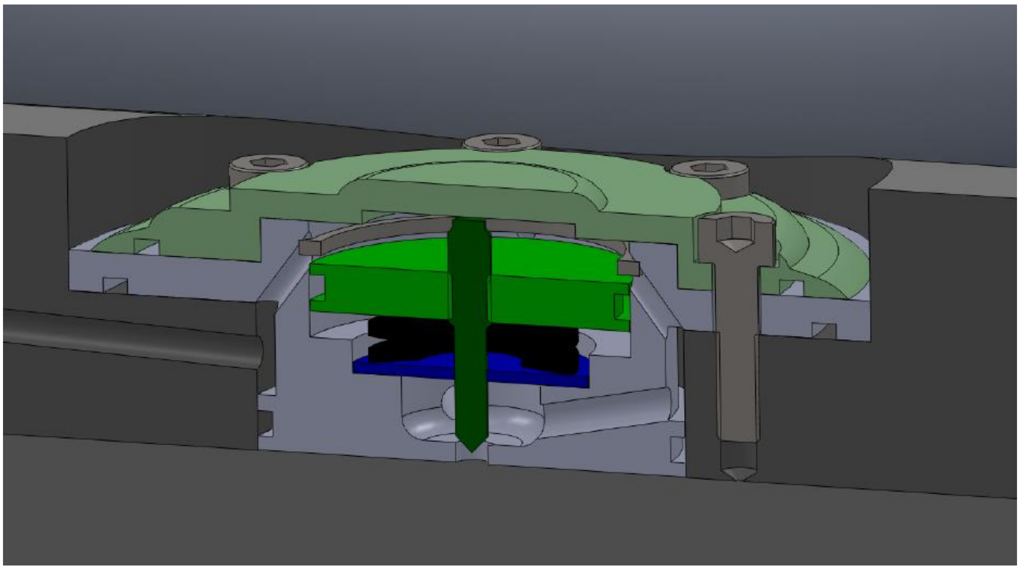

Figure 3.5c: Three-D view of the BECH AICD. Aadnøy and Hareland, 2009; Gimre, 2012. SPE.org.

Figures 3.6a, b and c give a more detailed view of the BECH AICD which illustrates a design of a prototype valve. In order to keep impurities from entering the mechanism, the entire piston is oil-filled and enclosed within two seals.

An interesting feature about the Autonomous Inflow Control Device patented by Prof. Aadnøy apart from its ability to shut-off flow when water/gas contacts the orifice is that it provides constant fluid flow regardless of variation in pressure. This is achieved by a reservoir pressure controlled piston which is set to a pre-determined flow rate. Its percentage stem opening is hydraulically adjusted by the varying reservoir pressure to satisfy the pre-set flow rate.

The functional versatility of ICDs, justifies their inclusion in oil well completion design in terms of project economics. This versatility is seen in its multi-operational usage as listed below.

a) Implemented in extended reach wells, especially in thin pay reservoirs where there exists a very small tolerance/window in the oil-water contact and oil-gas contact. In such reservoir condition, highly sophisticated drilling technology such as Managed Pressure Drilling is used to avoid the intersection of the oil-water contact or oil-gas contact with a rather non-practical chance for fulfilling the required precision. The satisfaction of this requirement in drilling precision is deemed non-practical for the following reasons.
   i. Un-even oil-water and oil-gas contact profile along the reservoir section.
   ii. Bit walk which may not be adequately estimated.

iii. Poor understanding of pressure regimes.

b) Flow control in injection wells.
c) Hole cleaning.
d) Matrix acidizing / fracture acidizing.
e) Included at the various levels of TAML.

Upper design utilizes a spring loaded membrane to compensate for pressure variation while lower design utilizes piston connected to a needle to achieve the same purpose.

The upper drawing shows a design where the spring-loaded membrane is replaced by a piston with seals on both sides of the piston to avoid dirty oil from plugging/restricting the free movement of the piston.

It should be noted that the autonomous valve can be calibrated both for constant flow, increasing flow and decreasing flow thereby allowing an optimal design to be reached in a complex reservoir.

2 PARTS:

1) FLOW ADJUSTMENT PART (conventional ICDs utilize shut nozzles)
2) PART WHERE CONSTANT FLOW IS SET (compensation part)

The flow first goes into a chamber which has a lower pressure thank the reservoir pressure due to the set point restriction. Here a spring loaded membrane or piston connected to a needle is used. This accounts for the compensation part.

Where there is variation in pressure drop in the reservoir or production tubing, the piston moves accordingly thereby allowing a constant flow through the piston/nozzle entering the production tubing.

FORCE BALANCE BETWEEN THE RESERVOIR AND THE NOZZLE IS GIVEN AS

$$P_{res} \times A - P_2 \times A - KX = 0 - - - - - - - - - - - - equation\ 1$$

Where: $P_2 = Pressure\ at\ the\ chamber$

$$k = Nozzle\ constant$$

$$x = Distance\ travelled\ by\ spring$$

FORCE BALANCE BETWEEN THE CHAMBER AND PRODUCTION TUBING

$$P_2 - P_{tubing} = k_v \times \rho \times Q^2$$

$$P_{res} = Resevoir\ pressure\ on\ outside\ of\ system$$

$$P_2 = Pressure\ in\ chamber\ after\ flow\ setting$$

$$P_{tubing} = Pressure\ in\ production\ tubing$$

$$A = Area\ of\ piston$$

$$X = Displacement\ of\ spring\ loaded\ piston$$

$$K_v = Nozzle\ constant$$

$$K = Spring\ constant$$

$$\rho = Fluid\ density$$

$$Q = Fluid\ flow\ rate$$

Combining equation 1 and 2 yields;

$$P_{res} - P_{tubing} = {}^{kx}/_{A} + k_v \rho Q^2$$

$$Q = \sqrt{{}^{1}/_{k_v \rho} \times \left\{ \left(P_{res} - P_{tubing} \right) - \frac{kx}{A} \right\}}$$

Spring force kx is calibrated to move when the differential pressure is varied. The expression on the right hand side of the equation is calibrated such that it is nearly constant.

Since the pressure is influenced by the density, there is little concern about having a very large $\Delta P = P_{res} - P_{tubing}$ which would normally create a scenario that spring cannot compensate for by "kx". This is due to the fact that the density variation in the well is very minimal throughout the productive life of the reservoir.

3.7 Schlumberger – Simulation of flow control devices with feedback control system as applied to oil sands

Factors such as hydraulic gradients in the horizontal completion, geologic and fluid variations in the reservoir and placement issues can produce very poor steam performance in Steam Assisted gravity Drainage (SAGD). A technique popularly used in oil sand recovery in Western Canada. The use of Proportional-Integral-Derivative (PID) feedback coupled with Inflow Control Devices to control steam injection can lead to improvements in SAGD.

The foregoing presents detailed wellbore simulation of a SAGD process in which wells are completed with a combination of ICD and PID feedback control. The figure below illustrates the concept in which 2 closely positioned horizontal wells are placed such that the upper well injects steam and the lower well collects reservoir fluids which gets drained by gravity from a constantly evolving steam chamber. Interestingly, the actual pattern of SAGD well pairs show irregular steam chamber development along the lengths of most of the pars in the pattern as shown in Figures 3.6a, b and c below.

Figure 3.6a: An overview of a typical SAGD process. January 2014 edition of the Journal of Petroleum Technology. SPE.org.

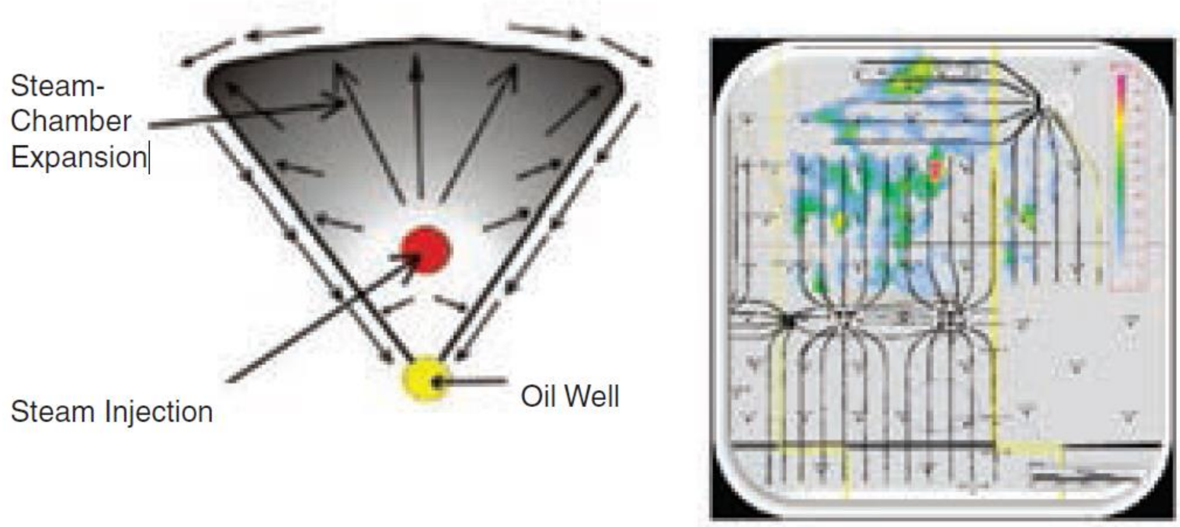

Figure 3.6b and c: An overview of a typical SAGD process. January 2014 edition of the Journal of Petroleum Technology. SPE.org.

Figures 3.7a, b and c give an overview of a typical SAGD process. Shown are the locations of the well pair relative to surface facilities (left), a cross-sectional view of the evolving steam chamber (center), and a plan view of a pattern of well pairs demonstrating non-uniform steam-chamber development along the well pairs (right).

It is important to prevent the risk of the steam chamber touching the local producer, which would then remove hot steam instead of using it more efficiently in the upper reaches of the chamber. This is achieved by pre-setting the injection and production rates to maintain a prescribed temperature difference between fluids exiting the upper injector and entering the lower producer. This temperature difference is also referred to as a sub-cool because it is set to be several degrees below a water saturation temperature. This may be controlled at both the heel and the toe of the well pair by use of the ability to inject and produce from 2 tubing strings landed at these points. The use of a feedback controller to monitor temperatures of produced and injected fluids automatically, with a target sub-cool at the heel and toe of the well pair became necessary to set the injection and production rates to reflect the current state of the reservoir and current sub-cool.

The benefits of targeting the same sub-cool includes but are not limited to:

a) Prevention of steam from entering the lower producer
b) Uniform production from both toe and heel halves is facilitated because they both target the same sub-cool temperature.

Regarding the PID controller, 2 separate controllers are used for the heel and toe tubular each with an error term incorporated into it.

ICD DESIGN TO CONTROL FLUID CONFORMANCE, SUB-COOL AND UNWANTED WATER/GAS.

A high temperature ICD design was chosen that combines a sand control screen with a choke, which that is designed to give a linear production or injection profile throughout the length of the horizontal well bore. These devices are installed in 7 inch base pipe joints each with a length of 46 ft. Each joint is equipped with a flow constriction nozzle. Flow across the nozzle produces a Bernoulli relation (i.e. pressure drop versus flow rate).

CASE STUDIES.

4 cases were run which included combinations of dual-string injection with PID control in wells equipped with ICDs. The following give a brief description of the cases.

1st Case – PID injector/ICD producer, was configured with an injector containing dual 3 inch – inner diameter tubing strings landed at the heel and toe in which steam –injection rates to heel/toe strings were PID controlled with a specified sub-cool target The producer was equipped with ICDs and hence contained only a single 6.3 inch -inner diameter tubular with no additional tubing string landed at the toe.

2nd Case – This featured a PID injector and dual string producer. The injector and producer both contained dual tubing strings. The injector was PID controlled by a heel/toe sub-cool target. The producer produced equally from both heel and toe.

3rd Case – ICD injector/ICD producer contained both injector and producer fitted with ICDs along their entire horizontal length. There was no additional tubing string landed at the toe for this case.

4th Case – A dual string injector and a dual string producer was a base case in which the injector and producer both contained dual tubing strings. Steam injection rates were constant and equally split between the heel and toe strings and production was split also between heel and toe.

Figure 3.7 shows a graphical representation of the steam efficiency in SAGD applications in the 4 different scenarios delineated above

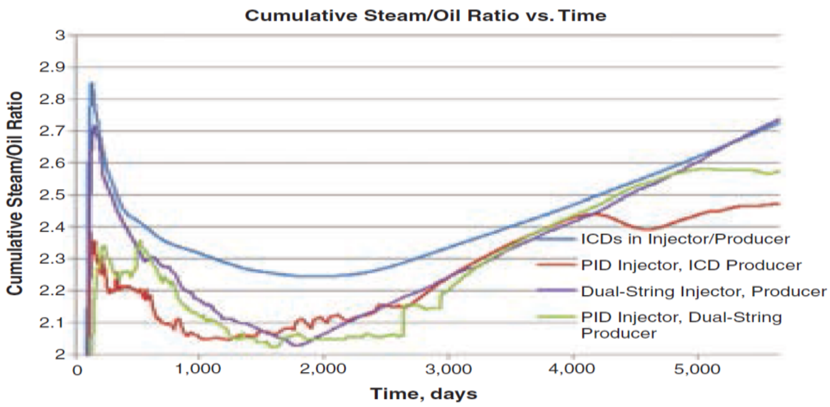

Figure 3.7: Comparison of cumulative steam/oil ratio for 3 SAGD well-pair configurations and the base case. January 2014 edition of the Journal of Petroleum Technology. SPE.org.

At 2 years, temperature and gas-saturation profiles are similar between the three cases—PID injector/ICD producer, PID injector/dual-string producer, and ICD injector/ICD producer. ICD injector/ICD producer displays a slightly greater coolness in the mid-region and lower gas saturations although with similar chamber growth near both ends, possibly because injection and production are both occurring only at the heel, while the first two cases have injection at both the heel and the toe. All are showing a good degree of uniformity along the length of the well pair. By 7 years, the two PID-injector cases are showing equivalent steam chamber growth along the entire length while the ICD-injector/ICD-producer case is showing slightly less growth near the toe. Temperatures in the first case

(PID injector/ICD producer) are looking somewhat cooler than those for both the PID-injector/dual-string-producer and ICD-injector/ICD-producer cases because the PID controller in the former is just beginning to hit its sub-cool target at this time (7 years) and the second PID case will achieve this shortly after.

By 12 years, the first two PID cases are showing cooler steam chambers than the ICD-injector/ICD-producer case because both are achieving their sub-cool targets. The two cases with dual-string producers, dual-string injector/dual-string By 12 years, the two PID-controlled injection cases are showing comparable low pressures around the well pair, while the ICD injector/ICD producer case is showing considerably higher pressures because steam has broken through to the producer and is causing higher pressure drops across the ICD nozzles.

In summary, the results suggest that a hybrid method of using feedback- (PID-) controlled steam injection from dual-tubing strings with a producer equipped with ICDs may have several benefits.

First, there are reduced capital and operating expenditures because there is one less tubing string in the producer.

Second, an ICD equipped producer provides a more-even inflow, which results in better-controlled sub-cool throughout the production cycle.

Third, later in the production cycle, the ability of the PID-controlled injection to force a specified sub-cool target appears to keep the steam chamber farther from the producer and improve the economics of the process.

4 EXPERIMENTAL METHOD

4.1 Presentation of fluid samples used for experimental work

Table 4.1 below is a presentation of the properties of fluids used in this experimental work. As indicated in the second column of the table below, all fluids were experimented at a uniform temperature of 20 °C. However, at the end of the flow experiments, the measured temperature of the fluids seemed to differ by 1-2 °C, which has an insignificant impact on the calculations presented in later in Chapter 5.

FLUID	TEMPERATURE ($°C$)	DENSITY $(kg/m\text{^}3)$	VISCOSITY (cP)
Pure Supreme gear oil 20W-50	20	874.5	341
Pure Mobil gear oil 426 4W-10	20	883.53	120
Pure tap water	20	1000	1
Pure White Spirit	20	796.44	0.75 – 1.65
Supreme 20W-50 mixed with Mobil 4W-10, tap water and white spirit.	20	879.86	198.8
Mobil fluid mixed with residual tap water and white spirit in hose	20	884.22	117
Tap water mixed with residual dry white spirit and Mobil fluid in hose	20	Non-Homogeneous	Non-Homogeneous
Dry white spirit mixed with residual tap water and Mobil fluid in flow line	20	800.55	1.3 – 4.9

Table 4.1: Fluid viscosities and densities used in experimental thesis work.

<u>Criteria for fluid selection</u>

Let it be noted that the fluids listed in Table 4.1 were carefully selected to depict typical fluid viscosities obtainable in the NCS including its artic regions.

a) **Tap water** – Water conditioned to temperature of about 20°C was used as the reference fluid to perform an initial test run of the experimental rig-up shown in Figure 4.1. It was used to investigate the flow properties of a fluid having high density but low viscosity. Data obtained from water based experiments formed a basis for drawing comparison and correlation with respect to the other fluids that were flow-tested.

b) **White Spirit** – The white spirit which features properties of low viscosity and low density was used to provide more information on ICD/AICD nozzle flow regime. Once again the experiments were done at similar temperature conditions as tap water. Since the flow through constriction had been determined to be turbulent so far, the white spirit which similarly to tap water has low viscosity was used to confirm the pre-determined flow regime in a density driven flow.

   This fluid equally served the purpose of cleansing the system of residues before transiting from one fluid to another fluid of different viscosity and density. Its function in this capacity was not very efficient as the new fluid upon circulation through entire system showed reduced viscosity and slightly higher density.

   As seen in the attached Risk Analysis in Appendix A.1, due-diligence was done by the Institute of Petroleum Technology at the University of Stavanger and the experimentalist to avoid hazards associated with this fluid.

c) **Mobil 4W-10** – Commonly referred to as Mobil 426 gear oil, it was used for its low density but very high viscosity (see Table 5.4). Flow-test of this fluid provided a better understanding of the flow regime associated with highly viscous oils such as that obtainable in the arctic region of the Norwegian Continental Shelf. It also provided sparse understanding of the viscosity limit above which viscous effects become predominantly evident in laminar fluid flow. Its use presented very little or no health hazard as it can be compared to the hazard level in a typical domestic car garage.

d) **Supreme 20W-50** – As presented in Table 4.1, this fluid which has higher viscosity than the Mobil 426 fluid was used in our experimental work to provide a confirmation of the laminar flow regime conclusion drawn earlier. Once again, the flow of this gear oil presented very little hazard which is comparable to that obtainable in a typical domestic car garage. It was observed that our 100 bars rated positive displacement pump did not have the capacity to pump this fluid at its pure state having a viscosity of about 341 centi poise. In order to solve this problem, a combination of 70% of the Mobil 426 fluid and 30% of the Supreme gear oil which combined for a mix viscosity of 198.8 centi poise was used. Our pump worked relatively efficiently with this mixture.

4.2 Description of experimental apparatus

The physical simulator developed for this study can be seen in Figure 4.1. It consists of:

a) A common water faucet and sink; a minimum of 20 liters of fluid was used for flow experiments as this allow sufficient hydrostatic head needed for the suction side of our PDP;
b) A ventilation chamber with an integrated suction unit. This chamber/fume hood will serve the purpose of spill protection as well;
c) A tank, with the following inner dimensions:
    - length of 1260 mm;
    - width of 251 mm;
    - height of 250 mm;
    - thickness of 15 mm;
    - volume of 79,065 Liter;
d) A bucket with capacity of 1 Liter;
e) A PDP (with capacity of 100 bars, 4 KW, 3-15 L/min, CAT PUMP model 341); This pump has a suction that operates without pressure feeding or gravity feeding;
f) Hoses to connect everything, with inner diameters varying mainly from 8 (the smaller, transparent ones in the figure) to 12 mm (the yellow one, to drain the water to the sink);
g) Pressure gauges;
h) Pressure regulators;
i) Pressure valves, including 2 ball valves, 2 choke valves, a relief valve, a hydraulic feedback valve and a bleed line valve;
j) A conventional ICD;
k) The AICD developed by Prof. Aadnøy for this study;

The equipment is placed at a height of 93 cm from the floor. The total (external) height of the tank is

26 cm, and the nozzles are also 26 cm above the top of the tank. So, in total it is 145 cm.

The task involves the use of a 100 bar rated pump in pumping fluids with viscosities of 0.5 centi poise and higher which are typical viscosities obtainable in the North Sea. The water from the tap is first pumped to the 2 ICDs, through pressure regulators, to set a pre-defined pressure. When it passes through the nozzle of the conventional ICD, the flow rate will change with the pressure. When it passes through the AICD, the flow rate won't change. However, the pump pressure has to be ramped up to a minimum of 10 bars in order for flow to occur through both valves.

Shown in Figures 4.1a, b, c and d are pictures of the experimental rig-up used for this thesis work. It shows a tank enclosed in a fume hood which housing up 20 liters of fluid at a given time. To the extreme right of this picture in green color is the PDP used to pump the fluids.

Figure 4.1a: Front view of experimental apparatus for fluid throw measurement.

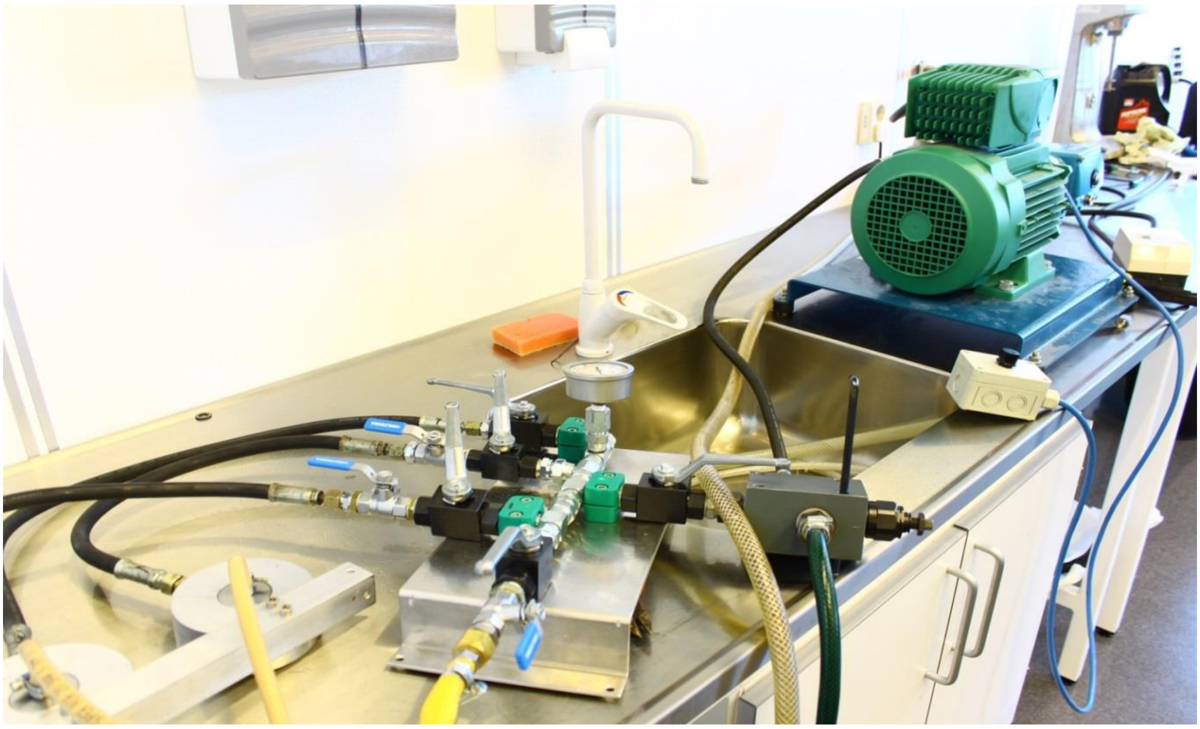

Figure 4.1b: View of valve arrangement and PDP – It consists of ball valves, choke valves, bleed valve, relief valve and differential pressure feed-back valve.

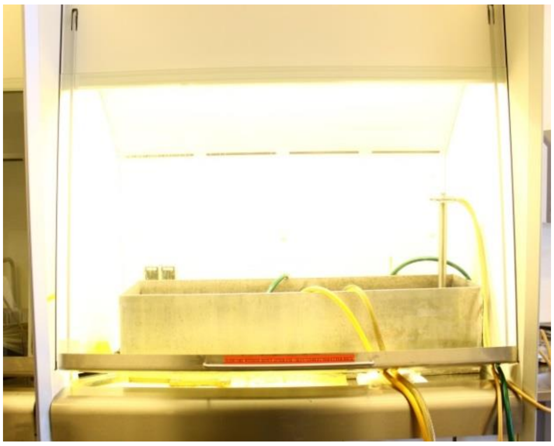

Figure 4.1c: Tank view with fume hood close.

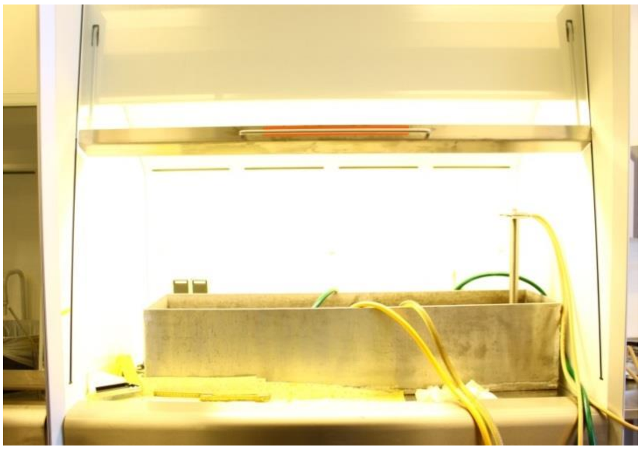

Figure 4.1d: Tank view with fume hood open.

Section 4.3 presents a step-wise procedure that ensures the safe operation of the experimental apparatus shown in Figure 4.1.

4.3 Experimental procedure

In this section a comprehensive description of the technical know-how of operating our experimental rig-up and taking measurements is presented.

4.3.1 Procedure to start the equipment for initial flow test with water

a) Fully open the tap;

b) Open the pressure feedback valve;

c) Open the bleed line;

d) Open the relief valve;

e) Close the nozzles valves;

f) Open the pressure feed-back valve;

g) Start the pump (in this case by pressing the black button in the rear of the green PDP as shown in Figure 4.1b);

h) Set the desired pump flow rate (if not previously set);

i) Set the relief valve to the desired pressure (less than 100 bars, because this is the limit of the pump);

j) Adjust the bleed line valve until the desired pump pressure is achieved (the main pressures used in this experiment ranged from 2 to 90 bars);

k) Adjust the nozzles valves according to the desired flow rate;

l) Check all the adjustments again and make corrections where necessary;

m) Start making the measurements.

N/B - When working with oil, special considerations should be made as follows:

a) An oil tank, a feed pump, and a return line, should be included, to conduct the oil back to the oil tank. The necessary minimum pressure, and the corresponding tank dimensions, must be determined. With this feeding system, the pump used for the water would not be necessary.

b) To reduce the minimum required volume of oil, tilting the tank could be considered, provided it maintains the original horizontal position of the nozzles. However, this was not necessary in these experiments.

Another possibility is simply to use the same pump – firstly connected to the tap – to suck the oil from the same tank. It is the easiest way because the return system is automatically created this way. But in this case it is important to be careful with some irregularities that may occur with the sucking system, like air entering into the hose. This was the selected arrangement for the experiments conducted in this study. Thus for testing with all fluids including water, it is a matter of filling the tank with a minimum of 20 liters of the desired fluid, and adjusting the pump to suck directly from it. This equipment configuration/arrangement also necessitated putting the bleed line in the tank, instead of in the sink.

4.3.2 Method for calibration of fluid throws

The filling of a 1 liter bucket shown in Figure 4.2a and b is timed using a stop-clock. This process is repeated again and an average value is calculated in order to account for any human error in timing and uncontrollable fluid loss into the tank. Calibration for the ICD nozzle is done separately from the AICD nozzle.

Figure 4.2a: 1 liter calibration bucket.

Figure 4.2b: Illustration of calibration process.

4.3.3 Method for measurement of fluid throws

The pictures in Figure 4.3 show the measurement tools used for estimating the fluid throws and the actual act employed in taking the measurements.

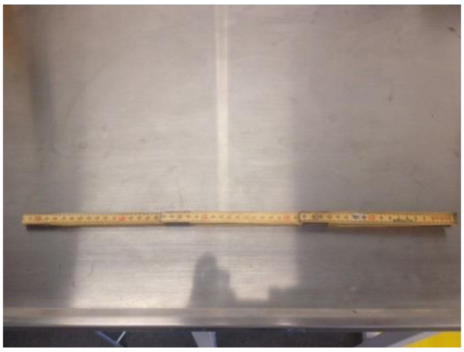

Figure 4.3a: Meter rule

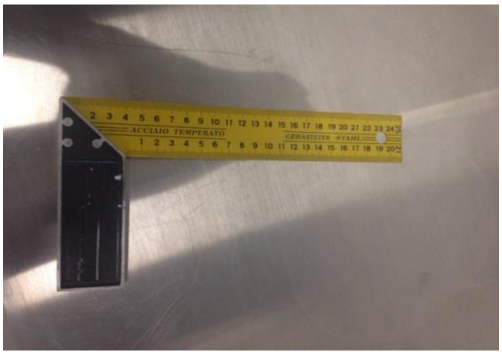

Figure 4.3b: Right angled meter rule

Figure 4.3c and d: Measurement of fluid throws from nozzles.

a) Adjust the pressure on the AICD and ICD in the highest desired level (in this case it was up to 90 bars), taking note of this pressure in a proper table;
b) Make adjustments until the same flow rate is achieved through both nozzles;
c) Orient the right angled meter rule to be in a direction perpendicular to tank thickness and ensure it makes contact with the mid-point of the fluid throw. The mid-point is used as our reference point because of the spread in fluid that occurs somewhere very close to the end of the parabolic throw path. It is observed that the highest percentage by volume fluid accumulates at the middle of the fluid spread;
d) With the use of another meter rule, take measurement of the horizontal distance x between the nozzles and the point where the right angle meter rule makes contact with the tank

thickness. This coincides with the point where the fluid crosses the top of the tank. Take note of this in a proper table;

e) Repeat the steps above by reducing pump pressure as many times as necessary until final throw measurement at 2 bars is obtained.

4.3.4 Procedure to stop experiment

a) Shut the faucet (if working with tap water);
b) Turn off the pump (in this case by pushing the red button at the right rear end of Figure 4.1b)
c) Remove the remaining fluid in the tank (the pump can be used to suck the fluid into an adequate container);
d) Leave the bleed line, relief line and pressure feed-back line open;
e) Shut the choke and ball valves;
f) Perform thorough clean-up of all equipment/component
g) Check if everything was done in the most proper and safest manner and make corrections where necessary before introducing different fluid into system.

A Risk Analysis Report is attached in Appendix A. This shows a detailed consideration of the main risks for the equipment, environment, and especially for the people using it.
It includes the following information.

a) The necessary (PPE), like safety glasses, hearing protectors (to protect from the noise of the pump), and aprons.
b) The use of a fume hood to enclose the tank in order to prevent spillage on individuals, equipment and floor.
c) Use of an adjustable suction system (fume hood) which must be placed over the nozzles, to protect individuals against possible fumes.

4.4 Theoretical premise for calculating flow rates based on experimental data of pump pressure and fluid throw

During testing of the Autonomous Flow Device and the comparable ICD, a particular flow measurement system was set up. The fluid stream from the outlet nozzle forms a parabolic shape, where the length from the nozzle to the surface (i.e. the fluid throw) is proportional to the flow rate. Figure 4.4 below presents a simple drawing used to illustrate this measurement principle.

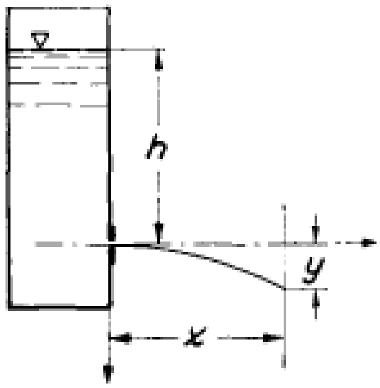

Figure 4.4: Details of the fluid throw components and configuration (AADNØY, B. S. 2012.). www.hansenenergy.biz.

A nozzle at the bottom of the tank shown will assume an outlet velocity of:

$$v = \varphi\sqrt{2gh} - - - - - 4.1$$

Where φ is the discharge coefficient varying from 0.96 to 0.99. The parabolic shape is defined by:

$$x = vt\ ;\ y = \frac{gt^2}{2}$$

Combining these 2 equations gives the final equation for the flow as follows:

$$v = x \times \sqrt{\frac{g}{2y}} - - - - - 4.2$$

Hence for a given drop height, the flow velocity or the flow rate is directly proportional to the length from the nozzle to the point of impact (i.e. the fluid throw).

However, the flow is initially measured by filling jar overtime to a volume of 1 liter and then this flow is scaled according to the specific length of the impact given by "x".

The above stated linear relationship is described as follows;

$$lets\ assign\ "m"\ meters\ to\ be\ our\ calibration\ impact\ length/throw$$

$$Assume\ it\ takes\ a\ time\ of\ \text{"t"}\ seconds\ to\ completely\ fill\ a\ volume\ of\ 1\ L\ cubic\ meters$$

$$Based\ on\ the\ above, the\ calibration\ flow\ rate\ can\ be\ written\ as\ {}^{1L}/_{t}\ \left({}^{cubic\ meters}/_{sec}\right)$$

$$An\ arbitrary\ throw\ of\ (m+1)\ meters\ at\ a\ given\ pump\ pressure\ would\ therefore$$

$$produce\ a\ flow\ rate\ of;$$

$$\left[\left(\frac{m+1}{m}\right) \times {}^{1L}/_{t}\right]\left({}^{cubic\ meters}/_{sec}\right) - - - - - 4.3$$

5 EXPERIMENTAL RESULTS, ANALYSIS AND CORRELATIONS

5.1 Initial analysis with tap water

In order to verify the claimed theory of our BECH AICD which says constant flow rate through nozzle irrespective of pressure variation, tap water was first pumped using our experimental rig-up and the following plot was obtained. Experimental data for the plot in Figure 5.1 can be found in Appendix A.2

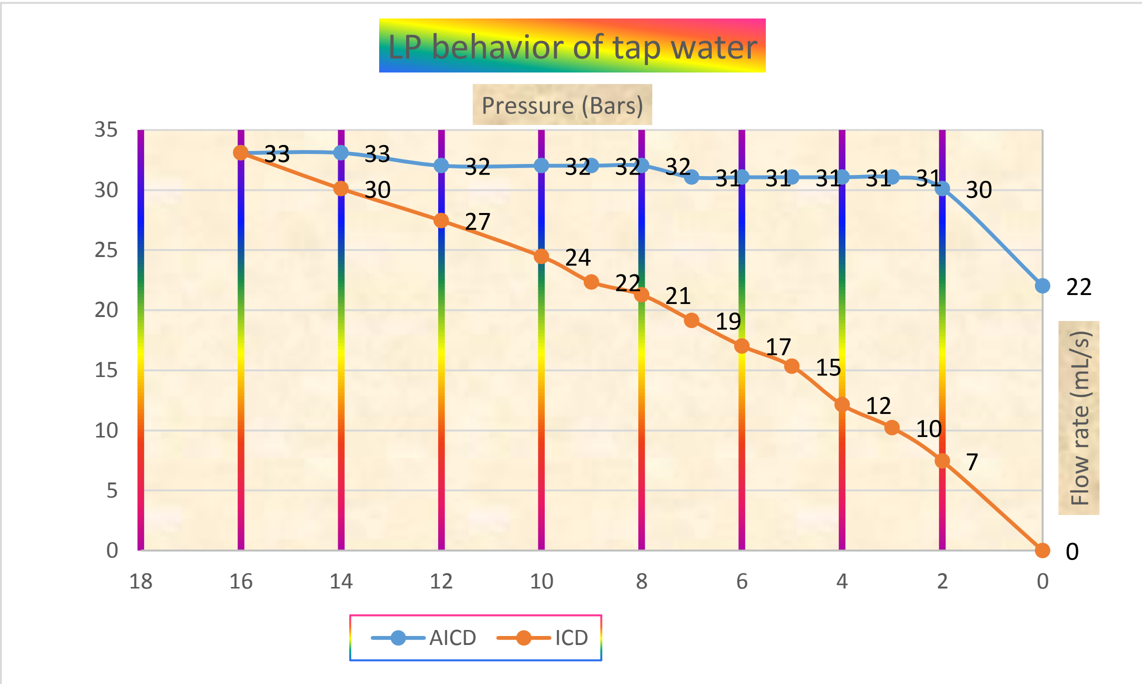

Figure 5.1: Plot showing insignificant BECH AICD flow variation of Tap Water flow rates at different pump pressures. Laboratory data is attached in Appendix A.2.

As shown in the Figure above, it was observed that the ICD shows a decrease in flow with dropping pressure, whereas the Autonomous Flow Valve (i.e. BECH AICD) shows a nearly constant flow regardless of pump pressure. However, it is later shown in figure 5.4 of section 5.2.1 that a malfunction of our positive displacement pump creates a non-uniform flow rate through the AICD nozzle which resembles the data obtained from the commercial ICD nozzle. Another reason for the non-constant water flow rate through the AICD nozzle is due to the conservative boundary condition one of which is the extremely small valve stem opening of 0.3 mm. A small valve opening is more conservative than a larger valve opening as far as flow parameters as concerned because it represents worst case scenario. By worst case scenario we seek to paint a picture that depicts the predominant flow regime as precisely as possible. In other words, when pumping a fluid of known viscosity at a given pump rate of revolution and pressure, the flow regime obtained at a very small valve opening as observed experimentally would be the same when the valve opening is increased. Hence the small valve opening gives a more reliable determination of flow regime.

5.1.1 Flow behavior of fluids with viscosities higher than 1 cP

<u>Dry White Spirit</u>

Figure 5.2 below shows an excel plot of data obtained during the flow test of the dry white spirit. As observed, the near constant flow rate by the BECH AICD irrespective of pump pressure, which forms one of the core objectives of this experimental thesis is obeyed.

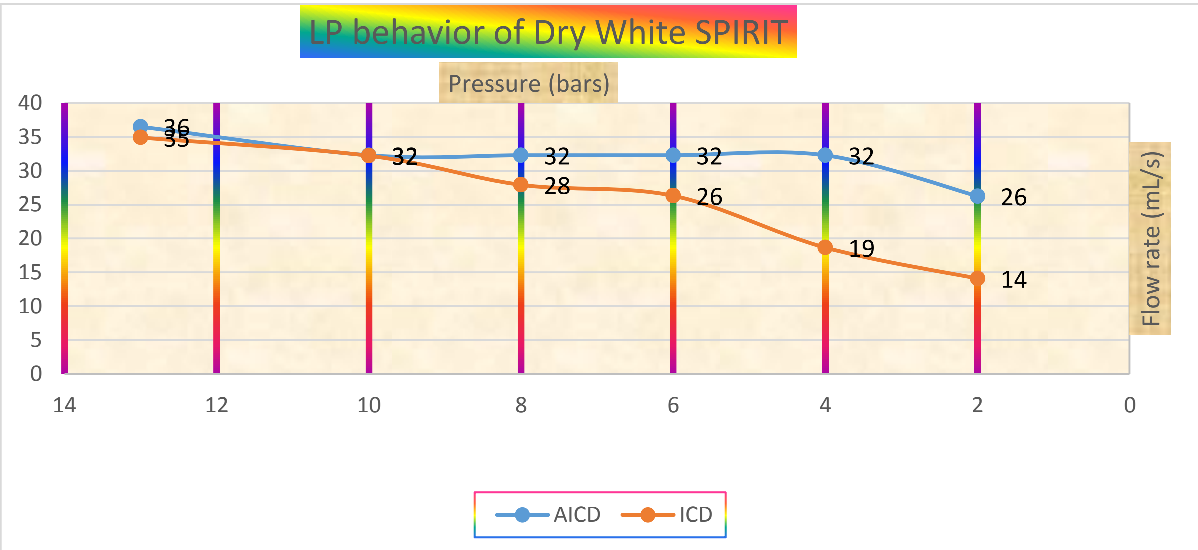

Figure 5.2: Plot showing insignificant BECH AICD flow variation of White Spirit flow rates at different pump pressures. Laboratory data is attached in Appendix A.3.

Mobil 426 Fluid

Figure 5.3 below shows an excel plot of data obtained during the flow test of the Mobil 426 gear oil. As observed, the near constant flow rate by the BECH AICD irrespective of pump pressure, which forms one of the core objectives of this experimental thesis is obeyed.

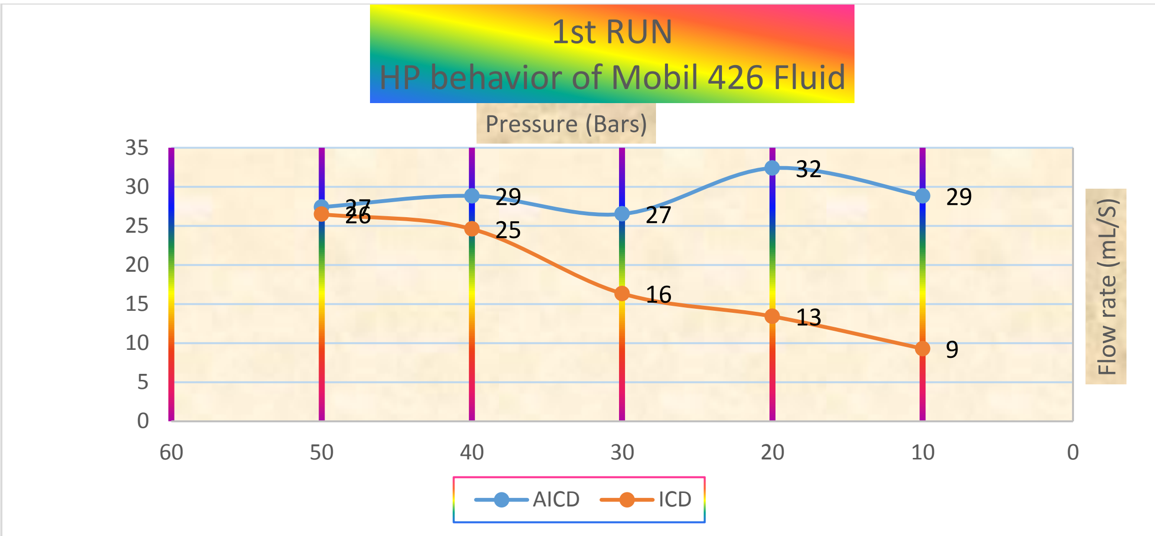

Figure 5.3a: Plots showing insignificant BECH AICD flow variation of Mobil 426 fluid flow rates at different pump pressures. Laboratory data is attached in Appendix A.4.

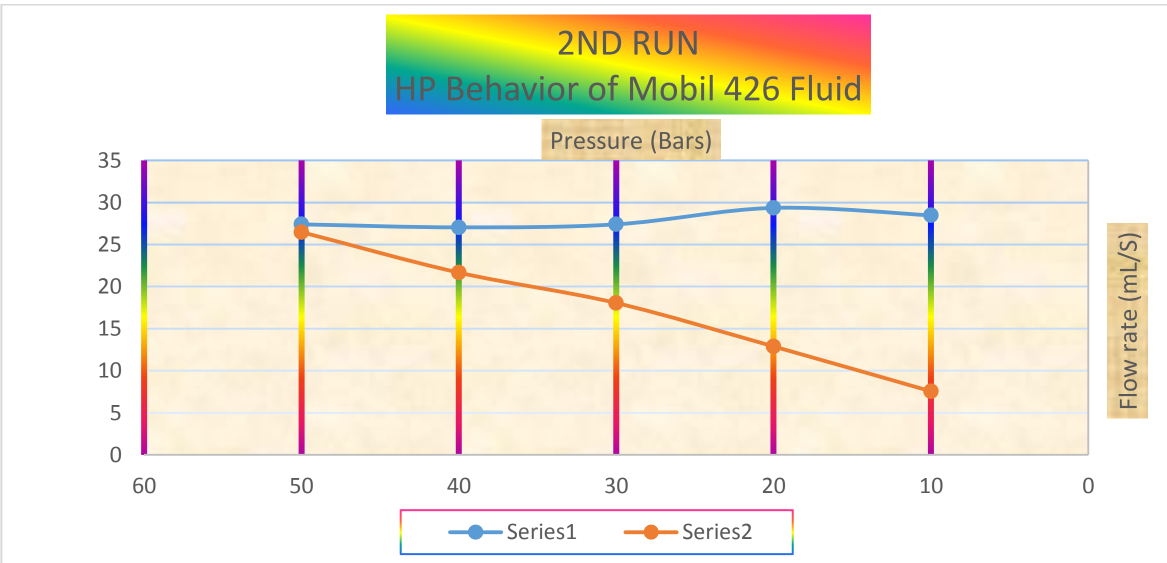

Figure 5.3b: Second run performed to account for uncertainties associated with the pumping of Mobil 426 Fluid.

The flow rate variation for Mobil 426 fluid was investigated at high pressures which is quite different from pressure ranges used for the Dry White Spirit and Water. This was due to the fact that at pump pressures below 10 bars, there was a high degree of irregularity and uncertainty in flow data obtained. The main non-conformance/irregularity associated with the BECH AICD is the sudden drop in flow rate for this highly viscous gear oil at pump pressures below 10 bars. This trend is shown clearly in Figure 5.4 below, where a plot for even more viscous gear oil is generated.

Interestingly, the observed uncertainty can form a deductive basis, which states the following – **"At reservoir pressures below 10 bars, the nozzles of both ICD and BECH AICD would only function adequately with fluids having viscosities much lower than 117 centipoise"**.

The exact critical viscosity value which would authenticate the above hypothesis has not been investigated further in this thesis. This is owing to a lack of resources in acquiring fluids with a wide range of viscosity properties more so, a minimum of 20 liters of gear oil is required in the tank in order to guarantee sufficient hydrostatic head pressure for the suction side of our PDP.

Supreme Gear Oil

Figure 5.4 below shows an excel plot of data obtained during the flow test of the Supreme gear oil. As observed, the near constant flow rate by the BECH AICD irrespective of pump pressure, which forms one of the core objectives of this experimental thesis is obeyed until a pump pressure of about 6 bars is attained.

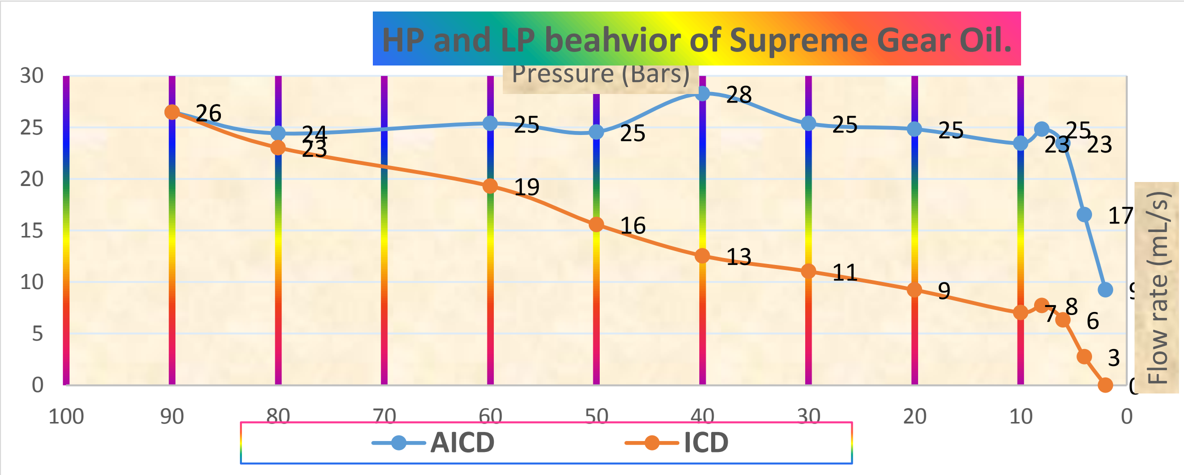

Figure 5.4: Plot showing insignificant AICD variation of Supreme Gear Oil flow rates at different pump pressures. Laboratory data is attached in Appendix A.5.

As seen in Figure 5.4, there exists an unacceptable sporadic/haphazard trend in flow rate data below 10 bars of pump pressure for this fluid which happens to have a viscosity of 198.8 centi poise in its mixed state – accounting for the highest fluid viscosity under investigation in this thesis. It is also observed that at about 6 bars of pump pressure, the decrease of flow through the AICD and ICD escalates (i.e. exhibits a much stepper slope) which again demonstrates the limitations in application of the BECH AICD and conventional ICD.

The following example serves as an illustration of the potential reservoir drainage benefits that can be obtained from utilizing the BECH AICD in completion design. The exact economic benefits which can potentially be derived from feature have not been further investigated as it lies outside the scope of this thesis.

Example 5.1

The following example demonstrates the positive consequences of these near constant flow rate characteristic of our BECH AICD. It is based on the assumption that available viscosities in the NCS would follow the same trend demonstrated above – i.e. infinitesimal AICD flow rate variation which has been experimentally proven using fluid viscosities shown in Table 5.4.

An Extended Reach Well having length of 3600 meters, an initial inflow rate of 24000 barrels per day and recoverable oil volume of 10^8 barrels can be analyzed for drainage time as follows.

The production rate ratios from Figure 5.1 are summarized in the table below.

Production rates	**ICD**	**BECH AICD**
Initial production rate	33 mL/sec	33 mL/sec
Final production rate	7 mL/sec	30 mL/sec
Production ratio	7/33 = 0.21212	30/33 = 0.90909

Table 5.1: Summary of production rate ratios.

The obtained ratios can be applied to my Example Problem 5.1 by performing the following calculation.

$$ICD\ final\ production\ rate: 24000\ bpd \times 0.21212 = 5090.88\ bpd$$

$$AICD\ final\ production\ rate: 24000\ bpd \times 0.90909 = 21818.16\ bpd$$

The above calculation is tabulated as follows:

Flow rates	**AICD**		**ICD**	
	Q_t (STB/D)	N_p(STB)	Q_t (STB/D)	N_p(STB)
Initial rate	24000	0	24000	0
Final rate	21818.16	10^8	5090.88	10^8

Table 5.2: Presentation of initial and final production rates and corresponding cumulative production.

Time taken by BECH AICD to drain entire recoverable reserve is calculated as follows:

$$\mathrm{D_i} = \frac{24000 - 21818.16}{10^8} = 2.18184 \times 10^{-5} Days^{-1}$$

Time taken to reach drain entire reservoir OR time taken to attain 21818.16 STB/D is calculated as follows:

$$\frac{\ln(24000/21818.16)}{\mathrm{D_i}} = \frac{4368.39 \text{ days}}{365} = 12 \text{ years}$$

Where $\mathrm{D_i}$ = Rate of decline

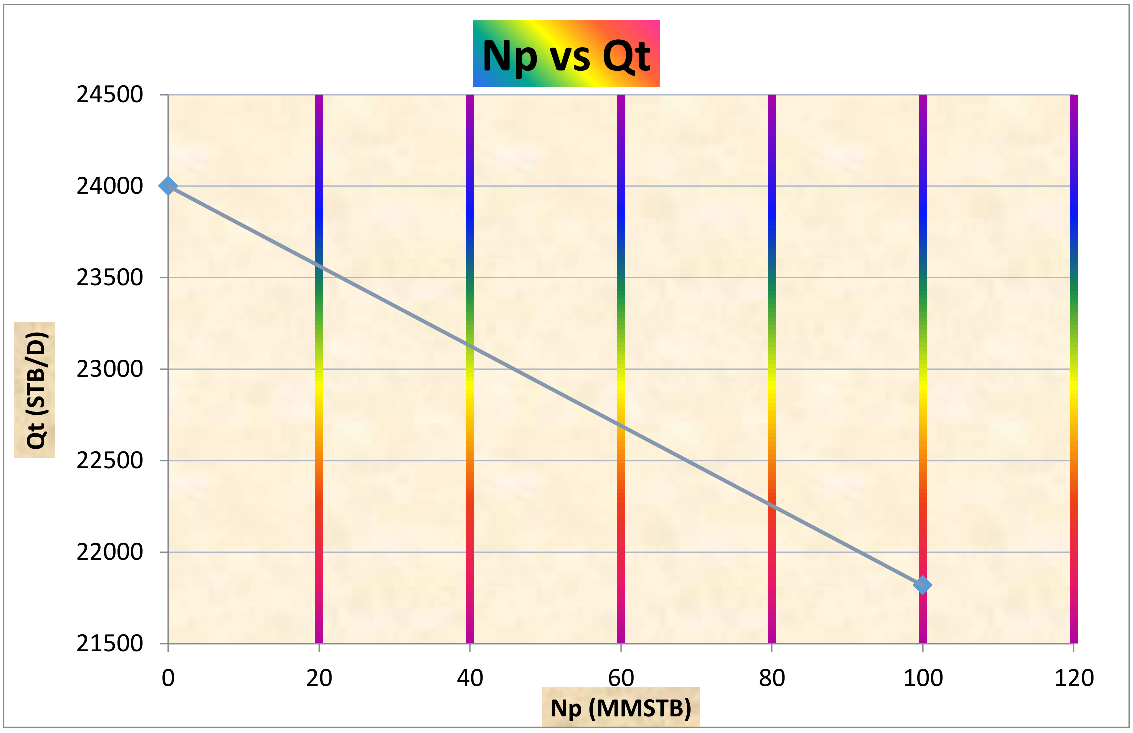

Figure 5.5: Reservoir drainage using BECH AICD

A similar calculation would be performed for the ICD as follows:

$$\mathrm{D_i} = \frac{24000 - 5090.88}{10^8} = 1.891 \times 10^{-4}$$

Time taken to reach 2100 STB/D is calculated as follows:

$$\frac{\ln(24000/5090.88)}{D_i} = \frac{8200 \text{ days}}{365} = 22.5 \text{ years}$$

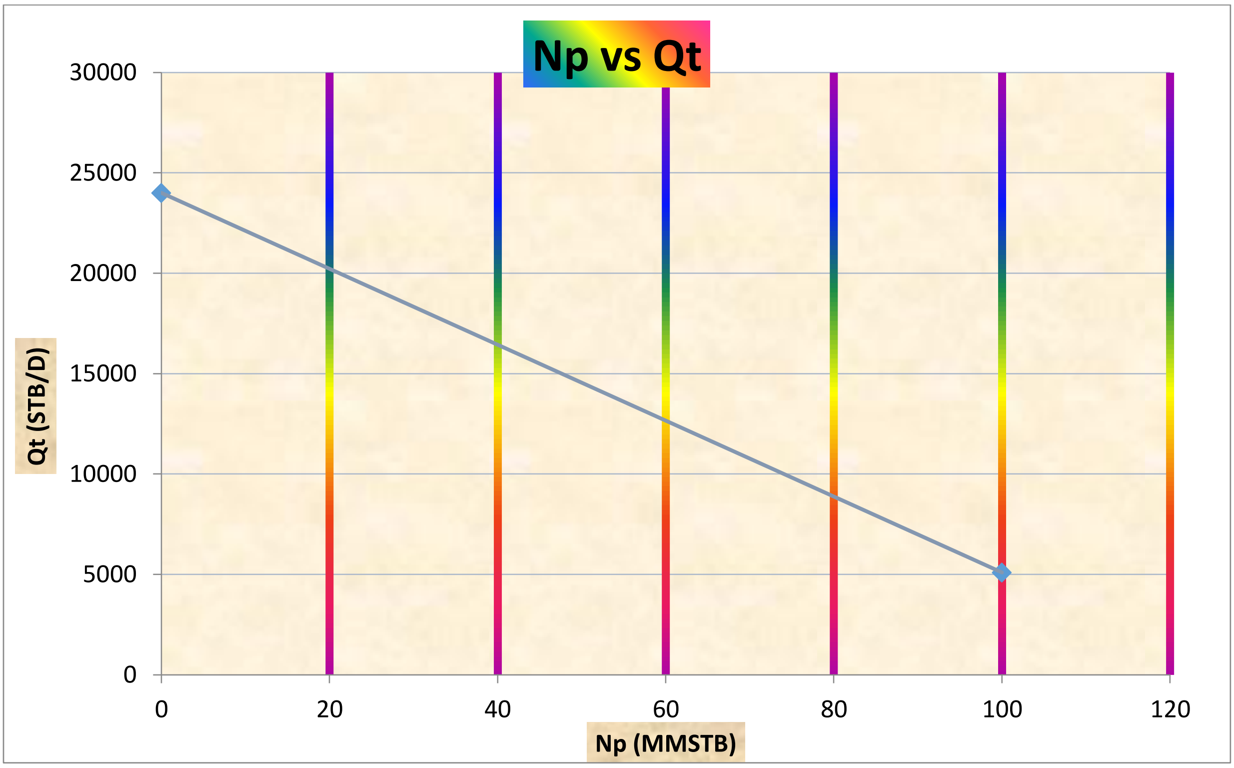

Figure 5.6: Reservoir drainage using conventional ICD

The results obtained from above analysis are summarized in Table 5.3 below.

Production rates	ICD	BECH AICD
Initial production rate	24000 bpd	24000 bpd
Final production rate	21818.16 bpd	5090.88 bpd
Time to drain reservoir	22.5 years	12 years

Table 5.3: Presentation of time taken to drain reservoir by conventional ICD and BECH AICD

The Autonomous Flow Device (AICD) drains the reservoir at nearly half the time it takes the conventional ICD to accomplish the same task. The AICD does this with an improved performance due to its constant flow rate at declining reservoir pressure.

Hence the main drivers for inclusion of the BECH AICD in completion design are summarized as follows.

- Higher production rates and reduced drainage time
- Largely minimized or delayed water/gas coning
- Controls flow in injection wells.

5.2 Correlation that shows contrast in flow rates due to different fluid densities.

The following analysis provides a mathematical model which relates the flow rates of the fluids having varying densities. This is based upon the premise that the different fluids are pumped through the nozzles at the same boundary conditions of nozzle exit area for ICD and AICD, pump pressure, choke valve percentage opening, relief valve percentage opening and feed-back valve opening.

<u>Laminar Flow</u>

$$\Delta P \sim \mu \times Q -----5.1$$

$$Where\ \ \mu = Dynamic\ viscosity$$

$$Q = Flow\ rate$$

<u>Turbulent Flow</u>

$$\Delta P\ \sim \rho \times Q^2 -----5.2$$

$$Q = \sqrt{P/\rho} -----5.3$$

The relation in equation 5.3 shows that flow rate would be higher with less fluid density.

If the same pump pressure of 20 bars is applied in the flow of both oil and water, then the following relations is true.

$$\rho_{water} \times Q_{water}^2 = \rho_{oil} \times Q_{oil}^2 ----- 5.4$$

From equation 5.4 we obtain the following.

$$Q_{oil} = Q_{water} \sqrt{\frac{\rho_{water}}{\rho_{oil}}} ----- 5.5$$

This serves to give an expected contrast in flow rate as oil and water are pumped separately from our positive displacement pump. It suggests that oil should have a higher flow rate than water at a given pump pressure since both fluids are assumed to be in the turbulent flow regime (i.e. density controlled flow) and the oil is of less density.

In Table 4.1 we have accounted for the mix effect in fluid properties that occur when a particular fluid is evacuated from pump and flow lines which is followed by pumping of new fluid. This has the capability of introducing an unwanted variable/error while taking measurement of desired parameters. Largely, the error owes to the inefficient cleaning and drying procedures implemented in this experimental thesis.

From Table 4.1, the fluid data are obtained to perform the following calculations.

<u>MOBIL FLUID 426 AND WATER</u>

$$Q_{mobil\ oil} = Q_{water} \times \sqrt{\frac{1000}{884.22}}$$

$$Q_{mobil\ oil} = 1.063 \times Q_{water} - - - - - 5.6$$

<u>DRY WHITE SPIRIT AND WATER</u>

$$Q_{white\ spirit} = Q_{water} \times \sqrt{\frac{1000}{800.55}}$$

$$Q_{white\ spirit} = 1.118 \times Q_{water} - - - - - 5.7$$

This serves to give an expected contrast in flow rate as oil and water are pumped separately from our positive displacement pump. It suggests that oil should have a higher flow rate than water at a given pump pressure since it is assumed to be a turbulent flow regime for both fluids (i.e. density controlled flow) and the oil has less density.

5.2.1 Combined plot of flow rates associated with different fluids

Figure 5.7 serves to provide a visual representation of the contrast model put forward in section 5.2 above. This will pave way for a better comparison of the data obtained from model to the actual experimental result. Please note that at the set boundary condition, it was not possible to pump the Supreme gear oil mainly due to the high viscosity.

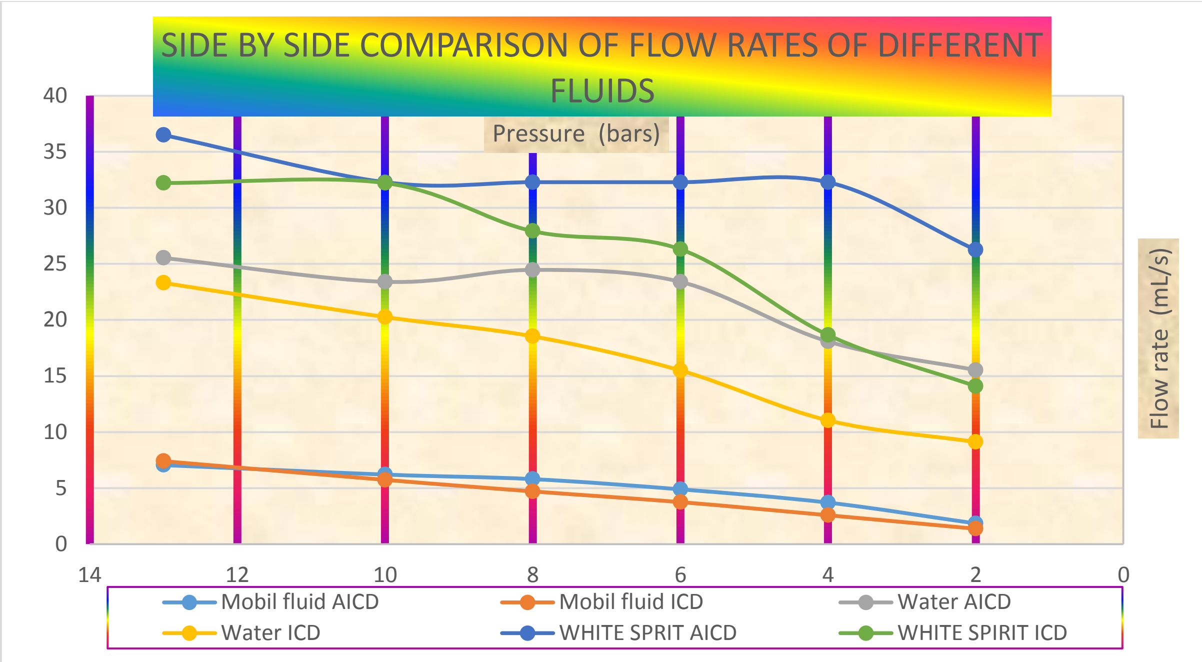

Figure 5.7: Combine plot showing different fluid behavior at same flow boundary conditions. Data is attached in Appendix A.6.

Taking a ratio of the flow rates of the fluids to that of water at 14 bars of pump pressure helps us to verify the accuracy of the above presented model. Through the Autonomous Inflow Control Nozzle the flow rate of the less dense dry white spirit exceeds that of the denser tap water by a factor of $36.49/25.53 = 1.42$. A similar calculation performed for the Conventional Inflow Control Device yields a factor of $32.23/23.31 = 1.38$. These values compare favorably with the model prediction of 1.118. However, the similarly less dense Mobil fluid 426 is observed not to conform to the presented model as it gives a less flow rate that the denser tap water when pumped at the same initial boundary conditions. The factor of comparison in this case is $7.06/25.53 = 0.28$ for the AICD and $7.41/23.31 = 0.32$ for the ICD; both of these factors are much less that the factor of 1.063 predicted by the model. We can therefore suggest that there exist a certain critical limit for viscosity, above which flow through an ICD or AICD nozzle is governed by viscosity and produces a laminar flow as observed with the Mobil fluid 426. Due to limitation in resources in terms of acquisition of multiple fluid specimens with varying properties, **a plot of fluid viscosities versus flow rates** which is necessary to clearly define the domain of viscous effect, has not been developed in this thesis project.

5.3 Investigation of flow regime in fluids

In the forgoing analysis we seek to establish a critical flow rate for each of the fluids based on a hypothetical transitional Reynolds number of 2300. Upon making comparison with data obtained from the laboratory, we would be able to conclusively determine the flow driving parameter of each fluid (i.e. either density or viscosity). This analysis is based on same boundary condition for pumping the three fluids.

$$Re = \frac{\rho v d}{\mu} - - - - - - 5.8$$

$$Where;\ Re = Reynolds\ Number$$

$$\rho = Density\ in\ \frac{kg}{m^3}$$

$$v = Velocity\ in\ \frac{m}{seconds}$$

$$d = Ball\ valve\ diameter\ in\ meters = 0.3 \times 10^{-3}\, m$$

$$\mu = Dynamic\ viscosity\ in\ \frac{pascal}{seconds}$$

$$But;\ v = \frac{Q}{A} - - - - - - 5.9$$

$$Where;\ \ Q = Flow\ Rate\ in\ \frac{m^3}{seconds}$$

$$A = Area\ in\ m^2\ = \frac{\pi}{4} d^2 = 7.065 \times 10^{-8}\, m^2$$

$$Implying;\ Re = \frac{\rho Q d}{\mu A} - - - - - - 5.10$$

$$Re - arranging\ yields;\ Q = \frac{Re\mu A}{\rho d} - - - - - - 5.11$$

$$Thus;\ Q_{supreme\ gear\ oil}^{critical} = \frac{2320 \times (198.8 \times 0.001) Pa.s \times 7.065 \times 10^{-8}\ m^2}{879.86\ \ kg/m^3 \times 0.3 \times 10^{-3}\ m}$$

$$= (1.23 \times 10^{-4}\ \ m^3/s \times 1000000) mL = 123.44\ \ mL/s$$

$$Q_{Mobil\ 426\ fluid}^{critical} = \frac{2320 \times (117 \times 0.001) Pa.s \times 7.065 \times 10^{-8}\ m^2}{884.22\ \ kg/m^3 \times 0.3 \times 10^{-3}\ m}$$

$$= (7.23 \times 10^{-5}\ \ m^3/s \times 1000000) mL = 72.29\ \ mL/s$$

$$Q_{Dry\ white\ spirit}^{critical} = \frac{2320 \times (4.9 \times 0.001) Pa.s \times 7.065 \times 10^{-8}\ m^2}{800.55\ \ kg/m^3 \times 0.3 \times 10^{-3}\ m}$$

$$= (3.344 \times 10^{-6}\ \ m^3/s \times 1000000) mL = 3.34\ \ mL/s$$

$$Q_{Water}^{critical} = \frac{2320 \times (1 \times 0.001) Pa.s \times 7.065 \times 10^{-8}\ m^2}{1000\ \ kg/m^3 \times 0.3 \times 10^{-3}\ m}$$

$$= (5.46 \times 10^{-7}\ \ m^3/s \times 1000000) mL = 0.55\ \ mL/s$$

Table 5.4 summarizes the critical flow rates calculated for the different fluids using the transitional Reynolds number of 2320. The will be used as a basis for determining the flow regime of the AICD and ICD nozzles.

SUMMARY OF CRITICAL FLOW RATES	
Fluids	$\mathbf{Q_{Fluid}^{critical}}$ **(mL/s)**
$Q_{\text{Supreme gear oil}}^{\text{critical}}$	123.44
$Q_{\text{Mobil 426 fluid}}^{\text{critical}}$	72.72
$Q_{\text{Dry white spirit}}^{\text{critical}}$	3.34
$Q_{\text{Water}}^{\text{critical}}$	0.55

Table 5.4: Summary of critical flow rates obtained for the different fluids.

The critical flow rate shown in Table 5.4 when compared to the plot in Figure 5.7 proves clearly that the white spirit and tap water are in the turbulent flow regime while the highly viscous Mobil 426 fluid is in the laminar regime. The claim about viscous effects on the Mobil 426 fluid is further consolidated by comparing the Supreme Gear Oil critical flow rate of 123.44 mL/seconds to the plot in Figure 5.4.

In order to conclusively authenticate the claim about laminar flow regime for Mobil 426 fluid and Supreme Gear Oil, we have changed the initial boundary conditions from that used in the figure above (i.e. valve stem opening has been changed from 0.3mm to 0.7mm) to allow a higher flow rate through the ball valve. The result of this is presented in Figure 5.8 below.

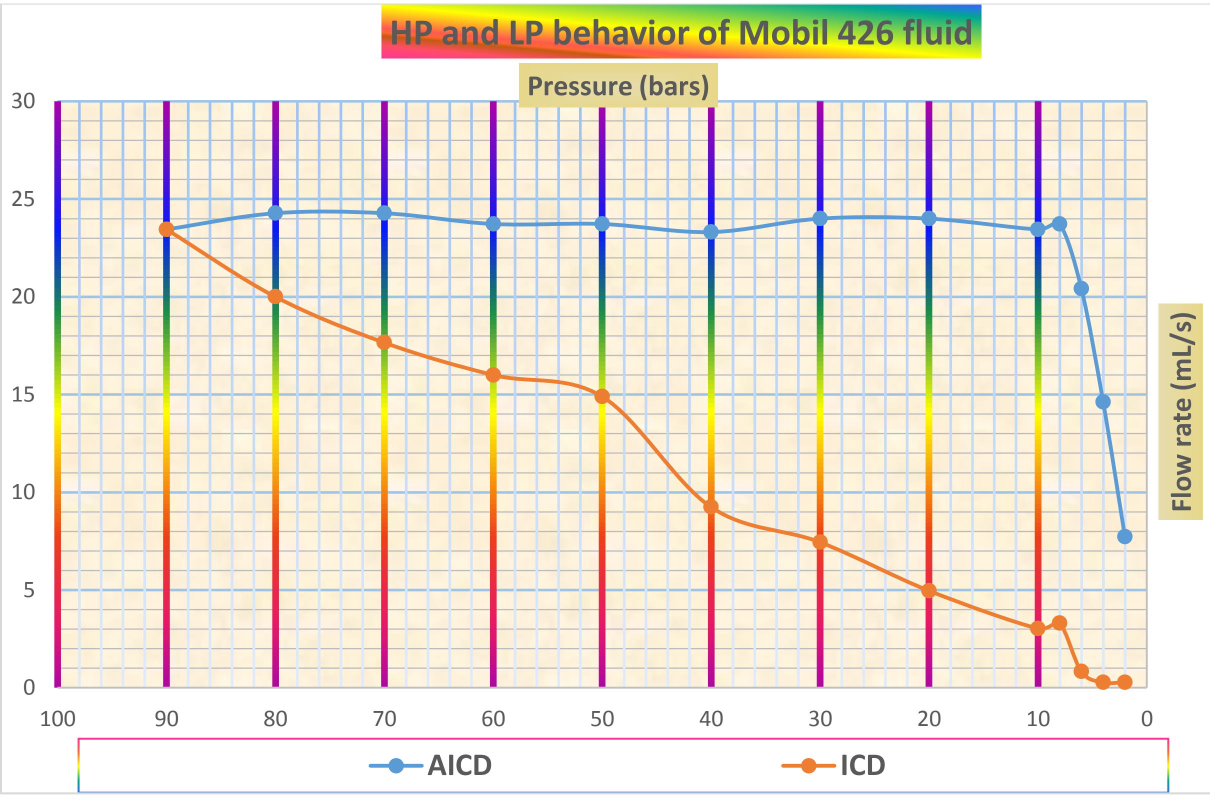

Figure 5.8: Plots of Mobil 426 at less conservative boundary condition. Data is given in Appendix A.7.

The term less conservative implies a larger valve opening of $0.7 \times 10^{-3}\,m$, which is a less accurate representation of the valve opening used downhole during a typical production operation. Generally the results obtained with the valve opening of $0.3 \times 10^{-3}\,m$ as presented in the previous sections of this chapter gives a more accurate depiction of a practical production scenario.

$$d = Ball\ valve\ diameter\ in\ \ meters = 0.7 \times 10^{-3}\, m$$

$$A = Area\ in\ \ m^2\ \ = \frac{\pi}{4} d^2 = 3.848 \times 10^{-7}\ m^2$$

$$Q = \frac{Re\mu A}{\rho d}$$

$$Thus;\ \ Q_{Mobil\ 426\ fluid}^{critical} = \frac{2320 \times (117 \times 0.001) Pa.s \times 3.848 \times 10^{-7}\ m^2}{884.22\ \ kg/m^3 \times 0.7 \times 10^{-3}\ m}$$

$$= (1.687 \times 10^{-4}\ \ m^3/s \times 1000000) mL = 168.7\ \ mL/s$$

Once again, when the critical flow rate of 168.7 mL/s is compared to the plot in Figure 5.8, it sufficiently puts the flow rates obtained at different pressures in the laminar domain. It is therefore safe to conclude that the flow of highly viscous Mobil fluid 426 through the ICD/AICD nozzle is governed by viscosity. This finding then presents a real problem as a constant flow rate cannot be guaranteed by the BECH AICD, since viscosity unlike density varies very significantly throughout the productive life of the reservoir.

5.4 Mobil fluid 426 – Bernoulli prediction VERSUS Actual flow rate from commercial ICD.

In the following analysis, we will apply the Bernoulli model to the non-Newtonian Mobil 426 fluid to predict the flow rates at different pressures and then compare the results with the experimental data obtained from the ICD nozzle. This is to establish the extent of conformance of the Mobil 426 fluid flow to the turbulent prediction given by the Bernoulli model. **Again this is performed on the basis of the same boundary conditions.**

Considering the inlet and outlet of the nozzle, the following equation is true.

$$\frac{{v_1}^2}{2} + gz_1 + \frac{P_1}{\rho} = \frac{{v_2}^2}{2} + gz_2 + \frac{P_2}{\rho} - - - - - 5.12$$

Since the nozzle inlet and outlet are at the same elevation and the velocity in the hose can be considered negligible when compared to the outlet velocity in the nozzle, the above equation reduces to the following;

$$\frac{\Delta P}{\rho} = \frac{v^2}{2}$$

$$\Delta P = \frac{\rho}{2} \times v^2 = \frac{\rho}{2} \times \frac{Q^2}{A^2}$$

$$Q = \sqrt{\frac{2A^2 \Delta P}{\rho}}$$

This then yields the following;

$$Q_{water} = \sqrt{\frac{2A^2 \Delta P_{water}}{\rho_{water}}}$$

And

$$Q_{oil} = \sqrt{\frac{2A^2 \Delta P_{oil}}{\rho_{oil}}}$$

Based on the boundary conditions;

$$\Delta P_{water} = \Delta P_{oil} - - - - - 5.13$$

And

$$A_{water} = A_{oil} - - - - - 5.14$$

Above equations can be written as follows;

$$Q_{water} = \sqrt{\frac{Constant}{\rho_{water}}}$$

And

$$Q_{oil} = \sqrt{\frac{Constant}{\rho_{oil}}}$$

Taking a ratio of equation 1 and 2 yields the following;

$$\frac{Q_{oil}}{Q_{water}} = \sqrt{\frac{\frac{Constant}{\rho_{oil}}}{\frac{Constant}{\rho_{water}}}} = \sqrt{\frac{\rho_{water}}{\rho_{oil}}}$$

This then implies the following for 2 data sets of pump pressures;

$$\frac{Q_{oil}}{Q_{water}} = \sqrt{\frac{\rho_{water}}{\rho_{oil}}} - - - - - 5.15$$

Equation 5.15 authenticates the turbulent relation shown in equation 5.16

$$\Delta P \sim \rho Q^2 - - - - - 5.16$$

Equation 5.16 implies the following;

$$\frac{\Delta P}{\rho Q^2} = Constant$$

Taking a ratio of 2 independent pump pressures (P_1 *and* P_2) and assuming an initial pump pressure ($P_{initial}$) of 0 bars in both cases, the following is obtained.

$$\frac{P_1}{\rho_{water} \times Q_{water}^2} = \frac{P_2}{\rho_{oil} \times Q_{oil}^2} - - - - - 5.17$$

Equation 5.17 holds true because the same boundary condition of pump pressure is applied irrespective of fluid properties. This equation can be re-arranged to make Q_{oil} the subject of the formula as follows.

$$Q_{oil} = \sqrt{\frac{P_2 \times \rho_w \times Q_{water}^2}{\rho_{oil} \times P_1}} - - - - - 5.18$$

Having established the above relationship, we can graphically illustrate the Bernoulli flow rate prediction for current commercial ICDs using calculated data set shown in Table 5.5. All flow rate calculations are based upon a reference flow rate of 23.45 mL/s obtained experimentally (See Appendix A.7) at a pump pressure of 90 bars.

SUMMARY OF FLOW RATES PREDICTED BY BERNOULLI MODEL	
Pump pressure (Bars)	$\mathbf{Q\ (mL/s)}$
90	23.45
60	20.36
40	16.62
20	11.75

Table 5.5: Presentation of flow rates predicted by the Bernoulli model using equation 5.18.

Using equation 5.18, a flow rate of 11.75 mL/Seconds is predicted at 20 bars for Mobil fluid 426 according to above equation when a reference pump pressure and flow rate of 90 bars and 23.45 mL/Seconds respectively are used. The statement above is demonstrated as follows;

$$Q_{oil} = \sqrt{\frac{20 \times 1000 \times 23.45^2}{884.22 \times 90}} = 11.75 \text{ mL/Seconds}$$

The model-predicted flow rate compares favorably to the actual flow rate of 4.96 mL/Seconds obtained from experiments giving an insignificant error. Hence we can emphatically conclude that the ICD nozzle conforms to Bernoulli Prediction. This implies that the flow rate of the Mobil 426 fluid should be turbulent. However, analysis shown in section 5.3 invalidates this claim due to high viscous effect thereby putting the fluid in a laminar flow regime.

Shown in Figures 5.9a and b below are graphical presentation of trend lines used to accurately determine the behavioral tendency of the Bernoulli model (i.e. either linear or quadratic), and also a presentation of how the prediction from the Bernoulli model compares with actual experimental data. Figure 5.9a presents a graph of the linear trend line while Figure 5.9b shows the polynomial trend line which mainly denotes a turbulent trend as seen in its quadratic equation.

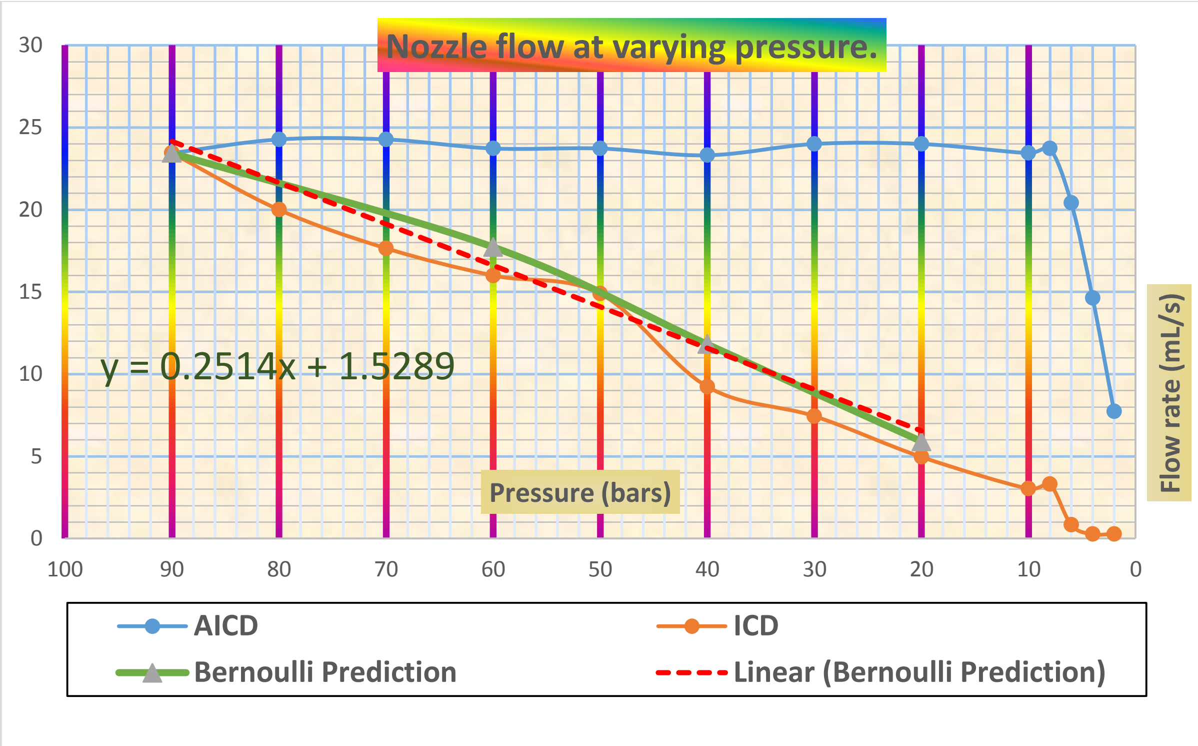

Figure 5.9a: Overlay of Bernoulli profile (linear trend line) on conventional ICD for Mobil 426 fluid. Data is given in Appendix A.7.

The linear trend line matches the Bernoulli prediction almost perfectly at 40 bars of pump pressure and below. This is a strong indication that the flow of highly viscous fluid within this pressure range is governed by viscosity and as such it is in the laminar regime according to the relation $(\rho \sim Q.)$

However, above 40 bars of pump pressure, the linear trend line shows significant disparity from Bernoulli expectations. This can potentially lead to the conclusion that the flow should be turbulent in this pressure range.

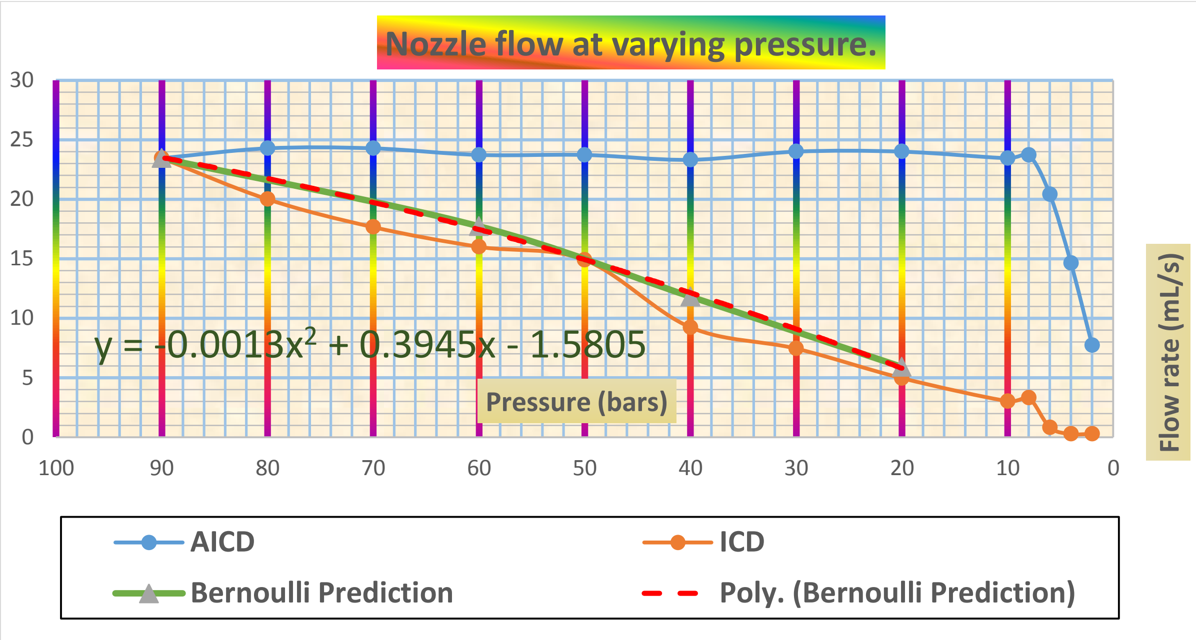

Figure 5.9b: Overlay of Bernoulli profile (polynomial trend line) on conventional ICD for Mobil 426 fluid. Data is given in Appendix A.7.

The plot above shows a strikingly close match between the polynomial trend line and the Bernoulli prediction above 40 bars of pump pressure. This conclusively implies that the flow of the Mobil 426 fluid through the nozzle should be in the turbulent regime (i.e. governed by density) at pump pressures above 40 bars. Furthermore the displayed polynomial equation $y = -0.0013x^2 + 0.3945x - 1.5805$ confirms that the square relationship between density and flow rate $(\rho \sim Q^2)$ is in operation.

However, Laminar flow is observed in laboratory data (see Appendix A.7) when compared to the calculated critical flow data in Section 5.3. This non-conformance is primarily owing to the high viscous effect of the Mobil 426 fluid. Un-avoidable variables encountered during collection of experimental data may have contributed to this non-conformance as well. These variables include the poor functioning state of our positive displacement pump which is observed to give pressure spikes as opposed to a smooth transition between pressures as observed during manual adjustment of ball valve. Furthermore, the poor functioning of our obsolete relief valve accounts for some of the non-conformance observed.

The observed decreasing trend in AICD flow rate below 8 bars of pump pressure, can be brought to the barest minimum by an iterative process of adjusting/fine tuning the distance between the inside piston and nozzle outlet in our AICD

6 CONCLUSION

6.1 Summary of findings

The ICD was initially developed in the early 1990s when water coning caused early water breakthrough in long horizontal wells offshore Norway. Due to the large pressure drop in the long horizontal wellbore completion, the production rates were higher at the heel of the well, leading to early water production. In addition to cost related to cleaning and disposal of produced water, a more severe effect was reduced recovery from the field. The oil at the very end of the well (the toe) was not efficiently produced.

A number of suppliers today offer ICDs for various applications. They present similar features, however some differences are seen. To avoid misunderstanding, an ICD can be seen as one or more nozzles installed in the production tubing. The main purpose is to restrict flow at given locations, e.g. near the heel of a horizontal well. The Bernoulli equation presented in earlier chapters of this thesis defines the relationships for nozzle parameters.

AICDs are better in depleted reservoirs as they control water and gas coning and produce the reservoir faster. In this thesis work, the applications of both ICDs and AICDs for high-viscosity/highly viscous oils have been successfully investigated. Preliminary findings are that with the ICD, viscosity plays an important role even at higher drawdown pressures. The AICD is fairly viscosity independent for lower pressures. For areas where higher oil viscosities are found, the AICD has potential to reduce coning and to deplete the reservoir faster. This experimental study also reveals that provided channeling is large enough to minimize viscous pressure drop outside the valve, the AICD is not so much affected by viscosity for high viscous fluids. Put simply, AICD valve opens up when reservoir pressure decreases.

The results obtained from the analysis presented in Chapter 5 would validate the conclusions listed below.

a) Today's commercial ICD is largely Darcy dependent implying that when reservoir pressure begins to deplete, flow through the ICD nozzle in a proportionate manner decreases as well.
b) An ICD reduces the Darcy dependence by introducing a choke. This choke is still sensitive to

reservoir and wellbore pressure.

c) Experiments have shown that the BECH AICD does guarantee a near constant flow rate in a manner that is Darcy independent for oil viscosities ranging from 1cP to about 198.8 cP. Further flow experiments for fluids with viscosities above 198.8cp were not performed due to limited capacity of flow equipment used in this thesis project.
d) Example 5.1 demonstrates the fact that the BECH AICD can indeed drain a reservoir 2 times as fast as today's commercial/conventional ICD. This obviously has positive economic implications on project.
e) Laboratory results shows that density governs flow in ICD and AICD nozzles when fluid with viscosities between 1cP and 116 cP are pumped. Above 116cP, viscosity driven characteristics are observed in a predominantly laminar flow. The stated broad range between 1cP and 116cP of fluid viscosities can be further investigated by flow testing multiple fluids with varying viscosities. This will create a more precise understanding of the turbulent versus laminar domain in a plot of **flow rate versus fluid viscosity**. Once again this has fallen beyond the scope of this thesis project due to limitations in resources.
f) Technically speaking, a well can be completed with minimum reservoir knowledge if the constant flow valve is used as it is independent on pressure drop variations.
g) It can be observed that water injection can greatly diminish the problems related to depletion. So, in these cases, the BECH AICD may not be so advantageous.
h) Also, when the reservoir is very thick, and the oil-water or gas-oil contacts are very far, a conventional ICD solution can be sufficient, or may not be required at all. Therefore, it is always important to analyze the reservoir to be produced before making a decision on **ICV versus ICD inclusion in completion design.**

6.2 Overview of viscous effects

A phenomena known as **viscous fingering** is usually evident in multi-phased porous media and has an overbearing effect on reservoir fracture conductivity, ESP performance, solvent displacement of heavy oil and relative permeability especially where there exists an unstable viscosity of reservoir oil overtime to mention a few.

Studies show that in a multi-phased reservoir, the recovery of a much higher fraction of the original highly viscous oil in place is attributable to the solution-gas drive mechanism which is very commonly referred to as foamy oil or bubbly oil. However, the mentioned mechanism does not give an exhaustive, crystal clear explanation of the reason behind the enhanced oil production in highly viscous reservoirs.

During production of highly viscous oils, excessive fatigue is introduced on beams, gear boxes and moving parts in general by imposing unusually high bending loads and torques. This scenario most times necessitates the use of exotic quality of material in the robust design of subsea equipment. In addition to this, there is a hike in project capital expenditure accrued from the implementation of highly sophisticated heating techniques and procedures to make the oil flow, such as seen in the SAGD process.

6.2.1 The fingering phenomena

Viscous fingering can be described as the manifestation of a finger-shaped interface between the displaced and displacing fluid occurring in a porous media where there exists either miscible or immiscible fluids in a mobile state. This effect is traceable to the instability of the viscous fluid being displaced by a more mobile fluid. The obvious variable which affects the degree of occurrence of the mentioned phenomena includes fluid mobility ratio, displacement velocity, distance of displacement and degree of packing of fluid molecules among others.

6.2.2 Theory of viscous coupling

Taking a 2-phased flow investigative approach, the viscous coupling effect or momentum transfer occurring in a porous media on a first impression basis, presents itself to be the driving mechanism for improved oil mobility in highly viscous oil reservoirs. Further experimental studies and subsequent development of capillary models has provided a new insight into the effect of viscosity ratio on relative permeability's and the importance of water lubrication in highly-viscous oil-water 2-phase flow.

6.3 Proposition for future study.

An in-depth experimental study of the aforementioned viscous fingering effect on porous media containing both miscible and immiscible fluids should be investigated in a future thesis work. This would consolidate on the results provided in this thesis work when performed with the aim of highlighting other governing parameters for the fingering effect, the merits and demerits thereof.

More so, for future work it would be suitable to employ the use of computational simulators to validate the experimentally and theoretically (i.e. Bernoulli predictions) obtained results, claims and deductions presented throughout the course of this thesis work.

A more complex experimental study which involves the configuration of a flow channel with undulations, to serve as a flow path from nozzle to tank would create an even more profound understanding of flow behavior and parameter governing properties in nozzles. This is considered true because an undulated flow path depicts more accurately, the way through the horizontal section of the well, as we know that no well is perfectly horizontal, and sometimes the geology study may suggest a more undulated trajectory, to find the most permeable zones of the reservoir. More so, this could be used to study the pressure drops encountered as the hydrocarbon makes its way into the production tubing.

In addition to this, an exhaustive field-data-based analysis of the potential economic benefits/pitfalls would further illuminate the grey areas associated with the inclusion of ICDs in completion design.

7 REFERENCES

1. AADNØY, B. S, SPE, University of Stavanger and GEIR HARELAND, G, SPE, University of Calgary. Analysis of Inflow Control devices. **SPE 122824, 2009.**
2. AADNØY, B. S. A Short Note on Inflow Performance Related to ICD's. University of Stavanger. Stavanger, 2012. Available at: <http://www.hansenenergy.biz/HANSEN_Energy_Solutions/ICDPerformance.pdf>. **Access in: 12 Jan. 2013.**
3. AADNØY, B. S. Facts and Fiction about Inflow Control Devices. University of Stavanger. 2012a. Available at: <http://www.hansenenergy.biz/HANSEN_Energy_Solutions/ICDPerformance.pdf>. **Access in: 12 Jan. 2013.**
4. AADNØY, B. S, AWANNEGBE EDOHAMEN PATRICK, SPE, University of Stavanger, DE AZEVEDO CABRAL RICARDO, University of San Paulo. Autonomous Inflow Control Device for Horizontal Wells in the Barents Sea. **SPE workshop in Harstad Norway, 2014.**
5. A. ALI DANESHY, Daneshy Consultants International, BOYUN GUO, University of Louisiana at Lafayette, VITALY KRASNOV, Rosneft, SERGEY ZIMIN, Rosneft. ICD Design: Revisiting Objectives and Techniques. **SPE 133234, 2010.**
6. ABDELFATTAH. T.A, GARCIA and G.A, BANERJEE, Baker Hughes Incorporated, GARCIA, L.A. SPE. Passive Inflow Control Device Autonomy – How much is too much?. **SPE/IADC 166730, 2013.**
7. ABDULLAH M. AL-DHAFEERI, Al-khafji Joint Operations (KJO); MAHMOUD ABD EL-FATTAH, SPE, Schlumberger; TAWAKOL I. MOHAMED; TAHA M. MOAWAD AND HANI A. BAJUNAID Al-khafji Joint Operations (KJO). Case Study: Utilizing of Inflow Control Device to Control Oil Wells from Water Production and Regulate Waterfront Encroachment. **OTC 24431, 2013.**
8. ABDULLAH M. QAHTANI, EXPEC ARC, Production Technology, Saudi Aramco. Flow Simulation in Inflow Control Valves Lattice Boltzmann Modeling. **SPE 136935, 2010.**
9. ALI MOJADDAM ZADEH, PER ARNE SLOTTE, ROBERT AASHEIM, ATLE JOHNSEN GYLLENSTEN, KRISTINE ARLAND, Statoil ASA. Optimal Inflow Control Devices Configurations for Oil Rim Reservoirs. **OTC 22963, 2012.**
10. BRANDON LEAST, STEPHEN GRECI, Halliburton; ANGEL WILEMAN, ADAM UFFORD, Southwest Research Institute. Fluidic Diode Autonomous Inflow Control Device Range 3B – Oil, Water and Gas Flow Performance Testing. **SPE 167379, 2013.**
11. DREW HEMBLING and ADEYINKA SOREMI, SPE, Saudi Aramco; NEALE CARTER, SPE, Tendeka;

GARTH NALDRETT, SPE, FlowQuest. **SPE 122448, 2009.**

12. E. DAVILA, R. ALMEIDA, I. VELA, J. PAZOS, K. COELLO, Petroamazonas; F. CHINELLATO, O. HUMBERT, Schlumberger; F. PORTURAS, Reslink. First Applications of Inflow Control Devices (ICD) in Open Hole Horizontal Wells in Block 15, Ecuador. **SPE 123008, 2009.**
13. ELIANA ARENAS, NORBERT DOLLE / Shell International Exploration and Production. Smart Water flooding Tight Fractured Reservoirs Using Inflow Control valves. **SPE 84193, 2003.**
14. ELIAS BIN ABLLAH, University Technology of Petronas; MUHAMMAD SANIF BIN MAULUT, Schlumberger; and SEAH CHIN LOONG, University Technology of Petronas. Application of Inflow Control valve in Water Injector Well: Case Study of Alpha Field. **SPE 144406, 2011.**
15. ESTHER CUI, SPE, BILL HAY, SPE, GONZALO A. GARCIA, SPE, Baker Hughes Incorporated. Inflow Control Device in Thin-Layer Bottom Water Drive Reservoir Enhances Oil Recovery in China South Sea. **SPE 167266, 2013.**
16. F.T. AL-KHELAIWI and V.M. BIRCHENKO, Heriot Watt University, SPE; M.R. KONOPCZYNSKI, Well Dynamics-Halliburton, SPE; and D.R. DAVIES, Heriot Watt University, SPE. Advanced Wells: A Comprehensive Approach to the Selection between Passive and Active Inflow-Control Completions. **SPE 132976, 2010.**
17. F.T. AL-KHELAIWI, SPE, Heriot-Watt University and Saudi Aramco, and D.R. DAVIES, SPE, Heriot-Watt University. Inflow Control Devices: Application and Value Quantification of a Developing Technology. **SPE 108700, 2007.**
18. GONZALO A. GARCIA, SPE, MARTIN P. CORONADO, SPE, and PAOLO GAVIOLI, SPE, Baker Hughes Incorporated. Identifying Well Completion Applications for Passive Inflow Control Devices. **SPE 124349, 2009.**
19. H. ASHEIM, SPE, NTNU, Trondheim-Norway. Analytical Solution of Dynamic Inflow Performance. **SPE 63307, 2000.**
20. HAAVARD AAKRE, InflowControl/Telemark University; BRITT HALVORSEN, Telemark University; BJORNAR WERSWICK, InflowControl; VIDAR MATHIESEN, InflowControl. Smart Well With Autonomous Inflow Control Valve Technology. **SPE 164348, 2013.**
21. Inflow Control Company located in Porsgrunn, Norway. Available at http://www.inflowcontrol.no/about-aicv-technology
22. IVAN VELA AND ROBERTO ALMEIDA, Petroamazonas; FRANCISCO FORTURAS and OLIVIER HUMBERT, Schlumberger. Well Conditioning Before and After the Installation of an ICD Completion Hardware: Block 15, Ecuador. **SPE 131526, 2010.**
23. J. AUGUSTINE, SPE, S. MATHIS, SPE, and H. NGUYEN, SPE, Baker Oil Tools and C. GANN, SPE,

and J. GILL, Vaalco Gabon (Etame) Inc. World's First Gravel-Packed Uniform Inflow Control Completion. **SPE 103195, 2006.**

24. J.D. ORTIZ-ARANGO and A. KANTZAS, SPE, University of Calgary, TIPM Laboratory. Visualization of viscous coupling effects in heavy oil reservoirs. **SPE/PS/CHOA 117675, 2008.**
25. JEANETTE GIMRE, University of Stavanger Master Thesis. Efficiency of ICV/ICD systems. **Spring semester 2012.**
26. Journal of Petroleum Technology, **January 2014** edition. Available at www.spe.org/jpt.
27. KAI SUN, SPE, Baker Hughes Incorporated, BOYUN GUO, SPE, University of Louisiana at Lafayette, and LUIGI SAPUTELLI, SPE, Hess Corporation. Applying Multi-Node Intelligent Well Technology for Active Control of Inflow Profile in Horizontal/Inclined Wells. **SPE 130490, 2010.**
28. KIM THORNTON AND RICARDO JORQUERA, Halliburton; and M. Y. SOLIMAN, SPE, Texas Technological University. Optimization of Inflow Control Device Placement and Mechanical Conformance Decisions Using a New Coupled Well-Intervention Simulator. **SPE 162471, 2012.**
29. Mannesmann Rexroth Engineering. Website - http://no.rs-online.com.
30. MEDHAT ABDOU, SPE, ADCO, ALI KSHADA, SPE, ADCO, MUHAMMAD SHAFIQ, SPE, Schlumberger, OLUSEGUN OGUNYEMI, SPE, Schlumberger, TEE SIN CHONG, SPE, ADCO, KARIM HADJAR, Schlumberger, EDMUND LEUNG, Schlumberger. Applied Production Completion Using Optimum Number of Inflow Control Devices. **SPE 138703, 2010.**
31. MICHEAL LORENZ, GENE RATTERMAN AND JODY AUGUSTINE; baker Oil Tools, SPE. Uniform Inflow Completion System Extends Economic Field Life: A Field Case Study and Technology Overview. **SPE 101895, 2006.**
32. OFFSHORE-TECHNOLOGY. Goliat Oil and Gas Field, Barents Sea, Norway. Net Resources International. Available at: <http://www.offshore-technology.com/projects/goliat/>. **Access in: 17 Feb., 2014.**
33. OYVIND GUSTAVSEN, OLAV MARTIN SELLE, FINN HALLSTEIN FADNES, PER EINAR SVELA, ERLEND GUDDING, and KARIN STENE, Statoil. Inflow Control Device Completion in a Scaling Environment: Findings and Experiences Obtained During Production Logging in the Heidrun Field. **SPE 134994, 2010.**
34. P.A. GOODE, SPE, and D.J. WILKINSON, SPE, Schlumberger-Doll Research. Inflow Performance of Partially Open Horizontal Wells. **SPE 19341, 1991.**
35. P. McELFRESH, C. WILLIAMS, and G. GARFILED, Baker Oil Tools. Maximizing Inflow

Performance in Soft Sand Completions Using New One-Trip Sand Control Liner Completion Technology. **SPE 94622, 2005.**

36. RUDY W.F. WELLING, FRANZ MARKETZ, RIYADH MOOSA, NOHA RIYAMI, EDWARD J. FOLLOWS, GERBERT DE BRUIJN and KHALID HOSNY, Petroleum Development Oman. Inflow Profile Control in Horizontal Wells in a Fractured Carbonate Using Swellable Elastomers. **SPE 105709, 2007.**
37. SAIF ALI AL ARFI, SALEM EL ABD SALEM, ASHRAF AL-SAIID KESHKA, SALEM AL-BAKR, ABDEL HAMEED AMIRI, and ABDALLA YOUSSEF EL-BARBARY, ADCO, and MAGDI ELASMAR and OMAR Y. MOHAMED, Baker oil Tools. Inflow Control Device and Innovative Completion Solution From Extended Wellbore to Extended Well Life Cycle. **IPTC 12486, 2008.**
38. SUDIPTYA BANERJEE, TARIK ABDELFATTAH, & HANG NGUYEN, SPE, Baker Hughes. Benefits of Passive Inflow Control Devices in a SAGD Completion. **SPE 165478, 2013.**
39. SVEIN M. SKJAEVELAN, University of Stavanger and JON KLEPPE, Norwegian University of Science and Technology. Recent Advances in Improved Oil Recovery Methods for North Sea Sandstone Reservoirs. **SPOR Monograph, 1992.**
40. T.A. INGLIS. Petroleum Engineering and Development Studies, Volume 2, Directional Drilling. **1987.**
41. T.D. BUI, SPE, Texas A&M University; O.A. VICENCIO, SPE, UT Austin; s. Sinha, SPE, R. KALITA, SPE and Y. JALADI, SPE, Schlumberger. In-Situ Diagnosis of Inflow Behavior in Horizontal Wells. **SPE 84873, 2003.**
42. T. MOEN, SPE, Reslink AS, and H. ASHEIM, SPE, NTNU. Inflow Control Device and Near-Wellbore Interaction, **SPE 112471, 2008.**
43. TARIK A. ABDELFATTAH, SUDIPTYA BANERJEE, GONZALO A. GARCIA, and HANG NGUYEN, SPE, Baker Hughes Incorporated. Effective Use of Passive Inflow Control Devices to Improve the Field Development Plan. **SPE 146521, 2012**.
44. TURHAN YILDIZ, SPE, The University of Tulsa. Inflow Performance Relationship for Perforated Horizontal Wells. **SPE 67233, 2001.**
45. V.M. BIRCHENKO and F.T. AL-KHELAIWI, SPE, Heriot-Watt University; M.R. KONOPCZYNSKI, SPE, WellDynamics (a Halliburton Company); and D.R. DAVIES, SPE, Heriot-Watt University. Advanced Wells: How to make a choice between Passive and Active Inflow-Control Completions. **SPE 115742, 2008.**
46. VIDAR MATHIESEN, BJORNAR WERSWICK AND HAAVARD AAKRE, InflowControl. The Next Generation Inflow Control, the Next Step to Increased Oil Recovery on the Norwegian

Continental Shelf. **SPE 169233, 2014.**

47. VIDAR MATHIESEN, HAAVARD AAKRE, BJORNAR WERSWICK, GEIR ELSETH, Statoil ASA. The Autonomous RCP Valve – New Technology for Inflow Control in Horizontal Wells. **SPE 145737, 2011.**
48. ZHUOYL LI, SPE, Schlumberger; PRESTON FERNANDES, SPE, Chevron; and D. ZHU, SPE, Texas A&M University. Understanding the Roles of Inflow-Control Devices in Optimizing Horizontal-Well Performance. **SPE 124677, 2011**.

8 APPENDICES

A.1 Risk analysis report for laboratory testing

Department (institute/section): Institute of Petroleum Engineering

Date of risk assessment: 9/03/2014

Definition of area that is risk assessed (with limitations, premise and simplifications):

a) **Room:** E-351
b) **Activity /lab work:** E-351

Risk assessment performed by:

Edohamen Awannegbe – UiS master thesis student.

Document information:

Version: 2

Valid from date: 01/01/2014

Approved by/ Signature laboratory manager /Lab engineer: Dr. Jostein Djuve

Purpose for RA: To investigate the flow regime and flow rates of highly viscous oils when pumped through the nozzles of both a Conventional ICD and Autonomous ICD.

General description of work: The task involves the use of a 100 bar rated pump in pumping fluids with viscosities of 0.5 centipoise and higher (typical viscosities obtainable in the North Sea). The experimental set/up comprises of a 100 bar rated pump, Conventional Inflow Control Device, Autonomous Inflow Control Device (patented by Prof. Aadnøy), 2 choke valves, 3 ball valves, 1 pressure feedback valve, 2 pressure gauges (1 calibrated to read 1 bar – 15 bars and the other reads 1 bar – 150 bars with no calibration below 10 bars), a faucet to supply feed water to the pump, a tank to carry pumped fluid and provide housing that enables measurement of fluid throw.

Table A.1.1 below shows the chemical hazards connected with the flow experiments performed in this thesis project. Also presented are the corresponding risk and safety phrases for each chemical.

LIST OF CHEMICAL CONSTITUENTS OF EXPERIMENTED FLUIDS AND ASSOCIATED HAZARDS			
Chemicals used	**R - phrases**	**S - phrases**	**Should be substituted**
MOBILFLUID 426: ZINC DITHIOPHOSPHATE, and CALCIUM SULFONATE	Excessive exposure may result in eye, skin or respiratory irritation.	Use of safety glasses, aprons, gloves. Use of a suction system / exhaust ventilation. Put inside a fume hood (laboratory ventilation system). Use of Basic Rules of Hygiene.	No.
WHITE SPIRIT: BENZENE, and NAPHTHA (PETROLEUM) HYDROESULPHURISED	Excessive exposure may result in eye, skin or respiratory irritation.	Use of all above. If ventilation is insufficient, suitable respiratory protection must be provided.	No.
20W-50: Mixture of hydro treated and hydrocracked base oil (petroleum)	Eye contact, Skin contact, Inhalation, and Ingestion: like above	Use all above.	No.

Table A.1.1: Identified chemical hazards associated with thesis flow experiments.

Table A.1.2 presents the operational risks connected with the flow experiments performed in this thesis project. Also presented are the mitigating actions and their completion status.

LIST OF LAB OPERATIONS AND DANGER POSED TO HEALTH, EQUIPMENT AND ENVIRONMENT				
Operations / Task	**Risk: (What can go wrong)?**	**Measure**	**Responsible (deadline: as soon as possible)**	**Completion status.**
Running the operational sequence of pumping and measuring fluid throw	Entire apparatus is placed at a height of 93 cm from the floor inside a fume hood but without adequate mounting to eliminate possibility of unwanted movement and tripping.	Experimental apparatus is operated as is. Precautionary measure is taken by the use of adequate personal protective equipment to prevent injury in case of tripping. The equipment is maintained in the most stable and safe position. As an added protection, it is operated from a fume hood/enclosure.	Edohamen Awannegbe and Ricardo Azevedo	Yes
Running the operational sequence of pumping and measuring fluid throw	Tripping of the equipment could lead to physical injury of experimentalist.	Experimental apparatus is operated as is. Precautionary measure is taken by the use of adequate personal protective equipment to prevent injury in case of tripping. As an added protection, it is operated from a fume hood/enclosure	Edohamen Awannegbe and Ricardo Azevedo	Yes

Undesired nearness of pressurized equipment to experimentalist.	There was the possibility of the fluid to spill to the floor below OR on the experimentalist while taking throw measurements. This is due to the fact that measurement of fluid throw requires that the experimentalist gets positioned very close to the throw.	Proper use of personal protective equipment such as safety glasses, and coverall. Taking extra precaution to avoid walking on floor with spilled fluid. Placement of experimental apparatus in the fume hood mitigates this problem as well.	Edohamen Awannegbe and Ricardo Azevedo	Yes
Operation of highly sensitive pump.	There is the possibility of the relief valve to fail and subsequently give a huge pressure surge while bleed line is been closed. This can cause irreparable damage to the pump and equipment.	Procurement of a new relief valve that functions precisely to desired pressure setting with near zero percentage of error. A different but also pre-used relief valve was used, and the pressure regulation became better.	UiS - Institute of Petroleum Technology.	No
Failure of 10 bar rated relief valve.	This could potentially occur as pump is rated at 100 bars. The immediate consequence of a surge in pressure during low pressure pumping is the failure of the ball valve.	Procurement of a relief valve with pressure rating of 100 bars or more. A different but pre-used relief valve was used and the pressure regulation became better.	UiS - Institute of Petroleum Technology.	No
Over-pressure of pump.	This can lead to breakage of hoses and flow lines.	Hose thickness design and material selection should adequately withstand over-pressure from pump. And now the relief valve is limiting the pressure under the safe limits.	UiS - Institute of Petroleum Technology.	Yes

Uncontrollable spread of fluid at approximately half way through the parabolic path of the throw.	This could potentially form a basis for slip hazard as spillage gets collected on the floor. This is an issue since the distance from the flow to the floor is only 1.30 meters.	Proper use of personal protective equipment such as safety glasses, and coverall. Taking extra precaution to avoid walking on floor with spilled fluid. Placement of experimental apparatus in the fume hood mitigated this problem as well.	Edohamen Awannegbe and Ricardo Azevedo	Yes
Uncontrollable spread of fluid at approximately half way through the parabolic path of the throw.	This would also cause reaction once in contact with human skin.	Use of coveralls and face mask when taking measurement of fluid throw, if necessary. But placement of experimental apparatus in the fume hood mitigated this problem as well.	Edohamen Awannegbe and Ricardo Azevedo	Yes
Fumes generated during pumping of oil.	In a case of non-activation of suction system due to negligence or outright suction system failure, inhaled fumes can have detrimental effect on respiratory system.	Use of respirators and proper ventilation. Placement of experimental apparatus in the fume hood mitigated this problem as well.	Edohamen Awannegbe and Ricardo Azevedo/ UiS - Institute of Petroleum Technology.	Yes

Poor ergonomics in taking fluid throw measurements.	The height where equipment is positioned necessitates an awkward posture of the experimentalist while taking measurements of fluid throw. This is based on the position/orientation of the arms (discomforting raising) and neck (abnormal bending) during such measurements. Experientially, this causes a lot of strain on the human body and as such can hamper efficiency in long duration test runs.	Taking breaks in between measurement.	Edohamen Awannegbe and Ricardo Azevedo	Yes
Repeated test operation	This can cause fatigue on human body and thus hamper accuracy of measurements.	Taking breaks in between measurement.	Edohamen Awannegbe and Ricardo Azevedo	Yes
Inadequate cleaning of equipment's (i.e. pumps, hoses, tank, area surrounding experimental set-up) while transiting from one fluid to another having different properties.	Use of table paper towel proves to be inefficient in cleaning oil spill.	Placement of experimental apparatus in the fume hood mitigated this problem as well. Anyway, a red bin will be available, to put the waste, if any cleaning is necessary.	UiS - Institute of Petroleum Technology.	Yes

Use of compressed air to blow hoses before pumping another fluid.	Non-precise fitting of compressed air unit into hoses.	It is not being used, so there is no risk.	UiS - Institute of Petroleum Technology.	No
Noise from pump	It is observed that up to 20 DB of noise occurs while pumping the highly viscous Mobil 426 fluid.	Use of hearing protection, when necessary. But the pump was lubricated, which reduced the noise considerably.	Edohamen Awannegbe and Ricardo Azevedo.	Yes.

Table A.1.2: Summary of operational hazards encountered during flow experiments. Listed also is a set of action items that can potentially prevent the occurrence of these hazards, the responsible parties and completion status of each line item.

A.2 Experimental data for Tap Water.

CALIBRATION RUNS (WATER)					
Reference volume	1	liter	0.001	m^3	
Reference Throw (AICD)	0.8	meters	Referene Throw (ICD)	0.8	meters
Reference pressure	1	bar			
Reference temperature	20	°C			
	AICD				
1st run	58.83	seconds			
2nd run	58.68	seconds			
Q from 1st run	1.69981E-05	m^3/seconds			
Q from 2nd run	1.70416E-05	m^3/seconds			
$Q^{AVERAGE}$	1.70199E-05	m^3/seconds			
	ICD				
1st run	58.83	seconds			
2nd run	58.68	seconds			
Q from 1st run	1.69981E-05	m^3/seconds			
Q from 2nd run	1.70416E-05	m^3/seconds			
$Q^{AVERAGE}$	1.70199E-05	m^3/seconds			

TAP WATER									
		Throws							
Pump Pressure (bar)	Pump Pressure (Pa)	AICD (cm)	ICD (cm)	AICD (m)	ICD (m)	Q^{AICD} (m^3/sec)	Q^{ICD} (m^3/sec)	Q^{AICD} (mL/sec)	Q^{ICD} (mL/sec)
16	1600000	155.5	155.5	1.555	1.555	3.30823E-05	3.30823E-05	33.08234477	33.08234477
14	1400000	155.5	141.5	1.555	1.415	3.30823E-05	3.01039E-05	33.08234477	30.10387
12	1200000	150.5	129	1.505	1.29	3.20186E-05	2.74445E-05	32.01860378	27.44451753
10	1000000	150.5	115	1.505	1.15	3.20186E-05	2.4466E-05	32.01860378	24.46604276
9	900000	150.5	105	1.505	1.05	3.20186E-05	2.23386E-05	32.01860378	22.33856078
8	800000	150.5	100	1.505	1	3.20186E-05	2.12748E-05	32.01860378	21.27481979
7	700000	146	90	1.46	0.9	3.10612E-05	1.91473E-05	31.06123689	19.14733781
6	600000	146	80	1.46	0.8	3.10612E-05	1.70199E-05	31.06123689	17.01985583
5	500000	146	72	1.46	0.72	3.10612E-05	1.53179E-05	31.06123689	15.31787025
4	400000	146	57	1.46	0.57	3.10612E-05	1.21266E-05	31.06123689	12.12664728
3	300000	146	48	1.46	0.48	3.10612E-05	1.02119E-05	31.06123689	10.2119135
2	200000	141.5	35	1.415	0.35	3.01039E-05	7.44619E-06	30.10387	7.446186927
0	0	103.5	0	1.035	0	2.20194E-05	0	22.01943848	0

Table A.2: Laboratory data obtained during the calibration and flow testing of Tap Water at room temperature.

A.3 Experimental data for Dry White Spirit

CALIBRATION RUNS (DRY WHITE SPIRIT)					
Reference volume	1	liter	0.001	m^3	
Reference Throw (AICD)	0.8	meters	Reference Throw (ICD)	0.5	meters
Reference pressure	1	bar			
Reference temperature	20	°C			
	AICD				
1st run	42.28	seconds			
2nd run	47.02	seconds			
Q from 1st run	2.36518E-05	m^3/seconds			
Q from 2nd run	2.12675E-05	m^3/seconds			
$Q^{AVERAGE}$	2.24597E-05	m^3/seconds			
	ICD				
1st run	75	seconds			
2nd run	74	seconds			
Q from 1st run	1.33333E-05	m^3/seconds			
Q from 2nd run	1.35135E-05	m^3/seconds			
$Q^{AVERAGE}$	1.34234E-05	m^3/seconds			

DRY WHITE SPIRIT									
		Throws				Scaled Flow rates			
Pump Pressure (bar)	Pump Pressure (Pa)	AICD (cm)	ICD (cm)	AICD (m)	ICD (m)	Q^{AICD} (m^3/sec)	Q^{ICD} (m^3/sec)	Q^{AICD}(mL/sec)	Q^{ICD}(mL/sec)
13	1300000	130	130	1.3	1.3	3.6497E-05	3.49009E-05	36.49700484	34.9009009
10	1000000	115	120	1.15	1.2	3.22858E-05	3.22162E-05	32.28581197	32.21621622
8	800000	115	104	1.15	1.04	3.22858E-05	2.79207E-05	32.28581197	27.92072072
6	600000	115	98	1.15	0.98	3.22858E-05	2.63099E-05	32.28581197	26.30990991
4	400000	115	69.5	1.15	0.695	3.22858E-05	1.86586E-05	32.28581197	18.65855856
2	200000	93.5	52.5	0.935	0.525	2.62498E-05	1.40946E-05	26.24976886	14.09459459

Table A.3: Laboratory data obtained during the calibration and flow testing of Dry White Spirit at room temperature.

A.4 Experimental data for Mobil 426 Fluid 4W-10

CALIBRATION RUNS				
Reference volume	1	liter	0.001	m^3
Reference Throw	0.7	meters		
Reference pressure	50	bars		
Reference temperature	20	° C		
	AICD			
1st run	41.11	seconds		
2nd run	39.23	seconds		
Q from 1st run	2.4325E-05	m^3/seconds		
Q from 2nd run	2.54907E-05	m^3/seconds		
$Q^{AVERAGE}$	2.49078E-05	m^3/seconds		
	ICD			
1st run	41.76	seconds		
2nd run	41.32	seconds		
Q from 1st run	2.39464E-05	m^3/seconds		
Q from 2nd run	2.42014E-05	m^3/seconds		
$Q^{AVERAGE}$	2.40739E-05	m^3/seconds		

MOBIL FLUID 426									
1ST RUN									
		Throws				Scaled Flow rates			
Pump Pressure (bar)	Pump Pressure (Pa)	AICD (cm)	ICD (cm)	AICD (m)	ICD (m)	Q^{AICD} (m^3/sec)	Q^{ICD} (m^3/sec)	Q^{AICD} (mL/sec)	Q^{ICD} (mL/sec)
50	5000000	77	77	0.77	0.77	2.73986E-05	2.64812E-05	27.39862271	26.48124349
40	4000000	81	71.5	0.81	0.715	2.88219E-05	2.45897E-05	28.82192778	24.58972609
30	3000000	74.5	47.5	0.745	0.475	2.65091E-05	1.63358E-05	26.50905704	16.33583202
20	2000000	91	39	0.91	0.39	3.23802E-05	1.34126E-05	32.38019047	13.41257787
10	1000000	81	27	0.81	0.27	2.88219E-05	9.28563E-06	28.82192778	9.285630833

2ND RUN									
		Throws							
Pump Pressure (bar)	Pump Pressure (Pa)	AICD (cm)	ICD (cm)	AICD (m)	ICD (m)	Q^{AICD} (m^3/sec)	Q^{ICD} (m^3/sec)	Q^{AICD} (mL/sec)	Q^{ICD} (mL/sec)
50	5000000	77	77	0.77	0.77	2.73986E-05	2.64812E-05	27.39862271	26.48124349
40	4000000	76	63	0.76	0.63	2.70428E-05	2.16665E-05	27.04279644	21.66647194
30	3000000	77	52.5	0.77	0.525	2.73986E-05	1.80554E-05	27.39862271	18.05539329
20	2000000	82.5	37.5	0.825	0.375	2.93557E-05	1.28967E-05	29.35566719	12.89670949
10	1000000	80	22	0.8	0.22	2.84661E-05	7.56607E-06	28.46610152	7.566069567

Table A.3: Laboratory data obtained during the calibration and flow testing of Mobil 426 Fluid at room temperature.

A.5 Experimental data for Supreme Gear Oil 20W-50

CALIBRATION RUNS				
Reference volume	1	liter	0.001	m^3
Reference Throw AICD	0.58	meters		
Reference pressure	60	bar		
Reference temperature	20	° C		
	AICD/ICD			
1st run	62	seconds		
2nd run	63	seconds		
Q from 1st run	1.6129E-05	m^3/seconds		
Q from 2nd run	1.5873E-05	m^3/seconds		
$Q^{AVERAGE}$	1.6001E-05	m^3/seconds		

Supreme 20W-50 mixed with Mobil 426									
		Throws				Scaled Flow rates			
Pump Pressure (bar	Pump Pressure (Pa)	AICD (cm)	ICD (cm)	AICD (m)	ICD (m)	Q^{AICD} (m^3/sec	Q^{ICD} (m^3/sec)	Q^{AICD} (mL/sec)	Q^{ICD} (mL/sec)
90	9000000	96	96	0.96	0.96	2.64845E-05	2.64845E-05	26.48445363	26.48445363
80	8000000	88.5	83.5	0.885	0.835	2.44154E-05	2.3036E-05	24.41535569	23.03595706
60	6000000	92	70	0.92	0.7	2.53809E-05	1.93116E-05	25.38093472	19.31158077
50	5000000	89	56.5	0.89	0.565	2.45533E-05	1.55872E-05	24.55329555	15.58720448
40	4000000	102.5	45.5	1.025	0.455	2.82777E-05	1.25525E-05	28.27767184	12.5525275
30	3000000	92	40	0.92	0.4	2.53809E-05	1.10352E-05	25.38093472	11.03518901
20	2000000	90	33.5	0.9	0.335	2.48292E-05	9.24197E-06	24.82917527	9.241970796
10	1000000	85	25.5	0.85	0.255	2.34498E-05	7.03493E-06	23.44977665	7.034932994
8	800000	90	28	0.9	0.28	2.48292E-05	7.72463E-06	24.82917527	7.724632308
6	600000	85	23	0.85	0.23	2.34498E-05	6.34523E-06	23.44977665	6.345233681
4	400000	60	10	0.6	0.1	1.65528E-05	2.7588E-06	16.55278352	2.758797253
2	200000	33.5	0	0.335	0	9.24197E-06	0	9.241970796	0

Table A.4: Laboratory data obtained during the calibration and flow testing of Supreme Gear Oil at room temperature.

A.6 Experimental flow rate data for the fixed boundary condition

DRY WHITE SPIRIT									
		Throws				Scaled Flow rates			
Pump Pressure (bar)	Pump Pressure (Pa)	AICD (cm)	ICD (cm)	AICD (m)	ICD (m)	Q^{AICD} (m^3/sec)	Q^{ICD} (m^3/sec)	Q^{AICD} (mL/sec)	Q^{ICD} (mL/sec)
13	1300000	130	120	1.3	1.2	3.6497E-05	3.22162E-05	36.49700484	32.21621622
10	1000000	115	120	1.15	1.2	3.22858E-05	3.22162E-05	32.28581197	32.21621622
8	800000	115	104	1.15	1.04	3.22858E-05	2.79207E-05	32.28581197	27.92072072
6	600000	115	98	1.15	0.98	3.22858E-05	2.63099E-05	32.28581197	26.30990991
4	400000	115	69.5	1.15	0.695	3.22858E-05	1.86586E-05	32.28581197	18.65855856
2	200000	93.5	52.5	0.935	0.525	2.62498E-05	1.40946E-05	26.24976886	14.09459459
TAP WATER									
Pump Pressure (bar)	Pump Pressure (Pa)	AICD (cm)	ICD (cm)	AICD (m)	ICD (m)	Q^{AICD} (m^3/sec)	Q^{ICD} (m^3/sec)	Q^{AICD} (mL/sec)	Q^{ICD} (mL/sec)
13	1300000	120	115	1.2	1.15	2.55298E-05	2.33051E-05	25.52978375	23.30505203
10	1000000	110	100	1.1	1	2.34023E-05	2.02653E-05	23.40230177	20.26526264
8	800000	115	91.5	1.15	0.915	2.4466E-05	1.85427E-05	24.46604276	18.54271531
6	600000	110	76.5	1.1	0.765	2.34023E-05	1.55029E-05	23.40230177	15.50292592
4	400000	85	54.5	0.85	0.545	1.80836E-05	1.10446E-05	18.08359682	11.04456814
2	200000	73	45	0.73	0.45	1.55306E-05	9.11937E-06	15.53061845	9.119368187
MOBIL FLUID 426									
Pump Pressure (bar)	Pump Pressure (Pa)	AICD (cm)	ICD (cm)	AICD (m)	ICD (m)	Q^{AICD} (m^3/sec)	Q^{ICD} (m^3/sec)	Q^{AICD} (mL/sec)	Q^{ICD} (mL/sec)
13	1300000	104.5	104.5	1.045	1.045	7.05847E-06	7.40877E-06	7.058465656	7.40876593
10	1000000	92	81	0.92	0.81	6.21415E-06	5.74268E-06	6.214151582	5.742679812
8	800000	86	66.5	0.86	0.665	5.80888E-06	4.71467E-06	5.808880827	4.714669228
6	600000	72.5	53	0.725	0.53	4.89702E-06	3.75756E-06	4.897021627	3.757555926
4	400000	55	36.5	0.55	0.365	3.71498E-06	2.58775E-06	3.714981924	2.587750779
2	200000	27.5	19.5	0.275	0.195	1.85749E-06	1.3825E-06	1.857490962	1.382496992

Table A.6: Laboratory data obtained using fixed conservative boundary conditions for the flow experiment of Tap Water, Dry White Spirit and Mobil 426 Fluid.

A.7 Experimental data for less conservative plot of Mobil 426 flow rate

CALIBRATION RUNS				
Reference volume	1	liter	0.001	m^3
Reference Throw AICD	0.58	meters		
Reference pressure	60	bar		
Reference temperature	20	° C		
	AICD/ICD			
1st run	62	seconds		
2nd run	63	seconds		
Q from 1st run	1.6129E-05	m^3/seconds		
Q from 2nd run	1.5873E-05	m^3/seconds		
$Q^{AVERAGE}$	1.6001E-05	m^3/seconds		

MOBIL FLUID 426									
		Throws				Scaled Flow rates			
Pump Pressure (bar)	Pump Pressure (Pa)	AICD (cm)	ICD (cm)	AICD (m)	ICD (m)	Q^{AICD} (m^3/sec)	Q^{ICD} (m^3/sec)	Q^{AICD} (mL/sec)	Q^{ICD} (mL/sec)
90	9000000	85	85	0.85	0.85	2.34498E-05	2.34498E-05	23.44977665	23.44977665
80	8000000	88	72.5	0.88	0.725	2.42774E-05	2.00013E-05	24.27741582	20.00128008
70	7000000	88	64	0.88	0.64	2.42774E-05	1.76563E-05	24.27741582	17.65630242
60	6000000	86	58	0.86	0.58	2.37257E-05	1.6001E-05	23.72565637	16.00102407
50	5000000	86	54	0.86	0.54	2.37257E-05	1.48975E-05	23.72565637	14.89750516
40	4000000	84.5	33.5	0.845	0.335	2.33118E-05	9.24197E-06	23.31183679	9.241970796
30	3000000	87	27	0.87	0.27	2.40015E-05	7.44875E-06	24.0015361	7.448752582
20	2000000	87	18	0.87	0.18	2.40015E-05	4.96584E-06	24.0015361	4.965835055
10	1000000	85	11	0.85	0.11	2.34498E-05	3.03468E-06	23.44977665	3.034676978
8	800000	86	12	0.86	0.12	2.37257E-05	3.31056E-06	23.72565637	3.310556703
6	600000	74	3	0.74	0.03	2.04151E-05	8.27639E-07	20.41509967	0.827639176
4	400000	53	1	0.53	0.01	1.46216E-05	2.7588E-07	14.62162544	0.275879725
2	200000	28	1	0.28	0.01	7.72463E-06	2.7588E-07	7.724632308	0.275879725

Table A.7: Laboratory data obtained using less conservative boundary conditions for the flow experiment of Mobil 426 Fluid.

A.8 Typical NCS fluid viscosities

Field	Group/ Form.	Age	T	D m ss	owc m ss	go/wc m ss	h_t m	h_n m	Θ °	h_g m	h_o m	ϕ %	k_h md	$\frac{k_v}{k_h}$	S_{wi} %	S_{orw} %
Balder	Heimdal	P	au	1680	1760	-	116	95	0-2	-	80	33	1-10 D	0.1-0.5	85	15
Brage	Statfj.	EJ	h	2300	2381	-	110	88	0	-	61	23	1 D	0.1-0.2	68	15
	Fensfj.	LJ	an	2080	2149	-	35	20	1-2	-	27	26	100	0.1-0.4	48	22
Draugen	Rogn	LJ	an	1596	1638	-	0-46	0-46	-	-	0-37	32	6-7 D	0.6-0.7	72-85	30-35
Gullf.	Brent	MJ	u	1740	1947	-	250-300	190	12	-	207	31	3.2 D	0.5-0.9	80	30
	Cook	EJ	u	1750	2090	-	50-75	48	0-15	-	340	28	550	0.05-0.2	72	21
	Statfj.	EJ	u	1860	2028	-	175	105	1-2	-	168	27	1 D	0.5	85	30
Gullf.-S	Brent	MJ	u	2850			300	135	17	0-470	5-250	20	5-250	0.1	70-95	32
	Statfj.	EJ	u	3000	3365	3222	200	170	17	222	143	20	0.01-3 D	0.1	60-85	28
	Lunde	LT	a	3250	3680	-	>420	>50	17	-		15	0-20	0.1	40-70	
Gyda	Farsund	LJ	au	3700	4155	-	50	45	4	-	45	17	30	0.1-1	47-83	15
Heidrun	Fangst	MJ	h	2080	2478	2283	70	63	7	203	195	28	0.7-20 D	0.9	86-97	25-35
	Tilje	EJ	h	2100	2452	2292	120	90	6	203	130	25	0.07-2 D	0.5	51-75	12-25
	Åre	EJ	h	2240	2415	2314	205	100	3	63	130	27	0.1-10 D	0.1	60-71	
Oseberg	Brent	J	ef	2120	2711	2497	186	111	8	377	214	23	0.5-3.5 D	0.1-1	60-89	27
Smørb.	Garn	J	u	3952	-	4077	40	36	6	125	-	11	>10		76	-
	Ile	J	u	4025	-	4550	60-70	2-45	6	525	-	12	>10		57-75	-
	Tofte	J	u	4143	-	4305	80	47	6	163	-	12	>10		64	-
	Tilje	J	u	4208			140-185	7-102	6			14	>10		61-84	-
Smørb.-Sør	Garn	J	u	3799	3982	-	87.5	70.6	<3	-	182.5	15	2-850	0.6	64-76	24
	Ile	J	u	3925	-	4039	71	21	<3	114	-	14	6		60	25
	Tilje-3	J	u	4125	-	4242	65		<3	117	-	12	1.7		60	17
	Tilje-2	J	u	4190	4242	-	52		<3	-	52	17	60		55	17
Snorre	Statfj.	EJ	u	2300	2595	-	90	40	9	-	120	24	1000	0.3	86	17
	L-DEF	LT	u	2360	2561	-	570	140	8	-	90	24	380	0.25	76	22
	L-BC	LT	u	2340	2574	-	180	45	8	-	50	24	125	0.25	71	22
Statfj.	Brent	MJ	u	2360	2586	-	155	115	7	-	226	28	2300	0.50	84	30
	Statfj.	EJ	u	2575	2806	-	125	63	7	-	231	21	1000	0.10	64	18
Statfj.-N	Volgian	LJ	u	2600	2718	-	46	37	10	-	118	25	785	0.30	83	35
	Brent	MJ	u	2620	2718	-	140	105	10	-	98	25	1000	0.4	80	35
Ula	Ula	LJ	u	3345	3561	-	110	100	10	-	90	17	300	0.15	82	30
Veslef.	Brent	MJ	u	2755	2906	-	125	71	1-3	-	151	18	200-700		72	30
	IDS	EJ	u	3000	3079	-	52	12	1-3	-	79	20	10-600		70	30
	Statfj.	EJ	u	3170	3208	3194	>200	>100	1-3	24	14	16	50		76	
Frigg	Frigg	E	a	1785	1957	1948	55	52	0	50	9	28	0.5-4 D	0.001-1	91	
Heimdal	Heimdal	P	an	2020	2150	2146	0-126	0-101		0-126	4	26	1000	0.01-0.8	86.7	20
Midgard	Garn	MJ	h	2300	-	2490	50	49	<10	200		29	5000	0.5	94	-
	Ile	MJ	h	2300	2500	2490	65	62	<10	200	12	27	5000	0.2-0.3	92	25
	Tilje	EJ	h	2350	-	2490	220	110	<10	200		25	1000	0.01-0.1	76	-
Sleip.-V	Hugin	MJ	au	3450	-		203	70-158	10	88-160	-	22	10-450	0.4-0.5	-	-
Sleip.-Ø	Heimdal	P	u	2260	-	2417	100	93	0	157	-	27	400	0.1	-	-
Snøhvit	Stø	LJ	u	2300	2419	2405	70-95	62-85	2	105	14	16	250	0.10	93	
	N-mdu	MJ	u	2300	2419	2405	60-105		2	105	14	14	10	0.10	93	
Troll	Sognefj.	LJ	rf	1300	1559	1547	230		1-4	230	0-26	27	10^3-10^4	0.25-0.9	30-95	20-40
Ekofisk	Ekofisk	Da	u	2900	3200	-	170	120	3-7	-	170	33	1-100	0.025-0.10	88	38-63
	Tor	Cr	u	3030	3250	-	85	60	3-7	-	85	30	1-100	0.025-0.10	82	38
Eldf.-A	Ekofisk	Da	u	2683		-	45	45	7-9	-	45	35	1.0	0.005-0.1	80	25-40
	Tor	Ma	u		2896	-	30	30	7-9	-	30	35	2.5	0.005-0.1	85	25-40
Eldf.-B	Ekofisk	Da	u	2807	2940	-	76	76	5-7	-	76	33	1.0	0.1	70	25-40
	Tor	Ma	u			-	91	91	5-7	-	91	35	3	0.1	80	25-40

Table B-1a: Properties Table —formation, fluids, composition, pressure, and temperature

contd.	S_{org} %	V_{clay} %	ρ_o	γ_g	ρ_c	μ_o cp	μ_g cp	μ_c cp	p_b bar	p_d bar	R_s	C_L	B_o	B_g^{-1}	C_1 %	C_{2-4} %	C_{5-12} %	C_s mg/l	C_{Di} mg/l	T °C	p bar
Balder Heimdal		0-25	914	0.677	-	3.0	0.016	-	155	-	53	-	1.15	120	53.9	5.9				77	177
Brage Statfj.			835		-	0.7		-	90	-	60	-	1.22	-	20.1	17.5		50210	5400	98	244
Brage Fensfj.	7		843	0.766	-	0.58	0.024	-	168	-	93	-	1.29	164	36.5	17.5		41710	2700	87	215
Draugen Rogn	-	< 10	824	1.010	-	0.68		-	59	-	52	-	1.19	-	16	23	60	37500	400	71	165
Gullf. Brent		5-25	882	0.793	-	1.12		-	244	-	94	-	1.25	-	45.4	6.2	47.0	41300	1970	72	310
Gullf. Cook		20-40	844	0.821	-	0.43		-	217	-	116	-	1.41	-	43.6	12.9	42.1			80	319
Gullf. Statfj.		15	838	0.810	-	0.40		-	270	-	171	-	1.46	-	49.6	13.6	35.7			80	320
Gullf.-S Brent	30	10	860	0.670	790	0.35	0.035		383	418	200	240	1.60	286	58	10	30	41200	1560	125	450
Gullf.-S Statfj.	30	5	860	0.670	790	0.35	0.035		386	463	200	310	1.60	278	56	12	29	38800	1210	125	470
Gullf.-S Lunde		15	865		-	0.41		-	381	-	180	-	1.60	-	58	10	31			129	510
Gyda Farsund	-	0-30	822	1.030	-	0.28		-	207	-	327	-	1.69	-	34.3	25.4	37.7	273000	33000	154	595
Heidrun Fangst	5-15	0.8	882	0.660		0.75	0.021		241	245	117	108	1.34	219	44.3	12.7	43.0	27000	Low	85	252
Heidrun Tilje	20-50	15	900	0.660		1.24	0.020		232	224	79	85	1.21	219	43.8	9.0	47			85	251
Heidrun Åre		9	922	0.660		2.29	0.020		201		60		1.16	219	40.8	3.4	55.8	32000	Low	85	251
Oseberg Brent	10	8	850	0.68	728	0.43	0.023	-	281	281	145	310	1.43	222	46.3	13.8	38.9	37800	1450	100	281
Smørb. Garn	-		-	0.905	766	-		0.13	-	447	-		2.32	238	73	13.9	9.2	*		143	467
Smørb. Ile	-							-	-		-			246	74.2	14.2	7.7			155	476
Smørb. Tofte	-		-	0.926	771	-		0.12	-	382	-		2.32	238	70.8	16.5	8.5			150	473
Smørb. Tilje			774	0.946			0.09			410	440		2.53	231	66.9	16.8	11.6			152	474
Smørb.-Sør Garn			832	0.961	-	0.14	0.055	-	362	-	433	-	2.48	-	56	17	14	50000		140	403
Smørb.-Sør Ile	20		-	0.992	768	-	0.052		-	386	1356		-	234	70	17	9	48000		140	414
Smørb.-Sør Tilje-3	20		-	1.146	788	-			-		1247		-	230						145	436
Smørb.-Sør Tilje-2	20		820	1.100	-		0.070	-	323	-	438	-		-	55	25	15	64350		145	436
Snorre Statfj.	10	6								-		-		-				34000	2000	90	383
Snorre L-DEF	-	10	690		-	0.42			179	-	133	-	1.40	-	37	23	40			93	383
Snorre L-BC	-	10	700		-	0.48			155	-	105	-	1.33	-	32	22	45	34000	2000	93	383
Statfj. Brent	-	13	824	0.771	-	0.31		-	276	-	190	-	1.58	-	49	17.7	32.6	14800	540	92	383
Statfj. Statfj.	5	17	840	0.848	-	0.29	0.032	-	196	-	155	-	1.54	-	39.5	19.5	40.3	14000	1250	99	404
Statfj.-N Volgian	-		842	0.844	-	0.74		-	131	-	93	-	1.30	-	27.6	21.1	30.0	22000	600	98	398
Statfj.-N Brent	-		846	1.154	-	0.71		-	109	-	66	-	1.24	-	23.5	19.5	30.4	22000	600	98	398
Ula Ula	-	0-15	689	1.293	-	0.37	0.015	-	166	-	164	-	1.35	-	28.1	20.6	28.4	200000	34000	143	491
Veslef. Brent		10	840	0.950	-	0.43		-	195	-	125	-	1.46	-	37.0	20.1	42.9	19800	250	122	321
Veslef. IDS	-	12	830	0.970	-	0.34		-	200	-	140	-	1.49	-	36.0	20.8	43.2	29500	990	128	346
Veslef. Statfj.	-	10	838	0.838	-	0.17		-	332		320		2.1		54.8	17.1	28.1	43727	1663	133	355
Frigg Frigg	-		835	0.581	797	4.83	0.021				61	5	1.15	194	95.5	3.7	0.07	60000		61	198
Heimdal Heimdal	-	9		0.712	710		0.022			210	156			211	86.3	10.3	3.4	60000		76	218
Midgard Garn	-		-	0.762		-	0.022		-	251	-	190	-	214	82	13.5	3.0	87000		90	251
Midgard Ile	10		663	0.762		0.36	0.022		251	251	159	190	1.48	214	82	13.5	3.0	87000		90	251
Midgard Tilje	-		-	0.762		-	0.022		-	251	-	190	-	214	82	13.5	3.0	87000			
Sleip.-V Hugin	-	10		0.84	649	-	0.047		-	356	-	360	1.54	271	70.8	15.2	4.1	70000		120	442
Sleip.-Ø Heimdal	-	5-10	-	1.456	653	-	0.009	1.2	-	235	1729	336	2.19	213	71.0	21.4	6.2	30986	2820	93	245
Snøhvit Stø	-		866	0.749	750	0.59	0.023		263	259	149	112	1.44	229	81.4	8.8	2.28	93000	5210	93	267
Snøhvit N-mdu	-		866	0.749	750	0.59	0.023		263	259	149	112	1.44	229	81.4	8.8	2.28	93000	5210	93	267
Troll Sognefj.	20-60		900	0.610	750	1.60	0.002	-	158	158	62	33	1.18	151	36	7	40	50000		68	158
Ekofisk Ekofisk		< 1	838	0.700	-	0.13	0.040	-	383	-	273	-	1.78	-	58	15	27	50000	4400	131	497
Ekofisk Tor		< 1	838	0.700	-	0.13	0.040	-	383	-	273	-	1.78	-	58	15	27	75000	3300	131	497
Eldf.-A Ekofisk		< 5	830	0.830	-	0.11	0.048	-	340	-	471	921	2.42	266	54.7	16.9	28.4	50000	850	126	472
Eldf.-A Tor		< 5	830	0.840	-	0.11	0.049				479	933	2.45	268						126	
Eldf.-B Ekofisk		< 5	842	0.880	-	0.10	0.061	-	400		458	1113	2.29	270	63.3	14.1	22.6	47000	1050	126	476
Eldf.-B Tor		< 5	842	0.880	-	0.10	0.061				458	1113	2.29	270							

Table B-1b: Properties Table contd. —formation, fluids, composition, pressure, and temperature

Table A.8: Typical viscosities prevalent in the NCS. Recent Advances in Improved Oil Recovery Methods for North Sea Sandstone Reservoirs. SPOR Monograph, 1992.